

ABSTRACT

DELLINGER, MARISSA. Distribution and Factors Influencing Blue Carbon Storage Within Coastal Wetlands of North Carolina. (Under the direction of Dr. Matthew C. Ricker).

The Natural Resource Conservation Service (NRCS) has completed soil surveys for 95% of the counties in the United States, but for non-priority areas such as tidal marshes and other coastal wetlands, surveys were lacking imperative information. Tidal marsh systems exist in a variety of geomorphic settings and provide many valuable ecosystem functions, such physical buffers against storms as well as functioning as a carbon sink. Understanding the factors of pedology that contribute to tidal marsh soil development can greatly improve our understanding of their potential to store soil organic carbon (SOC). In this study, four regionally representative pedogeomorphic units were identified and sampled: mineral soil back barrier and tidal creek marshes found in high-energy environments and organic soil lagoon island and submerged wetlands that form in low-energy estuarine environments. Total SOC pools were found to be highly dependent on the cumulative thickness of organic materials and the textural class of mineral marsh soils. High-energy sandy back barrier marshes had significantly ($p < 0.001$) smaller SOC pools to 200 cm depth (11.5 kg/m^2) compared to the maximum observed SOC storage in marshes formed over submerged wetlands (66.5 kg/m^2). Results suggest that tidal marshes vary significantly in their potential to store SOC between defined geomorphic settings, which can be used to refine regional blue carbon accounting efforts.

In coastal agricultural communities, increased salinization has also resulted in the abandonment of saline-sodic farm fields over the last century. Slowly these areas are transitioning from freshwater forests to ghost forests and ultimately into tidal marshes with the potential to store blue carbon and buffer storms. A total of 17 soil pedons were sampled to quantify the total carbon storage and net vertical accretion within abandoned fields along three transects,

representing defined ecosystem salinity gradients from forests to marshes. Carbon accretion rates were calculated from the volume of soil material that had developed on top of the prior agricultural surface (Ap horizon) and the estimates of years since abandonment at each sample location. Net accretion rates were calculated to range from 0.30 to 0.39 cm/yr across ecosystems, with an overall mean accretion rate of 0.36 ± 0.05 cm/yr. All soil accretion rates were less than relative sea level rise (0.49 ± 0.06 cm/yr, 1978-present) in the region. Mean soil carbon pools (to 200 cm depth) were also compared across abandoned farm fields (24.4 kg/m^2) to active farm fields (16.3 kg/m^2) and unaltered native tidal marshes (45.2 kg/m^2). Results from this study showed that abandoned fields are accumulating carbon relative to active farm fields, but not as much as unaltered marshes, which had significantly ($p < 0.05$) higher carbon stocks. In the future, proactive land management techniques will be needed in abandoned farm fields to increase SOC storage and vertical carbon accretion in order to keep pace with projected sea level rise.

© Copyright 2025 by Marissa Dellinger

All Rights Reserved

Distribution and Factors Influencing Blue Carbon Storage Within Coastal Wetlands of North
Carolina

by
Marissa Ann Dellinger

A thesis submitted to the Graduate Faculty of
North Carolina State University in
partial fulfillment of the
requirements for the degree of
Master of Science

Soil Science

Raleigh, North Carolina
2025

APPROVED BY:

Matthew C. Ricker
Committee Chair

Marcelo Ardón

Robert Austin

BIOGRAPHY

Marissa is a North Carolina native, born and raised in Raleigh. She began taking classes at Wake Technical Community College where she started out as a nursing major. At Wake Tech she took on a project involving biofilm formation in conjunction with surface area, which gave her the taste for scientific research. However, after two associate degrees and one trade degree, she decided to try a different path and began working and volunteering at the North Carolina Museum of Natural Science. From there she took an interest in soil science and, despite Wake Tech advisors telling her not to specialize, she went on to complete her Bachelors in soil science at NCSU. Marissa's participation in soil judging, working in the Land Use and Pedology lab, as well as her involvement with Ben Rose on his master's project "The ectomycorrhizal fungus *Paxillus ammoniavirescens* influences the effects of salinity on loblolly pine in response to potassium availability" encouraged her to seek a graduate position in soil pedology.

ACKNOWLEDGMENTS

Thank you to Dr. Matthew Ricker for giving me the opportunity to work on the project and providing your expertise. I have learned so much and I will take it with me throughout the rest of my professional journey.

To my lab mates, thank you Julia Janson for patiently answering all my questions about graduate school and salinity impacts in environments. Thank you to Jacob Cheers for putting so much time and effort as our laboratory technician. I was so fortunate to have your help sampling soils, running chemistry, and piloting our boat; your contribution was irreplaceable. My friendship with both of you is invaluable and I am grateful for it every day.

Thank you to Greg Taylor from the NRCS for not only piloting the airboat during our sampling expedition, but also for providing your professional expertise and experience.

Thank you to all the undergraduate students that were hired in the Pedology and Land Use lab, but especially Bennett Liverman who joined us out in Hyde County to sample. Your aid and company were appreciated.

Finally, thank you to both Bailey Parrish and Lori Gorczynski for their contributions in data and writing. Bailey provided almost all the data for my first chapter and her hard work was greatly appreciated. Lori's contributions of data as well as her expertly written thesis has guided me as I have written mine. I have truly stood on the shoulders of giants.

TABLE OF CONTENTS

LIST OF TABLES	vi
LIST OF FIGURES	vii
Chapter 1: Major Pedo-geomorphic Factors Affecting Blue Carbon Storage in Tidal Marsh Systems of North Carolina	1
Introduction.....	1
Methods.....	9
Geographic Information System (GIS).....	13
Statistics	14
Results.....	14
Series Mapped & Classified.....	14
Factors Influencing Development and Distribution of Tidal Marsh Soils.....	16
Carbon Extent Across PGUs.....	18
Estimations of Carbon Stock from Horizon Characteristics.....	21
Discussion	23
Series Mapped & Classified.....	23
Factors Influencing Development and Distribution of Tidal Marsh Soils.....	27
Carbon Extent Across PGUs.....	28
Conclusion	31
Chapter 2: Carbon Accretion and Salinization of Abandoned Agricultural Fields along the North Carolina Coastline	33
Introduction.....	33
Methods.....	38
Study Site	38
Field Collection.....	41
Laboratory Analysis.....	42
Geospatial Data.....	43
Calculations.....	44
Statistics	45
Results.....	46
Mapping Concepts: Ecosystems vs. Soil Series	46
Distinguishing Soil Factors Between Ecosystem	48
Discussion	53
Mapping Concepts: Ecosystems vs. Soil Series	53
Distinguishing Soil Factors Between Ecosystem	57
Salinity Gradient	61
Conclusion	64
References.....	65
Appendix A.....	79
Appendix Figure A1 C:N ratios by horizon for each ecosystem across salinity gradient	79
Appendix Figure A2 Representation of covariate relationship between mapped Soil Series and Ecosystem type.....	80
Appendix Figure A3 Boxplots of SOC pools across Soil Series and Ecosystem type.....	81

Appendix B: Carbon Stock Calculations	82
Figure B1: Regression analysis between estimates and measurements for the same Pedons	84
Appendix C: Site Metadata.....	86
Table C1 Summary of water and sampling data from transects (chapter 2).....	86
Table C2 Site location and vegetation by pedon (chapter 2)	87
Table C3: Pedon Horizon data.....	88
Table C4: Profile Descriptions.....	132
Appendix D: Taxonomic Classification.....	151
Table D1: Classification of Back Barrier Pedons	152
Table D2: Classification of Tidal Creek Pedons.....	153
Table D3: Classification of Submerged Wetland Pedons.....	154
Table D4: Classification of Lagoon Island Pedons.....	155
Table D5: Classification of chapter 2 soils per the Keys to Soil Taxonomy. Highlighted values are agreements between mapped and classified pedon.....	138
Appendix E: Shoreline Erosion	158
Figure E1: 1938 Shoreline Georeferenced.....	158
Figure E2: 2024 Shoreline Comparisons of Shoreline Erosion	159

LIST OF TABLES

Table 1.1	Summary of marsh soil sampling in North Carolina, means \pm 1 standard deviation	12
Table 1.2	Summary of mean pedon soil organic carbon (SOC) metrics by tidal marsh pedogeomorphic units (PGU).....	19
Table 1.3	Summary of carbon scale to 1 meter across pedogeomorphic units.	21
Table 1.4	Summary of carbon scale to 2 meters across pedogeomorphic units.....	21
Table 1.5	Summary of mean (\pm 1 standard deviation) tidal marsh soil organic carbon (SOC) stock properties by horizon type. Means with different letters by column are significantly different ($p < 0.05$) using one-way ANOVA and Tukey's HSD tests	22
Table 2.1	Mean Horizon Values of Soil Characteristics and Coefficient of Variation	47
Table 2.2	Average Rates of Carbon Development and Storage by Pedon	48
Table 2.3	NDVI values per ecosystem.	48

LIST OF FIGURES

Figure 1.1	Map of overall sampling sites and corresponding PGUs across NC coastline (left) and example of transect sampling within Tidal Creek marshes (right)	11
Figure 1.2	Boxplots showing the cumulative depths of organic soil horizons across PGUs. Note, that the Tidal Creek PGU had no organic horizons observed and was excluded from the analysis of organic thickness. Box plots with different letters are significantly different ($p < 0.05$) according to One-Way ANOVA and Tukey's HSD tests.	16
Figure 1.3	Color Map on Spearman's ρ for landscape-scale factors related to soil carbon storage. Variables in red hue squares are negatively correlated (-1) and variables in blue hue squares are positively correlated (+1)	17
Figure 1.4	Regression between the environmental factor distance to nearest non marsh soil (upland) and the carbon pools across all PGUs ($n = 51$).....	18
Figure 1.5	Regression between O horizon depths, or the accretion of organic matter on the surface, and SOC stock, or the pool of SOC across PGUs.	20
Figure 1.6	Regression analysis between estimates and measurements of pedon-scale SOC pools..	23
Figure 2.1	Map of all sampling locations and corresponding ecosystems within Hyde County, NC	40
Figure 2.2	Color Map of Spearman's (ρ) for environmental factors related to soil formation and carbon storage. Red hued squares are negatively correlated (-1) and blue hued squares are positively correlated (+1). The more positive the correlation, the higher the influence on a variable.....	50
Figure 2.3	The initial 1:1 pH reading taken after sampling and change in pH after 16 weeks of incubation regressed against 1:5 EC (dS/m) to observe the different ecosystems pH across a salinity gradient.	51
Figure 2.4	The amount of organic materials that had accumulated over the prior agricultural soil surface regressed against a salinity gradient.	52
Figure 2.5	Pedons in each condition were sampled to 2 m, and C:N ratios were calculated based on the carbon and nitrogen data from the sampled soils in each condition. (Active Fields $n: 24$; Abandoned Fields $n: 36$; Established Marsh $n: 28$).	53

CHAPTER 1: Major Pedo-geomorphic Factors Affecting Blue Carbon Storage in Tidal Marsh Systems of North Carolina

Introduction

In the United States, sea level has risen approximately 0.15-0.20 meters (m) in the last 100 years (Lindsey, 2022) and is projected to rise another 0.25-0.30 m over the next 30 years (Sweet et al. 2022). Some areas, like the Gulf of Mexico, have steeper projections than the national average due to significant coastal land subsidence (Lindsey, 2022). Sea level rise is caused by the expansion of the ocean's volume as water molecules expand in response to increasing temperature as well as the melting of ice sheets in the northern hemisphere (IPCC, 2010). As climate changes, global coastlines will progressively become more hazardous. For example, North Carolina's (NC) coast is expecting between 0.36 to 0.43 m in relative sea level rise by the year 2050 (Sweet et al. 2022) putting over 1 million people at risk of being significantly impacted by saltwater intrusion and flooding (NOAA, 2024). NC's extensive saltwater intrusion and flooding is caused by regional SLR but has been escalated by the melting of glacial ice since the end of the Wisconsin glaciation (Ohenhen et al. 2023). During the Wisconsin glaciation, the freezing of the ice sheets caused the global sea level to drop until around 25,000 years ago when glaciers began retreating (Lilly 1981). The weight of the ice compressed the Earth's crust and created an ice sheet forebulge, where the lithosphere on either side rises to compensate for the compression (Turcotte et al. 2002). Once glaciers retreated the compressed areas uplifted in isostatic rebound and the forebulge areas collapsed (Roy et al. 2015). Areas in the southeast, such as NC's coastlines, are currently subsiding in response to the forebulge collapse (Johnston et al. 2021; Riggs et al. 2003). Isostatic rebound induced sea levels have been rising ~0.30 m every 100 years in NC (Lilly 1981;

Riggs et al. 2003), but current models forecast an increase between 0.36 - 0.43 m by 2050 due to SLR induced by global warming (Sweet et al. 2022). The combination of both subsidence and SLR has resulted in an overall faster net rate of relative sea level rise in NC compared to other areas of the Atlantic Coastal Plain (Ohenhen et al. 2023; Ohenhen et al. 2024).

Current projections of sea level rise threaten the longevity of coastal ecosystems (Kirwan et al. 2013). Increased frequency and intensity of storms exposes freshwater vegetation to saltwater spray, killing off the vegetative fringe on shorelines (Riggs et al. 2003). Without the protection of vegetative fringe, sediments that accumulate on the coastline form different coastal environments that erode at higher rates (Riggs et al. 2003). Vegetated coastal ecosystems function as efficient carbon sinks, as they are an integral part of the carbon cycle, storing carbon in sediments from both local vegetative sources and external sources transporting organic coated sediments in (Mcleod et al. 2011). Stored carbon in these coastal ecosystems is referred to as 'Blue Carbon' denoting its proximity to the ocean. Blue carbon comes from many different sources such as the above and below ground living biomass of local vegetation as well as the non-living biomass of decaying organic material (Mcleod et al. 2011). Despite having a smaller spatial extent, the global distribution of these vegetated coastal ecosystems sequesters carbon at rates comparable to terrestrial ecosystems (Scott et al. 2022; Mcleod et al. 2011). For example, global carbon burial is estimated to be 5 to 87 million metric tons (Mg) per year in tidal marsh ecosystems, as compared to tropical terrestrial forests estimated to be 53 to 79 million Mg per year (Mcleod et al. 2011). The global soil and vegetation in coastal ecosystems store 10 to 24 billion Mg of carbon and, when

undisturbed, add 30 to 70 million Mg more carbon to their soils (Scott et al. 2022). However, any disruption to blue carbon stores result in the mineralization of organic materials and the release of carbon dioxide back into the atmosphere or fluxed as dissolved and particulate carbon back into the open ocean (Holmquist et al. 2018; Scott et al. 2022). With increases in SLR, blue carbon in coastal ecosystems is at heightened risk of disturbances losing their stored carbon through submergence and erosion (Kirwan et al. 2013).

Much of NC's original coastline was swamp and marsh ecosystems which developed over time due to the flat topography, high rainfall, and large distances between streams (Lilly 1981). These characteristics are ideal for waterlogging, creating anaerobic conditions and restricting lateral water flow, slowing the decomposition of litter, and generally permitting the accumulation of carbon (Batzer et al. 2014). Elevated levels of salinity in the sounds are expected with increases in SLR as inundation becomes more frequent and submerges the coast for longer periods (Li et al. 2022). SLR induced flooding creates waterlogging in soils which has been shown to stress plants physiologically and encourage the accumulation of carbon in vegetative biomass below ground (Minden et al. 2012; Li et al. 2022). However, waterlogging can also decrease photosynthesis under longer durations which reduces the amount of photosynthates, like carbon, stored in plant tissues. SLR induced flooding also promotes the transition in salinity gradients within soils along the coast (Costa et al. 2023). Even minor increases in salinity can alter the community of plant species present, influencing the amount of carbon that can be accumulated (Batzer et al. 2014). Increased salinization increases osmotic pressure in plants and reduces photosynthetic capacity (Batzer et al. 2014; Li et

al. 2022). The NaCl in brackish and saline water is toxic to vegetative species intolerant to salt stressors, often damaging the plant cellular functions before osmotic pressure affects the plant (Batzer et al. 2014). The suppression of CO₂ respiration in anaerobic soils with waterlogging and the toxicity of NaCl with increases in salinity both inhibit the typical carbon allocation patterns in plants, which can result in carbon accumulating in the root biomass instead of traveling through the phloem (Li et al. 2022). The influence, then, of SLR on the NC coastline has damaging effects for coastal ecosystems not adapted to tidal marsh conditions with increases in flooding frequency and duration of brackish and saline water (Morris et al. 2002). Areas that were predominantly freshwater can shift to brackish or saline environments, pushing plant species to migrate further inland, if able, or simply die off (Batzer et al. 2014; Morris et al. 2002). So, unless a plant species can photosynthesize underwater and adapt to salt stress, the vegetation will die (Mauchamp et al. 2004; Li et al. 2022).

The Albemarle-Pamlico Estuary System (APES) is a collection of drainage basins on NC's coastline undergoing that shift from freshwater to brackish environments due to increased SLR. It is part of a paleodrainage system that existed during the end of the Pleistocene, approximately 20,000 years ago (Riggs et al. 2003). Estuaries began to form around 8,000 years ago due to raised global sea levels and increased flooding across the low-elevation topography of the NC Coastal Plain (Riggs et al. 2003; Lilly 1981). Holocene age peat, with radiocarbon ages dating back to 700 to 4500 years old, have been accreting over Pleistocene mineral deposits (Riggs et al. 2003), though some ages for organic deposits on the surface have been estimated to only be a few decades old (Daniels et al. 1999).

Peat deposit depths are impacted by multiple geomorphic factors such as hydrology, dominant vegetation, and topography, which Li et al. (2024) notes as the most influential. Macro-topography features often have existed for thousands of years, creating ideal conditions for peats to accumulate (Frankard et al. 1998; Li et al. 2024). Radiocarbon dating has been utilized in multiple studies (Braswell et al. 2020; Aguilos et al. 2021) to understand the rate of peat deposits and subsequent carbon storage over time through observed soil ages. In one study, wood samples found in freshwater peat layers from the NC Alligator River National Wildlife Refuge were dated using C-14 to depths of 1 meter and organic soils in this region were estimated to be 235 to 1,780 years old (Aguilos et al. 2021). Cores that were sampled at shallower depths were noted as having decreasing soil carbon accretion; thus, it was estimated that cores with deeper cumulative depths of peat were older (Aguilos et al. 2021). In a more generalized study, basal peat cores from both field evaluations and literature reviews were analyzed for physical and chemical properties along with radiocarbon dating (Braswell et al. 2020). This study looked at 24 soil cores dated using ^{14}C from the field across the Atlantic and Gulf coasts as well as 387 soil cores dated within literature and found ages ranged from between 0 to 10,819 years old. Moreover, the wetlands closest to the ocean were more variable in age and were noted as having younger peat deposits compared to inland wetlands (Braswell et al. 2020). Therefore, the circumstances in which coastal environments form significantly impact the rate and longevity carbon is stored.

Due to the variety of geomorphic positions, the APES includes many different wetland ecosystems that can accumulate carbon at varying rates. The APES occurs within the boundaries of the barrier islands as a lagoon, receiving minimal astronomical

tidal input and minimal sediment input from river deltas (Riggs et al. 2003). Rather, mineral sediments are deposited and transferred with winds or storm events from the barrier islands into the estuaries. Multiple marsh ecosystems occur within the APES with variable salinity gradients, vegetation type, and soil characteristics (Riggs et al. 2003). Marshes also form on the NC mainland, facing the sound and within reach of are characterized as having micro-tidal inundation. Tributary estuaries form within the APES where rivers fan out into the Albemarle Sound from the Pasquotank River basin (Riggs et al. 2013). These estuaries have been carved out along the inside of the sound and the bottom of the tributary estuaries are submerged by freshwater generally but can transition to being submerged by brackish water with the progression of SLR (Riggs et al 2003). The submergence of the estuary valley creates an environment that encourages the accumulation of organic matter since it is unfavorable to microorganisms that can decompose litter, forming marshes (Batzer, 2014).

On NC barrier islands, back barrier marshes form in dynamic conditions where they dissipate wave energy and recollect displaced sediments after storms (RESTORE, 2017; Riggs et al. 2003; Rossi et al. 2019). Erosion rates are highly variable in these environments and require frequent over-wash events to prevent extensive erosion (Riggs et al. 2013). Organic matter accumulates quickly in above ground plant biomass then stabilizes after only a few thousand years (Rossi et al. 2019). Carbon accumulation is a function of increased plant productivity, which is influenced by proximity to open water (Batzer et al. 2014; Rossi et al. 2019). Tidal creeks form from the influx of semi-diurnal tides, where ocean water floods salt marshes and settles within channels on the landscape (Riggs et al. 2013). Tidal creeks serve as a barrier between the saltwater

ecosystems of the coastline and the freshwater ecosystems further inland (Magolan et al. 2020) and provide sediment and water inputs to estuarine habitats downstream (Bost et al. 2023). Channels are typically dry during low tide, permitting oxidation, and filled during high tide (Riggs et al. 2003; Conner et al. 2007).

Soils in these environments are mineral particles formed from deposited marine sediments coated in organic matter, with some locations having deeper organic topsoils (Lilly 1981). Histosols are mapped within the lower coastal plain region but only require 40 cm of organic material on the surface to classify as organic soil (Soil Survey Staff, 2022). Mineral soils mapped in the brackish systems include series such as Bohicket and Carteret. Bohicket is mapped along the southern coastline of NC, exposed to high-energy tidal oscillations. Carteret is mapped on the barrier islands of NC, both on the Atlantic side and the Sound side (Daniels et al. 1999). Soils in these high-energy coastal environments are highly variable and carbon storage capacity depends on the tidal deposition of sediments as well as vegetation established in that area (Deb et al. 2021).

Deeper organic soils in this region form in lower parts of the landscape with minimal disturbances, or in low energy environments (Dolman et al. 1968). Organic soil materials in NC are typically classified as sapric, meaning the organic matter is the most decomposed it can be, containing less than 1/8 by volume of visible fibers after rubbing the material (Soil Survey Staff, 2022). Sapric materials have the highest bulk density and lowest hydraulic conductivity due to the lack of pore space and are also the most resistant to chemical and physical changes (Boelter, 1965). Underlying mineral soils have been deposited within the last ~12,000 years during the Pleistocene epoch (Cohen et al. 2023), however the upper 30 cm of organic matter and mineral sediments are only

a few decades old (Daniels et al. 1999). Organic soil series mapped in the brackish systems of the Southeastern United States are Currituck, Backbay, Delway, and Longshoal. Currituck is predominantly mapped on the Outer Banks, specifically on the Sound side away from high-energy tidal oscillations. Currituck is classified as a deep organic soil regularly flooded with freshwater from estuaries or oligohaline classified water in tidal marshes. Backbay, Delway, and Longshoal are mapped along the fringe of the mainland drowned coastline, with deeper organics further away from upland soils (Daniels et al. 1999).

Carbon burial within coastal habitats contributes to high storage rates over longer periods, meaning soils are not only saturated with carbon, but organic matter is accumulating as its own layer (McLeod et al. 2011). Terric Histosols and Histic Humaquepts in the APES were identified in this study as soils that accumulate carbon as its own layer, or horizon. Their distribution in this region was documented and their formation in relation to the landscape and different soil characteristics were studied as well. Data was used to model where deeper organic deposits have the potential to accumulate carbon in the Southeast region.

Mineral tidal marsh soils were also identified for carbon accounting in this study. Mineral tidal marsh soils typically form in landscapes with frequent sediment deposition. There are 2 mineral tidal marsh soils (Carteret and Bohicket) most frequently mapped in the Southeast for both low and high-energy environments. Representative map units were chosen for mineral tidal marsh soils in the back barrier landscape to be evaluated for blue carbon storage and to be used for statistical comparison to similar geomorphic areas and their soils. With the onset of SLR increasing erosion potential and the shifts in

vegetation from changing salinity, carbon is at high risk of being lost. Therefore, taking inventory of available blue carbon is necessary to preserve what storage potential is left. Blue carbon ecosystems will prove to be vital as global warming continues to encourage the release of carbon into the atmosphere from the terrestrial environments where they are being stored.

Correctly identifying and mapping coastal wetlands serves to provide baseline information regarding the distribution and potential fate of stored carbon pools along our coast. Each coastal ecosystem has the capacity to store carbon to some degree, so in order to have an accurate blue carbon inventory, pedogeomorphic factors and soil properties need to be recognized as a key factor driving carbon accretion. To study this, different coastal ecosystems were hypothesized to have varying soil organic carbon pools the formation of which were theorized to be driven by different pedogeomorphic factors and soil properties. The primary goals of this study were to: 1) Identify pedogeomorphic units (PGU) that are representative of tidal marshes in NC. 2) Determine changes in soil properties across PGUs. 3) Quantify the organic carbon stocks in tidal marsh soils in the coastal Pamlico Sound region of NC using optimal sampling strategies based on PGUs.

Methods

Four major pedogeomorphic units (PGUs) were identified as representative of southeastern regional marsh systems and subsequently sampled and analyzed. Units identified were high-energy back barrier marsh (17-28 ppt mesohaline/polyhaline salinity), tidal creek marsh (29-32 ppt polyhaline salinity), submerged wetland marsh (7.5-12 ppt mesohaline salinity), and lagoon island marsh (4.2-6.2 ppt oligohaline/mesohaline salinity). PGUs were distinguished using geospatial analysis,

with sample transects taken to ensure variability across ecosystem salinity, soil series, distance to the nearest non-marsh soil, distance to the nearest open brackish water, height above mean sea level, and vegetation type. GPS coordinates of each soil sample were recorded so profiles could be compared to geomorphic factors such as distance to open water, distance to nearest upland, relative height above sea level, salinity, and sulfur content.

Back Barrier (BB) marshes are the tidal marshes that form on the backside of dunes and their extent in this study was 10,730 ha across the Southeast US from Virginia to Florida, with the sampling site located on the lagoon side of the Outer Banks (Fig. 1). The soil series commonly mapped in BB marshes is Carteret (Mixed, thermic Typic Psammaquents). Tidal creeks (TC) extend throughout salt marshes along the Atlantic seaboard due to the water input of incoming tides, and the total regional extent of this environment was 209,140 ha. The most representative soil series mapped in TC areas is Bohicket (Fine, mixed, superactive, nonacid, thermic Typic Sulfaquents). In the case of this study, the tidal creek marsh environment was a part of the Intercoastal Waterway, an extensive anthropogenic feature that runs parallel to the coastline for much of the Atlantic seaboard. Submerged wetlands (SW) are common in the NC coastline due to the low-lying and flat topography of the area. Most of these wetlands are inundated with brackish water under normal conditions and the extent for this environment was 37,026 ha. The SW PGU contains catena sequences composed of multiple different soil series with different cumulative depths of organic material deposition (range 20 to 200 cm in thickness). Soil series mapped in the SW marshes include: Longshoal (Euic, thermic Typic Haplosaprists), Delway (Loamy, mixed, euic, thermic Terric Haplosaprists), and Backbay (Fineloamy, mixed, active, nonacid, thermic Histic Humaquepts). Finally, the

lagoon island (LI) marshes are found on the estuary side of barrier islands and form relict flood tidal deltas or wash over fans that have been submerged. The extent of this tidal marsh PGU was 15,359 ha along the inland side of the Outer Banks and these areas are mapped as Currituck series (Sandy or sandy-skeletal, mixed, euic, thermic Terric Haplosaprists) (Fig. 1).

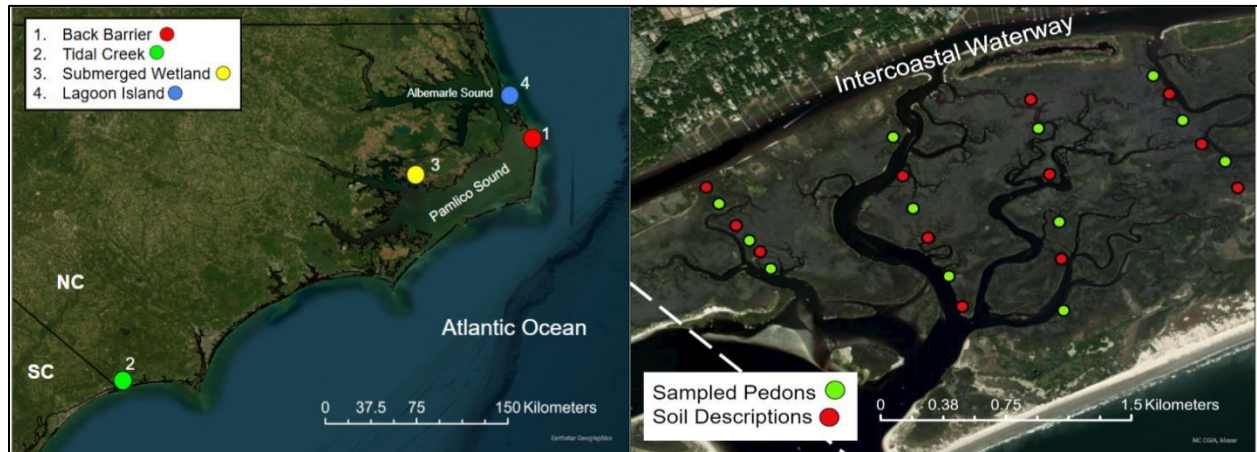


Fig. 1.1: Map of overall sampling sites and corresponding PGUs across NC coastline (left) and example of transect sampling within Tidal Creek marshes (right).

The main vegetation within study marshes was black needle rush (*Juncus roemerianus* Scheele.), smooth cordgrass (*Spartina alterniflora* Loisel.) and big cordgrass (*Spartina cynosuroides* (L.) Roth). Coordinates were taken at each location along with water sample dissolved oxygen (mg/L), pH, and salinity (ppt) were taken using a portable YSI meter at the nearest open water source to the sample point. Descriptions were made at 106 locations (Table 1.1) for both pedons sampled for laboratory analysis and unsampled pedons. All soil descriptions were completed using standard methods (Schoeneberger et al. 2012) and organic horizons were also evaluated using the von Post Humification scale (Von Post et al. 1926).

Table 1.1. Summary of marsh soil sampling in North Carolina, means \pm 1 standard deviation.

Pedogeomorphic Unit	Mean Water	Soil Series Mapped	Transects	Soil Descriptions	Pedons Sampled	Horizons Sampled
	Salinity (ppt)					
Back Barrier (BB)	21.51 \pm 4.59	Carteret	4	24	14	70
Tidal Creek (TC)	29.67 \pm 1.06	Bohicket	4	26	12	55
Submerged Wetland (SW)	9.50 \pm 1.43	Longshoal-DelwayBackbay	4	26	12	82
Lagoon Island (LI)	5.48 \pm 0.68	Currituck	6	30	13	77
		Totals	18	106	51	284

Pedons were sampled to two meters using a Macauley peat auger until refusal. Non-fluid sandy pedons were sampled using a gasoline vibracore to sample deep horizons (>100 cm). Of 18 transects, 106 descriptions were made and 51 pedons were sampled. Bulk density was taken at all sampled sites using either 5 cm Macauley auger cores, 5x5 cm metal cylinders, or cutting a “brownie” cube of known volume out of the marsh surface fibers and measured (length, width, height) using a handheld caliper (Blake and Hartge, 1986). Soil chemistry including 1:5 (soil: water volumetric ratio) electrical conductivity and 1:1 pH was taken in the field for all sampled pedons.

Soil horizon samples were characterized in the laboratory using standard metrics such as incubation pH for classification of sulfidic materials, electrical conductivity (EC) for salinity, total carbon and nitrogen content. Samples were combined with deionized (DI) water to create a soil water ratio and run for 1:1 initial pH, 1:1 and 1:5 electrical conductivity (Soil Survey Staff, 2022). Organic soil materials were also evaluated using 1:2 calcium chloride (CaCl₂) pH to determine Histosol taxonomic reaction class (Soil Survey Staff, 2022). After the initial pH measurement, samples were stored at room temperature for a 16-week incubation period under

moist aerobic conditions to identify both hyposulfidic and (hyper) sulfidic materials (Soil Survey Staff, 2022).

Particle size analysis was completed using the hydrometer method and wet sand sieving to identify mineral soil horizon texture (Gee and Bauder, 1986). Soil samples with organic-rich mineral horizons were pretreated with hydrogen peroxide to remove excess organic matter prior to determination of soil texture. Each horizon was analyzed for carbon and nitrogen concentration using thermal combustion on a LECO CN928 analyzer (LECO Corporation St. Joseph, Michigan, USA). Sample horizon depths and bulk density were used to convert soil C concentrations to landscape-scale mass per unit area (kg C /m^2) to fixed 1 and 2 m depths (see Appendix B for detailed calculations). Pedons were classified using morphology and laboratory data with the Keys to Soil Taxonomy, 13th edition (Soil Survey Staff, 2022).

Geographic Information System (GIS):

ArcGIS Pro (3.1.3) software was used to calculate the mean height above sea level and the nearest distance to open water. A Digital Elevation Model (DEM) was created using LAS files from the North Carolina Spatial Download database (“NC Spatial Data Download,” n.d.) to measure mean height above sea level. These files were derived from a Bare-Earth LiDAR NC floodplain mapping program. LAS files were converted to multipoint rasters, then to single-part, and finally the internal elevation or ‘Z’ factor values were added to the attribute table. Elevation values were referenced to the North American Vertical Datum of 1988 (NAVD 88) (“North American Vertical Datum,” 2018). The nearest distance to non-marsh soil, which were identified from soil data within the gSSURGO database, and open brackish water were determined using the GIS measure to find the shortest distance between the sampling location and the respective geomorphic variable.

Statistics:

Statistical analyses were conducted in JMP (Pro 17) and R-Studio (2023.06.2 + 561). Characteristics including soil organic carbon (SOC) stocks to 1 and 2 meters, depth of organic horizons, distance to nearest non-marsh soil, and open brackish water were compared using linear regressions across the different PGUs. A Spearman's Correlation matrix was used to identify relationships between the different geomorphic variables and average SOC pools at both 1 and 2 meters. The geomorphic variables included mean height above sea level, distance to nearest brackish water, distance to nearest non-marsh soil, SOC pool to 1 m, SOC pool to 2 m, average 1:5 EC, and average pH. Spearman's correlation (ρ) measures monotonic relationships, where positive correlations indicate that as one variable increases another variable increase along with it ("Spearman's Rank Order Correlation," n.d.). One-way ANOVA was run for SOC stocks to 1 and 2 meters for all PGUs and Tukey's HSD was used to look for statistically significant differences in means. ANOVA was also run for organic horizon depths across PGUs, excluding the tidal creek marsh locations, due to the lack of organic horizons.

Results

Series Mapped & Classified

The area of study was predominantly mapped as Entisols (51%), Histosols (41%), and Inceptisols (8%). The 6 soil series represented across the 4 pedogeomorphic units are listed in Table 1. All soil series are very poorly drained and contain marine sediment parent materials beneath the surface, and most series were described as having an organic surface layer of varying thickness ranging from 0 cm to 191 cm in depths. The 51 sampled pedons were reclassified based on laboratory analysis of carbon content and texture. Pedon-scale classified soils had a 31% agreement with the originally mapped classification done by the NRCS. Mapped series were reclassified as Entisols (55%) and Histosols (45%) with significant variation across subgroup classifications. Pedon-scale classifications deviated from mapped classification based

on depth to sulfidic materials, mineral horizon fluidity, soil salinity, and irregular decreases in organic carbon content with depth in the profile (for more detailed classification see Appendix A).

When calculating the cumulative depth of organic matter accreted over mineral parent materials, each PGU exhibited significant differences ($p < 0.05$) and trends that reflected their mapped series (Fig. 1.2). Of soils that contained organic horizons, BB marshes, the sandy Entisols, had the least organic matter depth, with a mean depth of 3.9 cm. TC marshes, the fluid mineral Entisols, had no observed organic horizons overlaying the mineral subsoil and could not be included in the comparison of PGUs (Fig. 1.2). SW marshes exhibited the largest range of organic horizon depths due to 3 different soil series that represent that PGU catena sequence, with a mean of 84 cm. LI marshes had the greatest cumulative depths of organic matter, with a mean thickness of 124 cm.

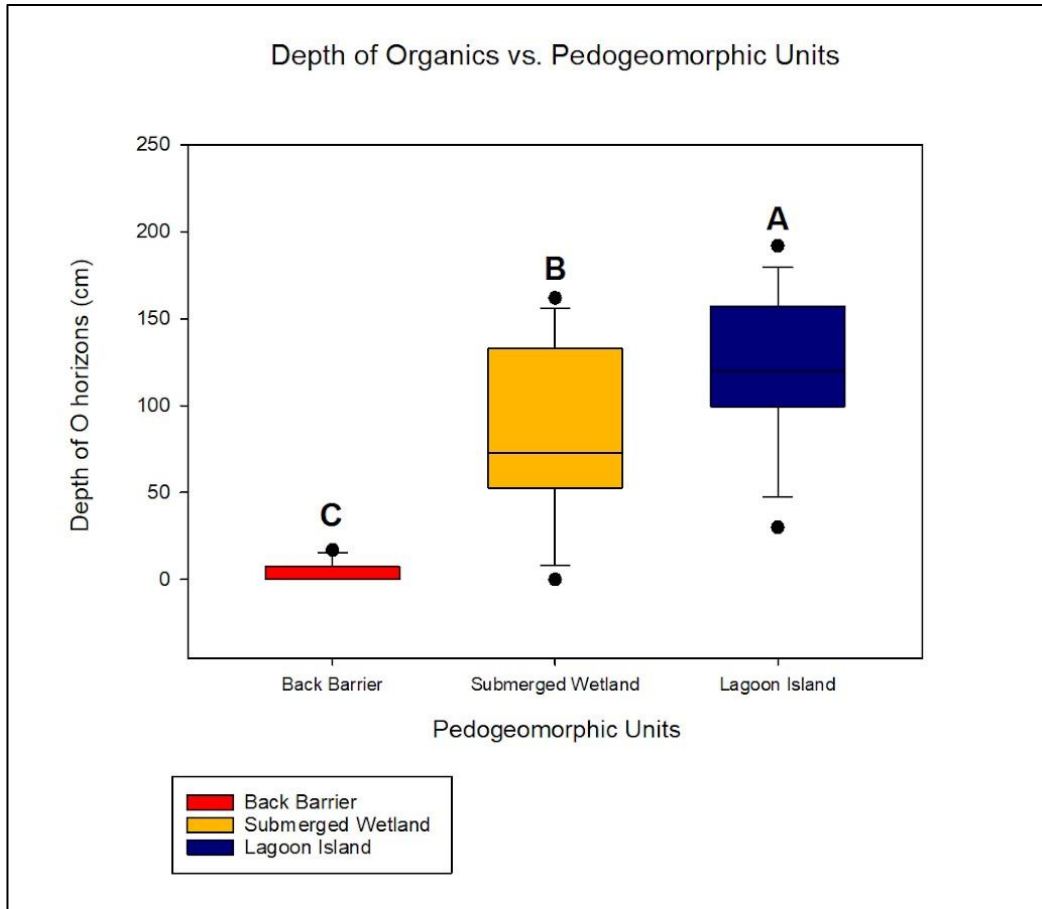


Fig 1.2. Boxplots showing the cumulative depths of organic soil horizons across PGUs. Note that the Tidal Creek PGU had no organic horizons observed and was excluded from the analysis of organic thickness. Box plots with different letters are significantly different ($p < 0.05$) according to One-Way ANOVA and Tukey's HSD tests.

Factors Influencing Development and Distribution of Tidal Marsh Soils

The SOC stocks for both 1 and 2 meter depths were summed across all PGUs for further analysis. Comparisons were made to determine the influence of height above mean sea level (m), distance to the nearest open body of brackish water (m), distance to nearest non-marsh soil (m), average 1:5 EC and pH have on the accretion of SOC pools in both 1 and 2 meters (Fig 1.3).

The correlations with the greatest significance (p -value: <0.001) between variables were found between distance to the nearest non-marsh soil (m) and SOC pools (kg/m^2) (1 m (ρ : 0.6), 2 m (ρ : 0.7)). Height above mean sea level (m) had a negative

correlation to SOC pools (kg/m^2), indicating that lower elevation locations within the study marshes have increased SOC pools. The rest of the variables tested did not have statistically significant correlations with SOC pools (Fig. 1.3).

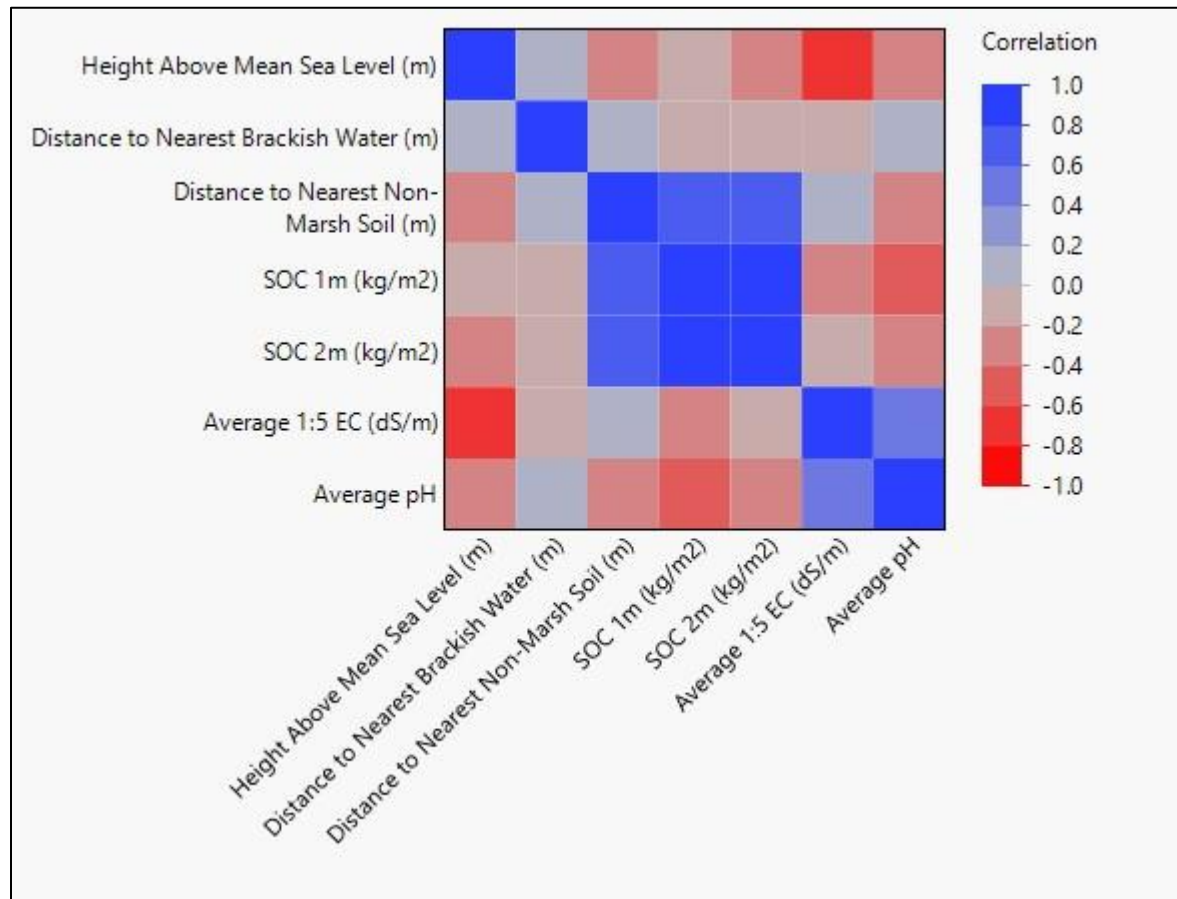


Fig 1.3. Color Map on Spearman’s ρ for landscape-scale factors related to soil carbon storage. Variables in red hue squares are negatively correlated (-1) and variables in blue hue squares are positively correlated (+1).

Because the only factor that influenced the SOC stocks was the distance to the nearest non-marsh soil, or in other words its proximity to the upland. SOC stock to 2 m was regressed against the proximity or distance to the nearest upland soil (Fig. 1.4). The correlations were highly significant across all PGUs (p-value: < 0.001), but the distance from uplands only explained <50% of the variation in tidal marsh SOC pools (R^2 : 0.477).

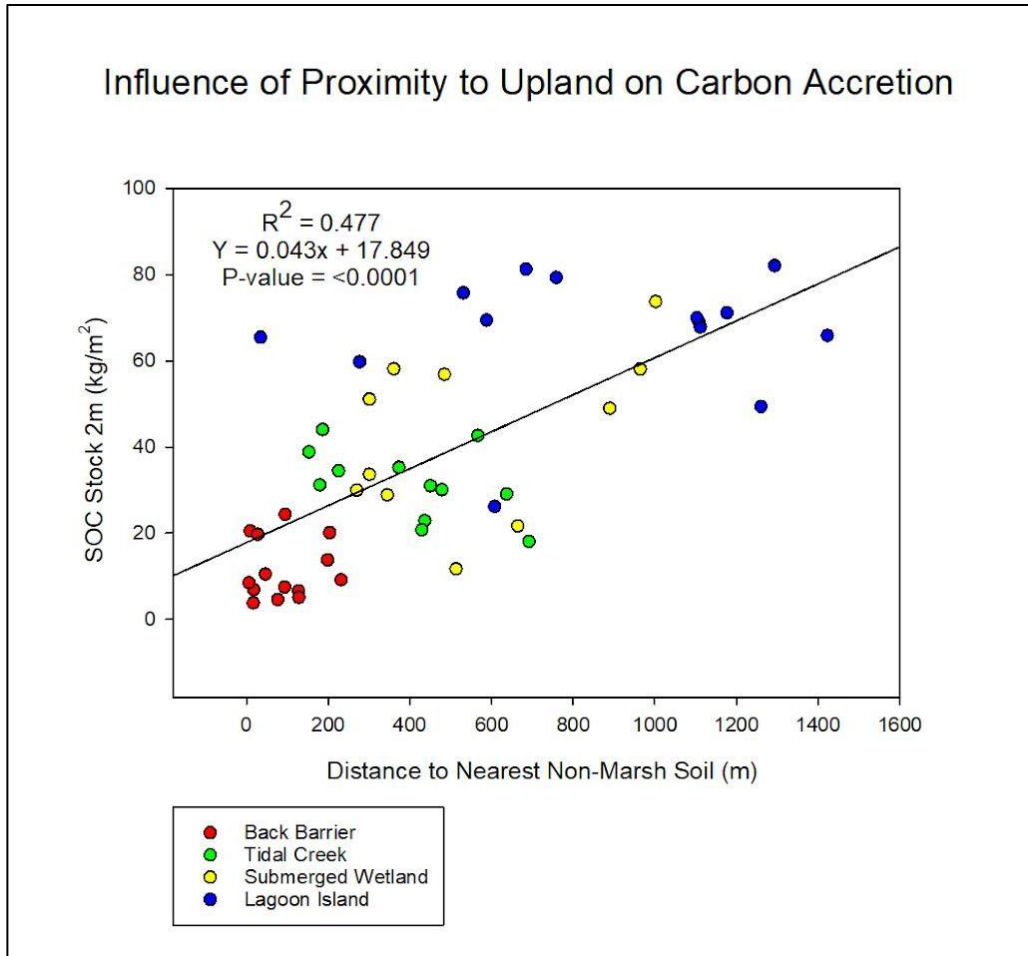


Fig. 1.4. Regression between the environmental factor distance to nearest non marsh soil (upland) and the carbon pools across all PGUs (n = 51).

Carbon Extent Across PGUs

Comparisons using One-Way ANOVA for both 1 and 2 meters found that each SOC pool was influenced by respective PGU sites. The mean SOC pools to 1 m were significant (p-value: <0.001) with differences between all PGUs, ranging from 8.4 ± 4.9 kg/m² in BB marshes to 40.3 ± 11 kg/m² in LI marshes. The SOC to 2 m also had significant differences (p-value: <0.001) between PGUs, ranging from 11.5 ± 6.9 kg/m² in BB marshes to 66.5 ± 15 kg/m² in LI marshes (Table 1.2). The proportion of total SOC stock in the upper 1 meter versus total SOC to 2 meters was significantly higher (p

< 0.05) in the BB marshes ($74.5 \pm 14\%$) compared to all other PGUs where <67.5% was stored in the upper 1 meter.

Table 1.2: Summary of Mean Pedon Soil Organic Carbon (SOC) Metrics by Tidal Marsh Pedogeomorphic Units (PGU).

PGU	n	SOC Pool 1m kg/m²	SOC Pool 2m Kg/m²	Proportion SOC in Upper 1 m %
Back Barrier (BB)	14	8.4 ± 4.9 d	11.5 ± 6.9 c	74.5 ± 14 a
Tidal Creek (TC)	12	17.4 ± 5.3 c	31.6 ± 8.2 b	55.0 ± 7.5 b
Submerged Wetland (SW)	12	27.8 ± 8.6 b	45.2 ± 19 b	67.5 ± 18 b
Lagoon Island (LI)	13	40.3 ± 11 a	66.5 ± 15 a	61.9 ± 14 b

Means ± 1 standard deviation, different letters by column are significantly different ($p < 0.05$) using one-way anova and tukey's hsd tests.

The depth of organic material was regressed to the 2 m SOC pools to look for influences on accreted surface organic matter (OM) and SOC pools across the PGUs (Fig. 1.5). The regression was significant (p-value; <0.001 , $R^2 = 0.847$) indicating there is a strong positive relationship between the depth of organic matter and the pools of SOC within 2 m pedons. Note that the TC marsh PGU contained no organic horizons so it could not be compared to the other PGUs that did have organic horizon depths and was therefore excluded from the analysis.

Table 1.3. Summary of carbon scale to 1 meter across pedogeomorphic units.

Pedogeomorphic Unit	Land		Soc Stock 1 m (Mg/ha)	Total Regional Carbon Storage (Gigagrams)
	Coverage (ha)	Soc Stock 1 m (kg/m ²)		
Back Barrier (BB)	10,730	8.4	84	901
Tidal Creek (TC)	209,140	17.4	174	36,390
Submerged Wetland (SW)	37,026	27.8	278	10,293
Lagoon Island (LI)	15,359	40.3	403	6,190
Total C (Gg)				53,775

Table 1.4. Summary of carbon scale to 2 meters across pedogeomorphic units.

Pedogeomorphic Unit	Land		SOC stock 2m (Mg/ha)	Total Regional Carbon Storage (Gigagrams)
	Coverage (ha)	SOC stock 2m (kg/m ²)		
Back Barrier (BB)	10,730	11.5	115	1,234
Tidal Creek (TC)	209,140	31.6	316	66,088
Submerged Wetland (SW)	37,026	45.2	452	16,736
Lagoon Island (LI)	15,359	66.5	665	10,214
Total C (Gg)				94,272

Estimations of Carbon Stock from Horizon Characteristics

Horizon-scale metrics were compared to quantify differences in bulk density, carbon concentration, and SOC density (Table 1.5). There were significant differences in all three metrics, depending on the horizon type identified. The highest SOC densities were in organic and mucky modified mineral A horizons compared to other mineral horizons.

Table 1.5: Summary of mean (± 1 standard deviation) tidal marsh soil organic carbon (SOC) stock properties by horizon type. Means with different letters by column are significantly different ($p < 0.05$) using one-way ANOVA and Tukey's HSD tests.

Horizon Type	n	Bulk Density g/cm³	Total Organic C %	SOC Density g C/cm³
Oi/Oe	47	0.16 \pm 0.09 d	25.28 \pm 8.66 a	0.0404 \pm 1.74 a
Oa	56	0.20 \pm 0.08 d	20.21 \pm 6.94 b	0.0404 \pm 1.35 a
Mucky A	35	0.50 \pm 0.23 c	8.09 \pm 2.32 c	0.0405 \pm 2.25 a
A	45	0.95 \pm 0.37 b	2.66 \pm 1.50 d	0.0253 \pm 1.40 b
Fluid Subsoil	44	1.03 \pm 0.38 b	1.72 \pm 1.14 d	0.0177 \pm 0.55 b
Sandy Subsoil	57	1.53 \pm 0.40 a	0.33 \pm 0.57 e	0.0050 \pm 0.75 c

Mucky modified A horizons are defined as having carbon concentrations from 5 to <12%. Fluid subsoil horizons are mineral subsoils with fluidity classes of slightly, moderately, or very fluid. Sandy subsoils were classified as non-fluid with sandy particle size classes.

SOC densities (g/cm³) were used as multipliers for pedons with described horizons, but no physical samples. Horizon thickness (cm) was multiplied against the densities based on a horizon's fluidity and horizon designation, which produces an SOC estimate for that horizon. Estimates were averaged for individual pedons. SOC estimate calculations were applied to sampled site pedons for further comparison of the calculations (Fig. 1.6). The relationship between estimated and measured SOC stocks was strong (R^2 : 0.9548) indicating that estimates based on empirical means can be useful in tidal marsh soils. For more information see Appendix B.

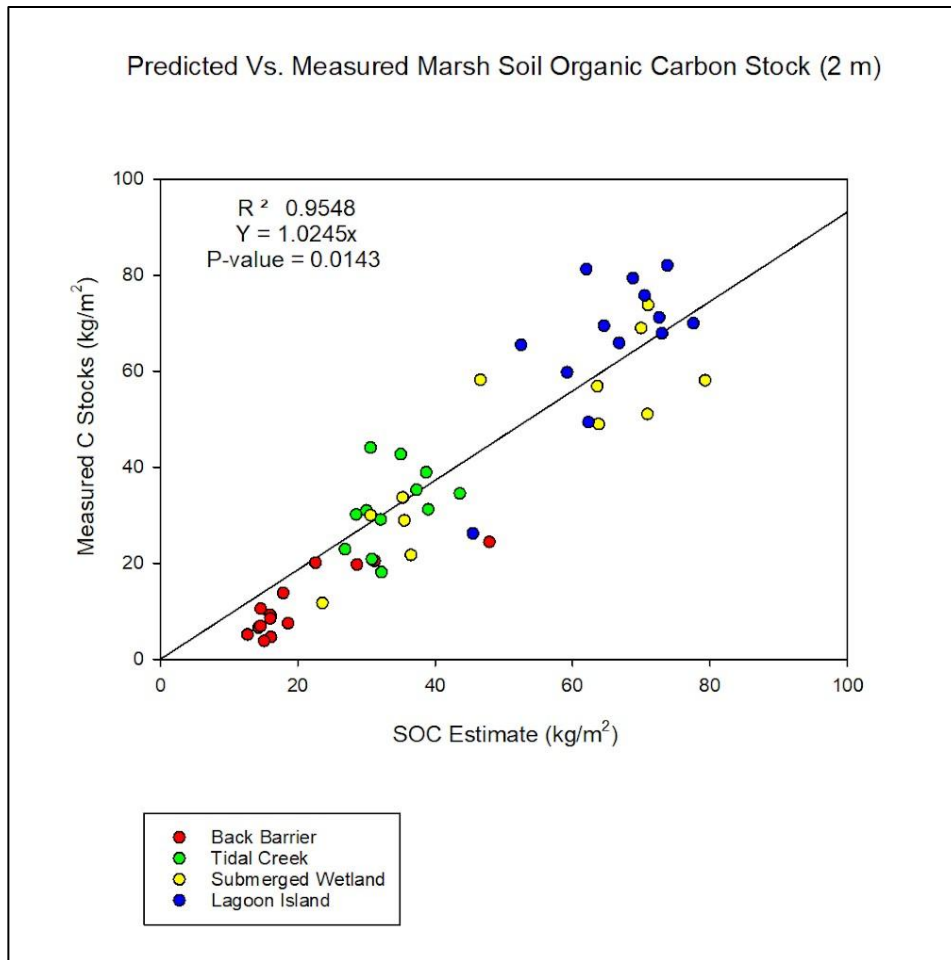


Fig. 1.6: Regression analysis between estimates and measurements of pedon-scale SOC pools.

Discussion

Series Mapped & Classified

Tidal marshes are the primary salt-tolerant coastal wetland in the Atlantic Coastal Plain and provide various beneficial ecosystem services (Finotello et al. 2020). When healthy, marshes regulate nutrient fluxes, act as a storm buffer protecting coastlines, and sequester significant amounts of carbon in their soils and above-ground plant biomass (McLeod et al. 2011). Despite their uses, tidal marshes have been considered non-priority lands in soil mapping because areas with little agricultural value were not given similar effort compared to working lands (Simonson, 1987). To date, the Southeast has very few sampled pedons that classify tidal marsh soils despite 259,025 ha of mapped marshes

within this region. Accurate descriptions and classifications of these wetland soils give a better understanding of how carbon can be both stored and lost as climate changes (Holmquist et al. 2018).

Each sampling point in this study corresponded to a specific soil series and pedons described were reclassified based on Keys to Soil Taxonomy. Based on their taxonomic classification, there was only a 31% overall agreement between soil series mapped and what was classified at a pedon-scale at each sampled site. When comparing PGUs to their organic horizon depths (Fig. 1.2) the averages reflected the general trends of their respective PGU soil series. BB marshes had the thinnest organic matter depths, since it is predominantly deep sands, and these areas are generally geomorphically unstable due to wash over storm events. Classified pedons had a 36% overall agreement in the BB PGU with their mapped series (Typic Psammaquents), with most of the discrepancies coming from the soils keying out as sandy Entisols with sulfidic materials within 50 cm of the surface (Haplic Sulfaquents). Mineral soils of TC sites had no organic surface materials, as would be expected in high-energy environments connected directly to the Atlantic Ocean with semi-diurnal tides (Conner et al. 2007; Riggs et al. 2003). Soils in TC PGUs were expected to have sulfidic materials near the soil surface (Typic Sulfaquents), however, most pedons sampled lacked sulfidic materials within the profile (Typic Hydraquents), resulting in only a 25% agreement between mapped series and pedon-scale reclassification between cores.

Organic-rich soils that had either histic epipedons (mineral soils with 20-40 cm of cumulative O horizons) or classified as Histosols (organic soils with >40 cm of cumulative O horizons) were predominantly found in the SW and LI marsh sites. Histosols are further separated by cumulative thickness of organic soil materials into

shallow Terric (40-130 cm cumulative thickness) or deep Typic (>130 cm cumulative thickness) subgroups. The SW sites had two soil series considered sapric Histosols, the most decomposed organic material. The third SW series was considered an aquic Inceptisol with a histic epipedon. The depth requirements to classify a histic epipedon, 20-40 cm, are shallower than histosols, 40 cm or more. SW had the greatest range and most observed variability of organic matter depth because these areas are mapped as complex catenas of soils ranging in predicted cumulative organic horizon thickness of 20-200 cm depth. SW are diverse in their distribution and development, and the mean cumulative organic thickness across the transects was 84 cm, indicating most soils were Terric Histosols. Within the SW transects, Histosols had a 25% agreement between mapped series and pedon-scale classification, whereas no pedons were classified as Backbay (Histic Humaquepts) despite being mapped in that location. Areas mapped as Histic epipedons were found to be incorrect at 75% of the pedon-scale sample locations due to >40 cm of cumulative organic horizon thicknesses resulting in Histosol classification. Overall, the catena mapping concepts used within SW transects were the most variable and had the least agreement with pedon-scale soil observations (17% agreement between mapped and pedon classification).

The LI marshes were mapped as Terric Haplosaprists and on average had the deepest mean organic matter depths (124 cm, Fig. 1.2). LI is a low-energy environment that develops on the sound side of the Outer Banks, away from the intensity of tidal oscillation and wave action, allowing for the accumulation of organic matter. For this PGU there was a 46% agreement between the mapped soil series and what was classified at a pedon-scale.

Significant discrepancies exist within the taxonomic subgroups between what was mapped and what was classified after analysis (see Appendix A). Many of the pedons that were reclassified after lab analyses were found to be more fluid or had different levels of organics than previously classified. Sodidity and the presence of sulfidic materials also influenced the deviation classified pedons had from their originally mapped subgroups.

PGUs were also identified as having distinct salinity regimes per geomorphic location. Based on mean field salinity measurements (Table 1.1), these were classified as polyhaline (1830 psu) for BB and TC sites and mesohaline (5-18 psu) for SW and LI sites. Variations in carbon and salinity data across PGUs in this study are likely rooted in the variability in their geomorphic positions. Across a variety of elevation gradients, the distribution of vegetation with plant productivity and sediment deposition increases the ability for a marsh to accrete carbon (Duarte et al. 2013; Elsey-Quirk et al. 2022). In this study, PGUs that exhibited lower carbon accretion, like BB and TC, were found to be more saline. Changes in salinity can alter plant populations, which drive the accretion of carbon through their above-ground and below-ground biomass (Deb et al. 2021). If a PGU had increased salinity, this could reduce the number of plant species present which would reduce the amount of carbon accreted. PGUs with more carbon in their profiles, such as SW and LI, were considered mesohaline which is lower in salinity.

Influences of salinity on carbon accretion can be indirect, like with the influence of salinity on vegetative biomass, or there can be a direct correlation between the factors. In the Li et al. (2022) study, higher salinity concentrations led to a decrease in microbial respiration and biomass in coastal soils. Decreases in microbial activities influence SOC turnover and would reduce the amount of carbon being decomposed in these

environments (Batzer et al. 2014). Conversely, Morrissey et al. (2013) observed a negative correlation between organic matter (OM) accumulation and salinity. Salinity was noted to disrupt the aggregation of soil and made organic particles more accessible to degradation by microorganisms, so increases in saline conditions increased the decomposition of OM.

Many factors contribute to carbon formation and degradation in coastal ecosystems. Our understanding of the distribution and accretion of blue carbon would improve by analyzing the pedogeomorphic factors with respect for each ecosystem. Detailed taxonomic classification provides information that might otherwise be overlooked. With these considerations, the mapping in the Southeast would need to be revised to consider the spatial and environmental variations different tidal marshes possess.

Factors Influencing Development and Distribution of Tidal Marsh Soils

Spearman's correlation matrix (Fig. 1.3) revealed that the SOC pools for both 1 and 2 meters were not significantly correlated to landscape-scale factors related to carbon storage, outside of distance to the upland soils. Based on each sample site's locations, different PGUs had different influences from pedogeomorphic factors on their SOC pools. In the Manetta et al. (2023) companion study, PGUs were hypothesized to increase organic horizon thickness closer to the open water's edge. The concept was that proximity to the water would bury organic materials and extend the marsh areas out into lagoons (Manetta et al. 2023). Sites further inland would have lower water tables which aerate the soil and encourage decomposition of organic matter rather than its accumulation. Conceptually, the assumption is reasonable but had little influence on the individual PGUs in their region. Manetta et al. 2023 found, instead, that proximity to

open water did not influence the depth of carbon accumulation. The trend was similar in this study.

Greater erosion potential impacts the longevity of carbon storage of the marsh edge along open water, especially in the wake of sea level rise. These considerations are not standard for every PGU but do suggest that the distribution and development of marsh soils are influenced by the pedogeomorphic factors that are location dependent. Each PGU's carbon accretion was influenced individually by its proximity to upland soils. As seen in figure 1.4, BB points were clustered at the lower end of the regression line revealing that there was no influence of distance to upland on the accretion of SOC stocks. In the Manetta (2023) companion study, back-barrier marshes also had no correlation in the relationship between distance to the nearest non-marsh soil and organic horizon thickness. LI points in this study were nearly linear, indicating that the distance to the nearest non-marsh soil could not be used to predict the 2 m SOC stock (kg/m^2) in this particular PGU. The rest of the PGUs exhibit a moderate correlation (R^2 : 0.477).

Observing Figure 1.4, the lack of correlation seen in the PGUs, except for distance to the nearest upland soil, is consistent with other literature (Miller et al. 2022; Aguilos et al. 2021). In Miller et al. 2022, North Carolina fringe marshes that increased in the landward direction often had a greater supply of organic carbon from decomposing leaf litter and grasses from the adjacent upland. In addition, distance from open water can correlate to the total organic carbon both in the vegetative biomass and soil, which was equated to multiple factors. Factors included production and decomposition dynamics, interruption of humus accumulation, soil microorganism activity, distance to open water, and others (Aguilos et al. 2021).

Carbon Pools and Regional Extent Across PGUs

Carbon storage rate is a function of both carbon burial within a coastal habitat's sediments and the accumulation of organic matter at the surface of soils (McLeod et al. 2011). When comparing the organic matter depth for PGUs (Fig.1.2), TC was excluded due to a lack of cumulative surface O horizons. TC marshes are high energy environments that limit the formation of organic horizons at the surface. Tidal creek ecosystems are highly productive in terms of biomass production and recycling (Sanger et al. 2016) but are vulnerable to degradation due to rising sea levels eroding stored sediments (Magolan et al. 2020). This limits organic matter accumulation in TCs, however, their SOC pools were greater than other high-energy mineral tidal marsh environments like BBs (Table 1.3 & 1.4). BB marshes undergo episodic erosion and deposition cycles from storm events, where SOC can accumulate before being eroded or buried by overwash events (Rossi et al. 2019). Despite its inability to accumulate more short-term stores of carbon, mineral TC soils had the highest regional carbon storage of all the PGUs (Table 1.3 & 1.4) at 66,088 Gg for 2 m, due to its widespread distribution (209,140 ha) in the Southeast.

Carbon burial within marsh soils is not the only indicator of carbon storage. The correlation between the 2 m SOC pools and the cumulative depth of organic soil horizons for each pedon (Fig.1.5, R^2 : 0.847) shows that the carbon accreted on the surface significantly influences SOC pools in coastal environments. The SW and LI PGUs were most influenced by the increases in depth of their surface O horizons. On the other hand, BB marshes had an overall low SOC pool and showed no significant influence from increases in surface O horizon depths, and yet had the largest proportion of SOC in its upper 1 meter (Table 1.2). This data suggests that marshes in lower energy

estuarine environments require uninterrupted, long-term organic matter accumulation to store carbon within soils.

Estimates of the regional spatial distribution of SOC within tidal marshes (Table 1.4) are consistent with other studies. One study determined that 461,996 ha, within the floodplains of the southeast region of the United States contained 97,900 Gg C when sampling to 2 m (Ricker et al. 2015). The spatial extent within this study was smaller by approximately half, 272,255 ha, but tidal marshes contained comparable carbon storage, 94,272 Gg to those of regional floodplains. In other literature, researchers compiled data from multiple different studies and estimated that across 17,454 data points in 29 different countries, the average stock of SOC in the top 1 m of tidal marsh soil was 231 Mg/ha in 2023 (Maxwell et al. 2023) and 268.4 Mg/ha to 1 m across 3710 unique locations worldwide in 2024 (Maxwell et al. 2024). In comparison to Table 1.3 in this study, the estimations were similar, with an average of 234.8 Mg/ha to 1 m across 51 sampled sites (Table 1.3; Table 1.1). It is worth noting that Maxwell et al. 2024 found that the relationship between total organic carbon and bulk densities in soil profiles is what controls most of the variability in SOC densities, and the deeper the profile is sampled the more stable it becomes. When making estimations on carbon stores, understanding soil morphological horizons and making accurate descriptions of their depths would be imperative since marsh SOC pools are driven by their cumulative depth of O and mucky A horizons (for more information, see Appendix B).

Data is available on the distribution of blue carbon, but the models used to calculate the estimations do not account for the variability existing across PGUs and varying climates. For example, blue carbon is estimated to store 10-24 Pg of carbon in the upper meter of the soil profile (Duarte et al. 2013), however, the storage rate is

unpredictable since the factors that encourage accretion will vary based on the location and scale (Noordwijk et al. 2023). Ideally, tidal marshes should be separated based on geomorphic location and individually characterized by carbon storage potential to account for the variation across different ecosystem types.

Conclusion

Past data of blue SOC pools fails to capture the full storage potential in tidal marsh ecosystems along the Southeast and Mid-Atlantic coast. To better understand the extent, this study reexamined the classification of mapped tidal marsh soils based on discrete PGUs. The PGUs reflected the general trends of soil series but differed at the subgroup level, based on characteristics such as organic matter depth and soil sulfidic chemistry. Regional companion studies, such as those completed by Manetta (2023) and Kim (2022) have significantly improved our collective understanding of blue carbon distribution and development in different tidal marsh environments along the Atlantic coast. In this study, the only significant landscape factor that had an influence on the development of SOC pools was the distance to the nearest non-marsh soil, whereas the PGUs themselves were most important for predicting significant differences in marsh SOC pools.

Among common tidal PGUs there were significant differences in how they stored carbon. Some PGUs had a large proportion of their carbon storage related to their accreted organic matter on the surface (LI and SW), whereas more high energy PGUs had relatively low carbon proportions overall but had a large regional extent (BB and TC). This comes as no surprise considering the diversity of tidal marsh soils across the Southeast. Data from this study reveals that there are different ways that carbon can be stored within tidal marsh soils and that the factors that influence that storage will depend

on site-specific pedogeomorphic factors. Data collected in this study will further our understanding of tidal marsh SOC pools and help regional modelling efforts to quantify their distribution and overall importance to the global carbon cycle.

CHAPTER 2: Carbon Accretion and Salinization of Abandoned Agricultural Fields along the North Carolina Coastline

Introduction

Global warming has induced multiple factors that contribute to saltwater intrusion along coastlines worldwide, the progression of which has altered the physical and chemical properties of soils (Brinson et al. 1985; Tulley et al. 2019). The most notable factor is global sea level rise (SLR), currently predicted to increase in the southeast United States at a rate of 0.36 - 0.43 m by 2050 (Sweet et al. 2022). The onset of SLR erodes coastlines allowing saline water to push further into freshwater environments (Gedan et al. 2019). Many areas are seeing increased rates of relative SLR due to land subsidence since the last glaciation period (Dixon et al. 2006; Mazzotti et al. 2009; Miller et al. 2021; Ohenhen et al. 2023; Riggs et al. 2003; Shirzaei et al. 2018). An isostatic rebound has caused areas of the Atlantic Coastal Plain to subside, putting their coastal ecosystems at a heightened risk of damage due to erosion and saltwater intrusion (Kirwan et al. 2013). Higher mean global temperatures have also increased the frequency and intensity of storm surges along coastlines (Knutson 2024). Larger, more energized surges push significant volumes of saltwater inland and, in tandem with SLR, accelerate salinization of freshwater environments (Riggs et al. 2003; Tully et al. 2019). Relict drainage canals from prior anthropogenic modifications have exacerbated surge damage in some areas, providing a channelized flow path for saltwater intrusion into freshwater environments (Bhattachan et al. 2018).

Saltwater intrusion fundamentally changes the physical and chemical properties of soils over time (Hebert et al. 2015). Saline and brackish waters contain significant amounts of dissolved salts, as well as other nutrients such as Ca^{2+} , Mg^{+} , K^{+} , and sulfate

ions. The introduction of these nutrients into soils increases the ionic strength of the soil solution and induces alkalization and sulfidization (Tully et al. 2019). Saltwater contains both sodium and exchangeable salts, and sodium ions at high concentrations replace other ions, such as calcium, on exchange sites (Amézqueta, 1998; Bronick et al. 2005). As a result, the structure of the soil pedis is altered, causing clay particles to disperse and settle into dense layers, instead of aggregating into distinct pedis with pore spaces (So, 1993). With frequent saline water inundation, H^+ ions are replaced by Na^+ on exchange sites after the salt ions are hydrolyzed (Breeman et al. 1983; Buol et al. 2011). Displaced H^+ ion weathers out of solution, lowering soil acidity thus alkalizing soils. (Breeman et al. 1983; Buol et al. 2011; Hussein et al. 2001).

As a result of anthropogenic landscape modifications and shifts in global weather patterns, overland flooding is often inconsistent and there are periodic shifts in alkalinity and sulfidation in coastal soils (Tulley et al. 2019). Freshwater inputs from precipitation can flush saltwater out of ecosystems for a time, lowering the ionic strength back to its prior state (Herbert et al. 2015; Tully et al. 2019). However, if sufficient sulfate ions and Na^+ or Ca^{2+} are retained with frequent saltwater inputs, ecosystems begin to transition to more salinized states (Tully et al. 2019). In response, freshwater vegetation migrates inland as soils become more salinized and salt-tolerant species begin out-competing freshwater species for resources (Anderson et al. 2021; Batzer et al. 2014; Riggs et al. 2003). If freshwater species are unable to migrate further inland, they are vulnerable to degradation via salt and flood stress (Desantis et al. 2007). With anthropogenic development in coastal areas, many wetlands are unable to escape shoreline erosion (Thorne et al. 2018) and must accrete vertically to survive SLR (Lovelock et al. 2020). Thus, SLR causes significant tree mortality in many freshwater wetland forests, leaving

behind stands of dead trees in the newly saline environments (Ury et al. 2021). Consistent exposure to salt and flood stressors hinders forest regeneration in the wake of storm and drought events, further exacerbating their gradual decline (Desantis et al. 2007). As salt tolerant vegetation invades declining forests, ghost forests develop as an ecotone between the migrating marshes and freshwater forests (Ury et al. 2021). The inundation from saltwater intrusion permits a reducing environment in these soils that slows decomposition and sequesters stores of soil carbon from litter and root additions (Krauss et al. 2018; Mcleod et al. 2011; Pierfelice et al. 2015). Shifts in salinity regulate landscape-scale plant composition (Batzer et al. 2014) and therefore alter net primary production as coastal ecosystems transition (Stagg et al. 2017).

Elevated saturation and salinity alter the carbon distribution within plants and induce shifts from above to belowground allocation (Li et al. 2023). Root productivity belowground can increase soil carbon accumulation (Krauss et al. 2018) due to increases in root turnover (Jolley 2009) in conjunction with higher nutrient contents within the soil matrix (Pierfelice et al. 2015). However, long-term increases in inundation and salinization can reduce the amount of organic carbon in soils by inducing osmotic stress in plants and lowering their productivity (Charles et al. 2019). Multiple studies of estuaries along the Atlantic Coastal Plain have indicated belowground carbon stocks (soil and roots) are greatest in mature ghost forest and tidal marsh ecosystems where herbaceous plants dominate (Krauss et al. 2018; Pierfelice et al. 2015). Conversely, the ecosystem aboveground carbon biomass is significantly reduced as salinization increases from freshwater forests to marshes (Krauss et al. 2018). An ecosystem comparison of ghost forests and healthy coastal forests found that further distance from open water strongly correlated to higher total plant and soil organic carbon (Aguilos et al. 2021).

The ghost forest ecotones, being the closest to open water in the Aguilos et al. study, were found to retain high above-ground biomass at first, which declined as salinization increased (Aguilos et al. 2021). Increased brackish water flooding makes the soil anaerobic and slows decomposition of organic carbon allowing for its accumulation, yet the same process introduces elevated salinity levels that lowers forest biomass, and subsequently the storage of organic carbon, with prolonged exposure (Charles et al. 2019). Loss of productivity and carbon stores will depend on the rate of SLR, which varies based on region (Sweet et al. 2022).

Within the Albemarle Pamlico Estuary system (APES) of North Carolina, land management practices have modified wetlands for agricultural purposes altering the ecosystem functions in this region. The area was historically an extensive network of wetlands, estimated to have covered 53% of the coastal land area (Bhattachan et al. 2018). Regional estimates on wetland drainage are that 202,345 ha of lower Atlantic Coastal Plain wetlands were drained by the 1920s (Richardson, 1983). Drainage canals were used to lower the water table which oxygenated soils and caused the mineralization and subsidence of many organic soils (Lilly 1981; Richardson 1983). Originally, the hydrologic flow paths into regional tidal marshes diffused gradually across the landscape, but with implemented drain lines the flow of water was channelized (Bhattachan et al. 2018). Freshwater is streamlined out of agricultural fields through drainage systems, and saltwater can be preferentially transmitted up the canals and ditches, depositing exchangeable salts further inland (Bhattachan et al. 2018). Despite best efforts, salinization could not be mitigated in regional farm fields, and many were left fallow as a result (Lynch et al. 1982). Land abandonment has progressed since the early 1900s from those fields closest to the brackish water source (Albemarle and

Pamlico Sounds) then inland over time. Abandoned agricultural land has been colonized by forest or marsh vegetation quickly, which does have implications for encouraging the development of new wetlands (Lynch et al. 1982). However, wetland restoration is highly variable and depends on the wetland's geomorphic position and acreage, both of which contribute to hydrologic processes, nutrient retention, and success of restoration (Ardón et al. 2010; Jackson et al. 2010; Moreno-Mateos et al. 2012).

Restored coastal wetlands with disturbed hydrologic processes like drainage ditches express lower rates of biogeochemical reactions than natural wetlands, specifically lower carbon and nitrogen stocks (Craft et al. 2003; Moreno-Mateos et al. 2012). Differences in nutrient storage have been attributed to restoration site age, frequency of inundation, sedimentation rates, and soil mineral composition (Craft et al. 2003). If sites are left undisturbed, restored wetlands can increase nutrient pools, organic matter stocks, and vegetative species richness and density as years progress (Craft et al. 2003; Moreno-Mateos et al. 2012). Within the APES region, abandoned agricultural fields have been left undisturbed for decades, allowing for some natural wetland regeneration to occur (Ardón et al. 2010). The new forested, ghost forest, and marsh habitats also function as physical buffers for agricultural fields further inland, dissipating energy from strong winds or waves during storm surges (Riggs et al. 2003). The ability to buffer storms is related to the health of wetland vegetation and landscape elevation relative to sea level, which is a function of soil accretion from mineral sedimentation or accumulation of organic matter based on geomorphology (Elsley-Quirk et al. 2022; Mcleod et al. 2011; Ury et al. 2021; Riggs et al. 2003). Within the APES there are infrequent mineral sediment inputs and land accretion is driven by soil organic matter accumulation and geomorphology (Riggs et al. 2003). The ability to accrete and store

soil carbon not only raises local elevation, but also provides mitigation to global warming through carbon sequestration (McLeod et al. 2011). Coastal wetland elevation will typically align with sea level height, however as the ocean continues to rise and outpace the elevation of regional shorelines, many coastal wetlands are being submerged (Gorczyński et al. 2024; Ury et al. 2021).

Currently there is great uncertainty regarding soil carbon sequestration and net accretion rates within abandoned coastal farmlands. Quantification of soil physical and chemical properties within these anthropogenically modified landscapes can ultimately improve our soil mapping concepts and provide insights regarding shifts in dynamic soil properties that are occurring due to saltwater intrusion. Ideally, these abandoned locations transitioning back to wetlands would be accumulating carbon in their soils. Therefore, this study's primary goals were to i) quantify carbon storage and accretion rates in abandoned areas to determine if soils were keeping pace with SLR and ii) compare rates of carbon accumulation based on ecosystem (forest, ghost forest, marsh) and soil survey (mapped soil series) approaches to assess the merits of these common methods of study.

Methods

Study Site

The study sites were located on the Pamlico morphostratigraphic unit on the lower Atlantic Coastal Plain within the APES. The region has a humid, subtropical climate and most topography is less than 6 m above sea level (HCP 2008). Rainfall is consistent throughout the year, with an average precipitation of approximately 127 cm annually (HCP, 2008; Lilly 1981). Historically, the region consisted of forest floodplains, mineral flats, marshes, and pocosins (Richardson 1983). Naturally occurring peat fires, where flames smolder for long periods of time would occur during dry

seasons and reduce the thickness of accumulated soil organic matter (Richardson 1983). However, due to high rainfall, low and flat topography, as well as significant distance between streams, organic matter could rapidly accumulate following disturbances (Lilly 1981). Beginning in the 1920s, large areas were anthropogenically burned to reduce deep organic deposits and expose the mineral soil surface underneath (Lilly 1981). These soils were then ditched to increase aeration for agricultural activities, but were highly acidic which decreased nutrient availability and required liming to increase crop productivity (Lilly 1981). Over time, saltwater intrusion progressed despite best efforts to mitigate the issue, and the impact was loss of crop productivity along the margins of the brackish shorelines of the Pamlico Sound (Lynch et al. 1982). Marginal farm fields were abandoned over time and allowed to grow in native forest or marsh vegetation with the oldest abandoned fields being closest to the current open water shorelines. Saltwater intrusion has continued within abandoned farm fields due to open relic ditch systems that transmit saline waters into the buffer zones. Continued salinization has created a sequence of ecosystems from inland to the shoreline that follows the pattern of increasing soil salinity from forest, ghost forest, and tidal marsh (Brinson et al. 1985; Ury et al. 2021). Currently, the major uses of these buffer areas are primarily for wildlife habitat and hunting, with no active wetland management practices being employed.

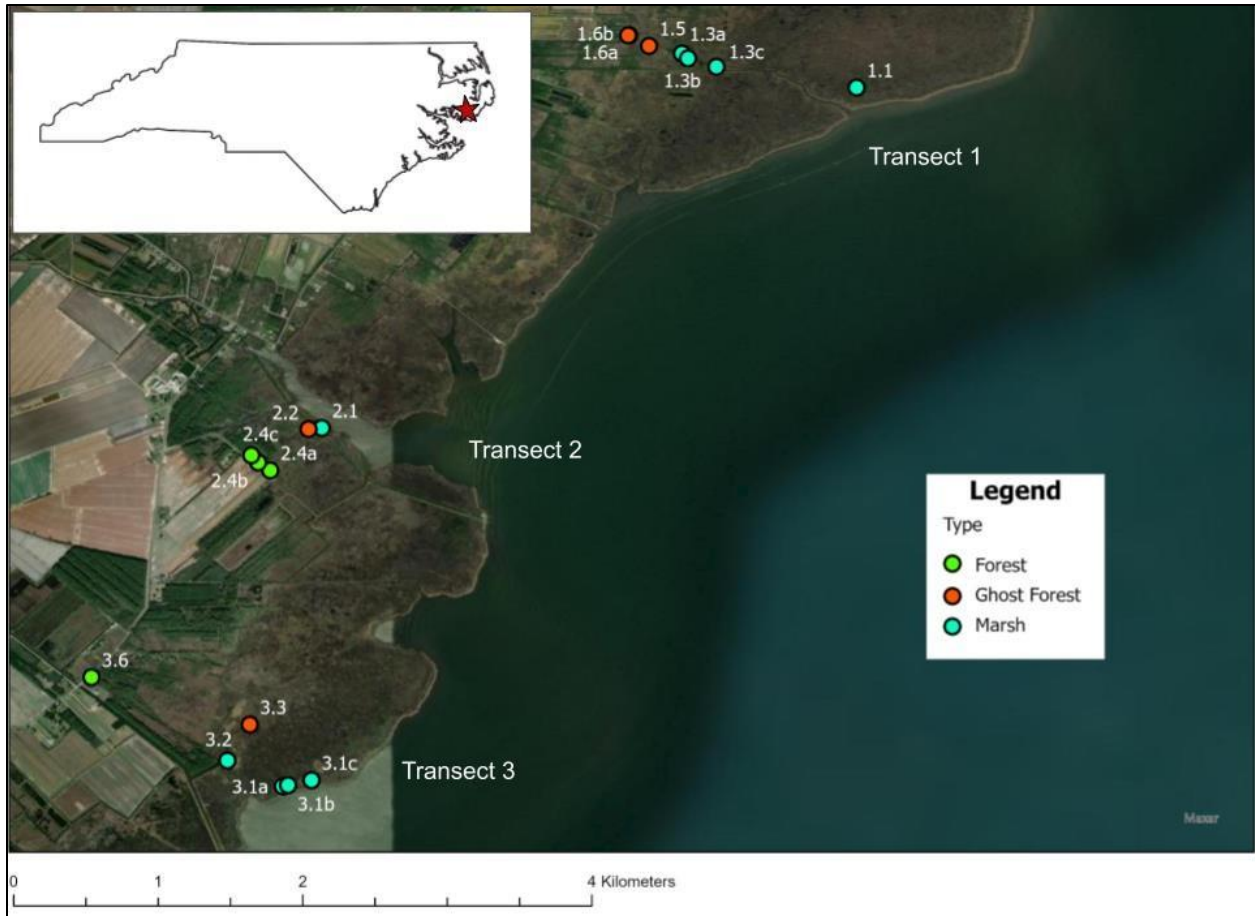


Figure 2.1: Map of all sampling locations and corresponding ecosystems within Hyde County, NC.

To study these buffer sequences of abandoned farm fields, we established three research transects that encompassed the forest, ghost forest, and marsh transition. Within transects, sampling sites were selected based on visual observation of ecosystem type (i.e. forest, ghost forest, marsh) and mapped soil series. Geospatial analysis through ArcGIS Pro and Google Earth Pro was used to identify transects that exhibited the transition from forest, ghost forest, to marsh using vegetation. Forests were identified as predominantly green and forested in recent (2023) aerial imagery. Sites were dominated by loblolly pines (*Pinus taeda* L.) which had naturally germinated or been planted in the past 20 years, as well as wax myrtle (*Myrica cerifera* (L.) Small). Ghost forests were

determined based on visual location as an ecotone between identified forest and marsh sites through (2023) aerial imagery and had understory marsh vegetation with sparse live tree cover. Sites were dominated by wax myrtle shrubs, stunted Atlantic white cedar (*Chamaecyparis thyoides* (L.) Britton, Sterns & Poggenb.) saplings and emergent species like invasive common reed (*Phragmites australis* (Cav.) Trin. ex Steud.) and native sawgrass (*Cladium jamaicense* Crantz) among standing dead tree stands. Marshes were identified based on proximity to the open sound as well as the visual appearance of black needle rush (*Juncus roemerianus* Scheele) in recent (2023) aerial imagery. (For more information, see Appendix B, Table B-B)

The three representative soil series mapped in 1991 for this study were Brookman, Backbay, and Delway with each series roughly corresponding to forest, ghost forest, and marsh sites, respectively. Within the study area, Brookman (fine, mixed, superactive, thermic Umbric Endoaqualfs) covered approximately 335 hectares (ha) and is classified as a very poorly drained Alfisol with a dark mineral surface (umbric epipedon with <20 cm cumulative O horizon thickness). Backbay (fine-loamy, mixed, active, nonacid, thermic Histic Humaquepts) covers 864 ha, classified as a very poorly drained Inceptisol with a histic epipedon (mineral soils with 20-40 cm of cumulative O horizons), mapped in oligohaline brackish coastal marshes. Finally, the Delway series (loamy, mixed, euic, thermic Terric Haplosaprists) covers 244 ha and is classified as a very poorly drained shallow sapric Histosol (organic soils with >40 to <130 cm of cumulative O horizons). Delway soils are mapped in mesohaline or polyhaline brackish marsh habitats and contain sulfidic materials (Soil Survey Staff, 2022; Soil Survey Staff, 2019).

Field Data Collection

In the field, GPS coordinates were recorded (± 3 m accuracy) of each sample point. At each transect, water data was collected using a portable YSI Pro Plus meter at the closest source of open water (see Appendix B, Table B-A). All transects fall within the same average salinity range of mesohaline (<5.0 to <18.0 ppt) with average water pH of 7.4. The 17 sampled pedons had descriptions made which included depth, texture or Von Post Humification scale (Von Post et al. 1926), fluidity, Munsell color, coarse fragments, hydrogen sulfide odor, reaction to peroxide, and unrubbed vs. rubbed fiber content using standard methods (Schoeneberger et al. 2012). Sampling was done to 2 meters for all 17 pedons either on foot or from the deck of an airboat. Organic soil pedons were sampled using a Macauley peat auger until underlying mineral sediment was reached, then sampling was completed using a gasoline vibracore to collect the deeper mineral horizons (>100 cm). Mineral soil pedons were sampled using a hand auger and gasoline powered REDI Boss Hammer to a total depth of 2 m (See Appendix C for detailed descriptions).

Bulk density samples of known volume were collected using multiple methods depending on the horizon sample characteristics. This included standard methods (Blake and Hartge, 1986; Stolt et al. 2017) such as segmented 5 cm Macaulay auger half-cores, 5x5 cm metal rings, 10 cm³ syringe cores from vibracores, or cutting “brownie” cubes of known volume out of fibrous surface peat horizons and measuring the length, width, and height using calipers.

Laboratory Analysis

Analyses were done per soil horizon to measure chemical and diagnostic properties for soil classification. Equal parts soil and deionized (DI) water were combined to create a soil:water ratio, used to measure 1:1 initial pH, and 1:5 electrical

conductivity (EC) by volume for each horizon. For organic soil horizons, 1:2 calcium chloride (CaCl_2) pH was also quantified to determine Histosol taxonomic reaction classes. Once initial 1:1 pH measurements were completed, samples were stored at room temperature under moist, aerobic conditions for a 16week incubation period to identify hyposulfidic and hyper-sulfidic materials (Soil Survey Staff, 2022). The difference between time zero and week 16 soil pH (delta pH) was used to determine sulfide classification, with a drop of at least 1 pH unit and final pH >4.00 being hyposulfidic and a drop of pH of at least 1 pH unit to a final pH ≤ 4.00 being classified as hyper-sulfidic.

Soil total carbon and nitrogen concentrations were quantified using thermal combustion on a LECO 928 CN analyzer (LECO Corporation St. Joseph, Michigan, USA). Mineral horizon texture was quantified using the hydrometer method and wet sieving sand fractions (Gee and Bauder, 1986). Horizons identified as being carbon-rich, either classified as O or mucky mineral horizons (all $>5\%$ C concentration), were pretreated with 30% hydrogen peroxide to remove excess organic matter (OM) prior to texture determination. Bulk density was calculated in the lab using the volume collected in the field and mass of oven-dry samples at 105°C as outlined by Blake and Hartge, 1986. After laboratory analyses, soil morphology and the laboratory data were used to determine pedon classification based on the Keys to Soil Taxonomy, 13th edition (Soil Survey Staff, 2022) (See Appendix C).

Geospatial Data

ArcGIS Pro (3.1.3) is a geographical information system (GIS) software that was used to identify potential sample sites prior to field investigation and sampling. ArcGIS Pro was also used to quantify sample location landscape factors such as distance (m)

from open water, mean height above sea level (m), and calculate the normalized difference vegetation index (NDVI) between different ecosystem sites. Mean height above sea level was measured off a Digital Elevation Model (DEM) created from LiDAR data from the North Carolina Spatial Download Database (“NC Spatial Data Download,” n.d.). LAS files were converted to multipoint rasters, singlepart, then a ‘Z’, or elevation, factor was calculated in the attribute table. The North American Vertical Datum of 1988 (NAVD 88) was the geodetic vertical datum (U.S. feet) used in this study, which were converted to meters (m) for calculations. NDVI was estimated using satellite imagery from PlanetScope satellites.

Calculations

Calculations were made to determine the net rate of vertical soil accretion and soil C sequestration for each study pedon to make comparisons between ecosystems and mapped soil series. Horizons above the morphologically identified plow horizon (Ap) were assumed to have accumulated since the sites were last in agricultural production. Total vertical depths (cm) of that upper proportion of soil materials were then divided by the estimated years since the field site was abandoned.

$$\text{Depth above Ap (cm)} / \text{years since abandonment (yrs)} = \text{Rate of net accretion (cm/yr)}$$

Similarly, carbon sequestration rates were calculated using SOC pools (kg/m²) above plow layers and the years since abandonment.

$$\text{SOC pool above Ap (kg/m}^2\text{)} / \text{years since abandonment (yrs)} =$$

$$\text{Net rate of sequestration (kg C/ m}^2\text{/yr)}$$

Ages of abandonment estimated for each pedon site were made using either records provided by the landowners (Dawson and Earl Pugh, personal communications) or by comparisons using aerial imagery over time (1938 to 2023) in Google Earth (Map

data: Google, DigitalGlobe) and from the U.S. Department of Agriculture Photograph Collection (1938) within the State Archives of North Carolina. Each pedon location was assigned an agricultural abandonment year and all field ages were calculated until 2023, when soils were sampled in this study. In some cases, archived aerial photos from 1938 were also used to date progressive saltwater intrusion through the observed transition of vegetation between ecosystems (forest, ghost forest, marsh) over the last century. Estimated ages of abandonment ranged from 21 years in recently converted forests to 153 years in tidal marsh areas of the transects.

Statistical Analyses

To conduct statistical analyses, JMP (pro 17) and SigmaPlot (14.5) were used to analyze and visualize data. An attempt was made to utilize 2-way ANOVA to determine interaction effects between mapped series and ecosystems. However, the two mapping concepts are covariates, where the soil series mapped were based on the type of ecosystem that had been visually observed (For more information, see Appendix A, Figure 7). Therefore, one-way ANOVA with Tukey's HSD test was used to compare soil horizon ($n = 139$) and 2 m depth pedon ($n = 17$) means across groupings of either soil series mapped (Brookman, Backbay, Delway) and ecosystems identified (forest, ghost forest, marsh). Factors compared include initial 1:1 pH, delta pH, 1:5 EC, bulk density, C:N, depth of accreted organic matter (cm), and SOC pools. Mean coefficient of variations (CVs) were calculated across all soil characteristics to assess which mapping concept pair had the greatest variability. When assessing the CVs, calculations are interpreted as percentages so the lower the percentage between mapping concepts, the lower the variability of data from the mean. CV values were generally greater than 30%, indicating there was high dispersion around the mean (Brown, 1998). Mean 2 meter

SOC pools from all abandoned farm fields in this study ($n = 17$) were also compared to active farms fields ($n = 12$, data from Julia Janson, Dissertation in Preparation, 2025) and unaltered reference tidal marshes within Hyde County ($n = 17$, data from Chapter 1 and Gorczynski, 2022). Data collection from these studies followed the same field and laboratory sampling protocols outlined for this research, making for valid comparisons along a gradient of human alteration. Active farm fields are regarded as the “time zero” state the abandoned farm fields would have been in before they began accreting organic matter on top of the agricultural plow layer. Over time the ecosystem conditions should change sufficiently within abandoned farm fields to resemble unaltered tidal marsh sites in the region. The unaltered marsh was sampled within Swanquarter National Wildlife Refuge and was used as reference for how much organic C could be accreted in a stable marsh condition.

Spearman’s Correlation matrices were used to evaluate the influence distance to open water and elevation had on the formation and characteristics of the soils in that area. Characteristics included 1:5 EC, initial 1:1 pH, C:N ratios, and bulk density at a pedon scale. Linear and polynomial regressions were created to quantify the relationships between soil factors across salinity gradients derived from measured 1:5 EC (dS/m). Regressions used the horizon measurements to one meter in each pedon, because it is assumed that the overwash of brackish waters on the surface is the primary driver causing the shifts in salinity in these soils. All statistical analyses were considered significant with $\alpha = 0.05$.

Results

Mapping Concepts: Ecosystems vs. Soil Series

Soil horizon data were compiled from field classification and laboratory analysis for comparisons. Results indicate that there is statistical significance, or difference, across

group means in pH, delta pH, EC, and the depth of accreted organic matter on the surface. Between ecosystems and mapped soil series, both were statistically significant (Table 2.1). Out of the three pairs, the forest ecosystem and Brookman soil series concepts generally had the greatest variability in each of the measured soil characteristics (Table 2.1).

Table 2.1. Mean horizon values with Coefficient of Variation (CV) as a percent in parenthesis. Means with different capital letters by column are statistically different ($p < 0.05$) according to one-way ANOVA and Tukey's HSD test.

Mapping Concept	n	1:1 pH	Delta pH	1:5 EC (dS/m)	Bulk Density (g/cm³)	C (%)	C:N Ratio
Forest	32	4.99 (13) C	0.05 (862) B	0.82 (44) C	1.40 (39) A	3.95 (209) A	12.11 (52) A
Ghost Forest	34	6.80 (7) B	1.35 (94) A	2.89 (39) B	1.07 (55) A	5.03 (173) A	14.11 (33) A
Marsh	73	7.25 (6) A	1.58 (75) A	4.48 (43) A	1.16 (54) A	4.53 (155) A	12.48 (38) A
Brookman	59	5.54 (17) B	0.39 (165) C	1.61 (68) B	1.29 (100) A	4.51 (195) A	12.74 (45) A
Backbay	22	7.20 (5) A	2.01 (62) B	4.03 (41) A	1.07 (54) A	5.11 (148) A	13.50 (35) A
Delway	58	7.32 (7) A	1.37 (92) A	5.08 (40) A	1.21 (57) A	3.65 (150) A	11.82 (38) A

Carbon data acquired from laboratory analyses were used to determine the means for depth of new organic matter accreting over prior Ap horizons (plowed mineral surface), pools of SOC (kg/m²), rate of accumulation over Ap horizons, and rate of sequestration (Table 2.2). Pedon comparisons only showed significant differences ($p < 0.05$) in mean depth of accretion, with the highest values being found in the marshes and Backbay soil series. All other soil carbon metrics were not significantly different among ecosystems and mapped soil series.

Table 2.2. Mean (\pm standard error) pedon comparisons based on ecosystem or soil mapping concepts. Means with different letters are significantly different ($p < 0.05$) according to One-Way ANOVA and Tukey's HSD tests.

Ecosystem	n	Depth of Accretion (cm)	Abandonment			C Sequestration (kg C /m ² /yr)
			SOC Pool (2 m, kg/m ²)	Time (yrs)	Accretion Rate (cm/yr)	
Forest	4	7.0 \pm 12 B	24.0 \pm 6.2 A	31 \pm 12 C	0.30 \pm 0.11 A	0.15 \pm 0.05 A
Ghost Forest	4	38 \pm 12 AB	19.7 \pm 6.2 A	93 \pm 12 B	0.39 \pm 0.11 A	0.10 \pm 0.05 A
Marsh	9	47 \pm 8 A	26.7 \pm 4.1 A	131 \pm 8 A	0.37 \pm 0.07 A	0.12 \pm 0.03 A
Soil Series						
Brookman	7	13 \pm 8 B	19.7 \pm 3.9 A	57 \pm 10 B	0.28 \pm 0.07 A	0.12 \pm 0.03 A
Backbay	6	58 \pm 8 A	32.2 \pm 4.2 A	111 \pm 11 A	0.52 \pm 0.07 A	0.16 \pm 0.03 A
Delway	4	41 \pm 10 AB	18.0 \pm 5.1 A	153 \pm 13 A	0.27 \pm 0.09 A	0.07 \pm 0.04 A
Grand Means	17	36 \pm 7	23.5 \pm 2.9	98 \pm 11	0.36 \pm 0.05	0.12 \pm 0.02

Distinguishing Soil Factors Between Ecosystems

Ecosystem sites were identified visually and mean NDVI was calculated for each ecosystem region for each season over 2023. Means were significantly different when compared across ecosystems ($p < 0.0001$) and corresponded to the gradient of salinity moving inland. Between ecosystems, the average NDVI ranged from 0.66 for forest, 0.51 for ghost forest, and 0.43 for marsh sites indicating relatively healthy dense cover within the forest ecosystems relative to the others evaluated (Table 2.3).

Table 2.3. Mean annual NDVI values (\pm standard error) per ecosystem. One-way ANOVA comparison of ecosystem type and NDVI was statistically significant ($p < 0.0001$) according to Tukey's HSD.

Ecosystem Sampled	Min NDVI	Max NDVI	Mean NDVI
Forest	0.38 \pm 0.03 A	0.79 \pm 0.02 A	0.66 \pm 0.03 A
Ghost Forest	0.33 \pm 0.02 A	0.73 \pm 0.02 A	0.50 \pm 0.02 B
Marsh	-0.16 \pm 0.02 B	0.63 \pm 0.02 A	0.43 \pm 0.02 B

Site characteristics were also examined through Spearman's Correlation matrix (ρ) to determine monotonic correlations between soil characteristics and site conditions. To compare mapping concepts, distance from open water (m) was the primary focus, or comparative standard, when determining monotonic relationships across other soil characteristics across sampled pedons (n: 17). In Spearman's Correlation matrix significant (ρ) positive correlations were found between distance to open water, SOC pools 2 m (ρ : 0.08) and C:N ratio (ρ : 0.26).

Sites further from the brackish open water had increases in their SOC pools and C:N ratios. Significant negative correlations were found between distance from open water, 1:5 EC (ρ : 0.83) and 1:1 pH (ρ : -0.74) as well. This indicates that sites further from the open water had lower soil EC and pH values. Elevation was not statistically different across all ecosystems (p = 0.24) and could not be used to make meaningful interpretations of collected soil data.

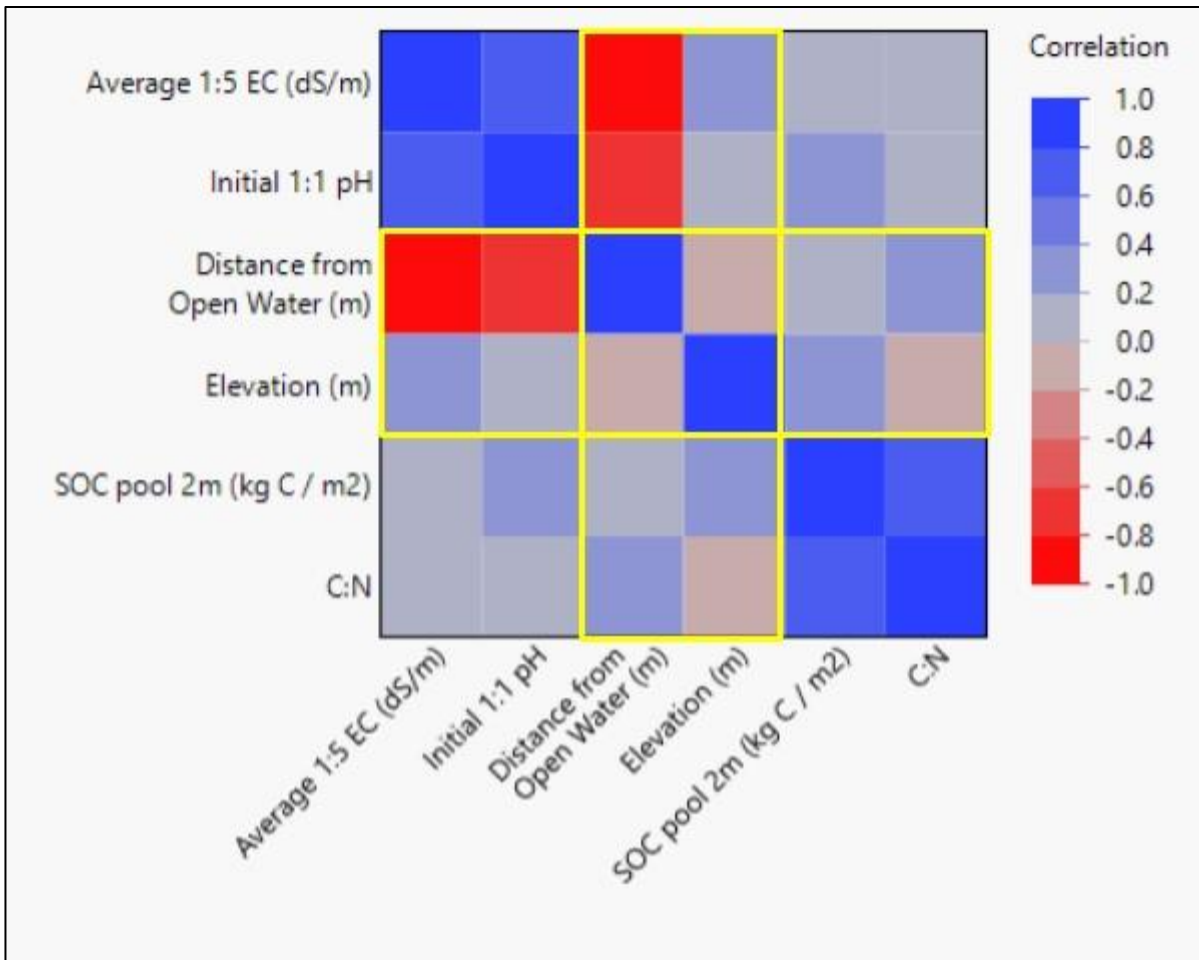


Fig 2.2. Color Map of Spearman's (ρ) for environmental factors related to soil formation and carbon storage. Red hued squares are negatively correlated (-1) and blue hued squares are positively correlated (+1). The more positive the correlation, the higher the influence on a given variable.

Soil characteristics were regressed across the salinity gradient to observe effects on the chemical and physical characteristics of the sampled soils at the horizon scale. The measured 1:5 EC (dS/m) to 1 meter was used to represent the salinity gradient across the different ecosystem types (Figure 3).

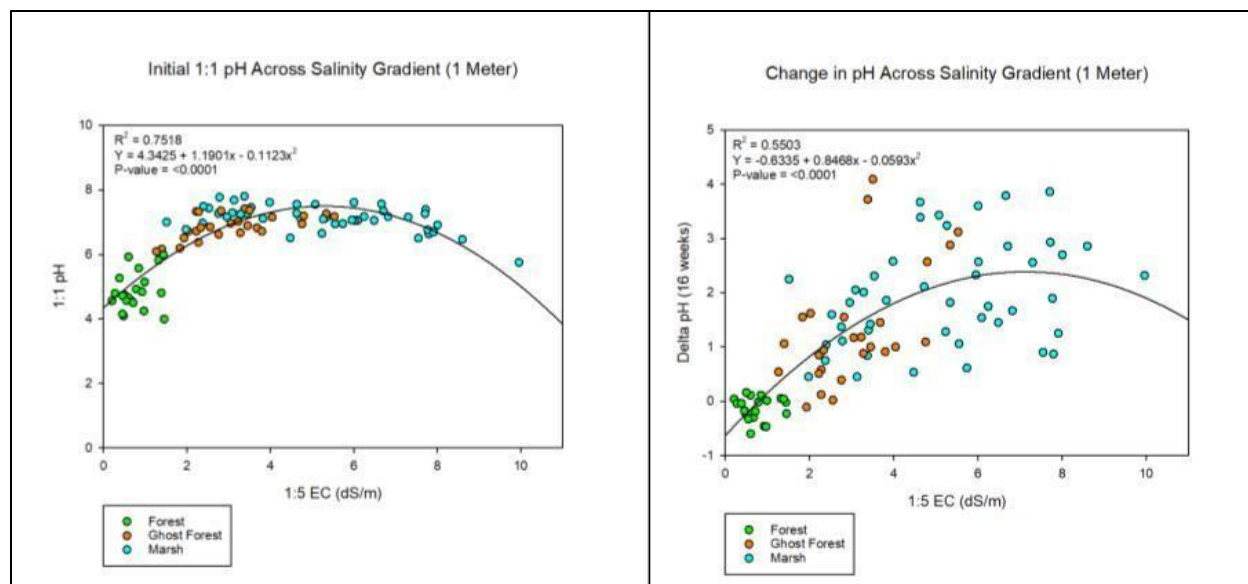


Figure 2.3. Regressions illustrating relationships between 1:1 pH and delta pH (sulfide content) regressed against 1:5 EC (dS/m) to evaluate changes in intrinsic soil properties as soil salinization progresses across abandoned farm fields.

The 1:1 pH across salinity gradients had a highly significant polynomial relationship ($p < 0.001$, $R^2: 0.75$). Initial 1:1 pH measurements increased with 1:5 EC (dS/m) until pH 8. Between ecosystems, the forest (green) points congregate at the base of the curve, showing no interaction between 1:1 pH and 1:5 EC, but 1:1 pH increased through ghost forest and marsh soils, until reaching a plateau before pH 8. The change (Delta, Δ) in pH versus salinity gradient regression also illustrates significantly increasing ($p < 0.001$, $R^2: 0.55$) reduced soil sulfides (higher delta pH) as soil EC increases from forest to ghost forest, and marsh.

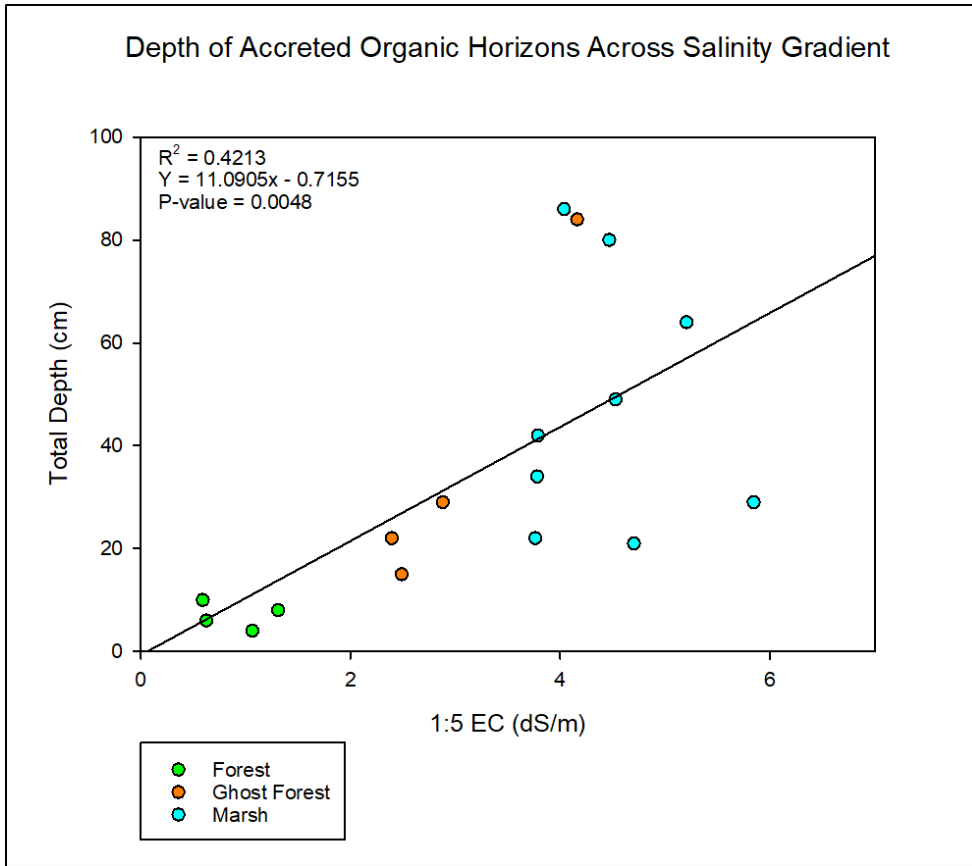


Figure 2.4. Linear regression showing depth of organic materials (cm) that had accumulated over the prior agricultural soil surface (Ap horizon) across a salinity gradient.

Increases in cumulative thickness of organic surface horizons were regressed across the salinity gradient of the abandoned farm fields (Figure 2.4). The regression had less of a relationship with EC than soil pH and delta pH did (R^2 : 0.4213, $P = 0.0048$) however, the general trend of increasing organic matter accretion across the ecosystem salinity gradient suggests elevation is increasing over time within abandoned farm fields. However, this data illustrates that less organic material has accumulated within abandoned fields relative to soil mapping concepts that predicted >40 cm of organic horizon thickness within marshes of the region.

Abandoned farm fields were further compared to active farm fields and established (unaltered) native marsh systems in the same geographic region of Hyde County, NC (Fig.

2.5). Comparisons showed that abandoned fields have numerically higher SOC pools compared to active fields but were significantly ($p > 0.05$) less than established marsh sites, suggesting that additional SOC can be stored in these systems over time. Mean soil C:N ratios showed a similar trend, with significantly ($p < 0.05$) lower C:N in active farm fields and abandoned fields compared to unaltered marsh ecosystems (23:1) in the region.

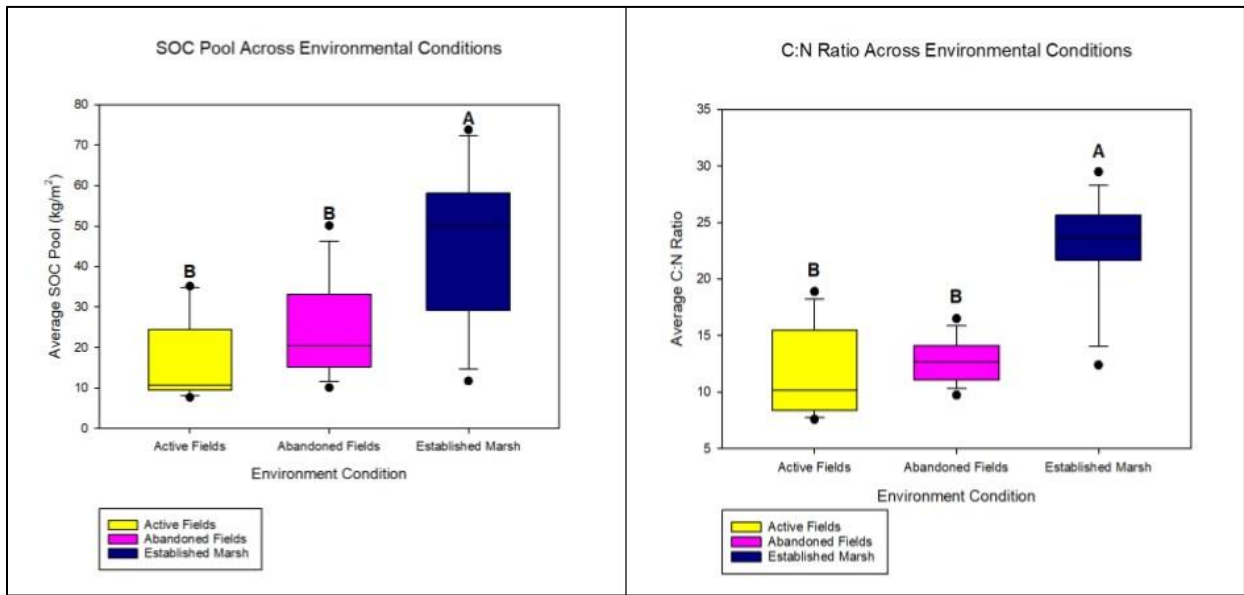


Figure 2.5. Comparison of SOC pools and C:N ratio means to 2 m depth among active farm fields, abandoned fields, and established tidal marshes of Hyde County, NC (Active Fields $n = 12$; Abandoned Fields $n = 17$; Established Marsh $n = 14$). Means with different capital letters are significantly different ($p < 0.05$) according to one-way ANOVA and Tukey's HSD tests.

Discussion

Mapping Concepts: Ecosystems vs. Soil Series

Soil surveys were completed by the NRCS to take inventory and provide land-use applications for priority areas in 95% of counties in the United States (Soil Survey Staff, 2019). For non-priority areas, such as salt marshes, ghost forests, or swamps, terrains are difficult to traverse and soil collection is challenging, so limited data was collected during initial mapping in the 1970s-1990s. Soil series were mapped based on

the gradient where forests transition to marshes as sites get closer to saline or brackish water sources. Soils were generally mapped in catena sequences based on cumulative depth of organic material at the surface from <20 to >40 cm going from inland forests outward towards the marsh shoreline (Soil Survey Staff, 2019). Our Soil classification after lab analyses and field investigation had minimal agreement with what had been mapped prior. Much of the discrepancies were from soils having more shallow organic matter compared to the mapping concepts of the wetlands evaluated. Between ecosystems and soil series, 24% of the classification matched its originally mapped series (n = 17). Out of the sites mapped as Brookman series, 3 of 7 sampled pedons matched mapped concepts; and in the forested areas of the APES region soils tend to have higher clay content (Daniels, et al. 1999), so it was reasonable that most of the sampled pedons were consistent with their mapped series. For areas mapped as Backbay series, none of the sampled pedons were classified as its denoted series (Histic Humaquepts), mainly due to insufficient cumulative organic matter thickness (20-40 cm predicted). Soils were also found to be highly sodic, indicated by an exchangeable sodium percentage (ESP) of >15% in the upper 100 cm of the soil profile (Soil survey staff, 2022). Thus, most of the pedons sampled in these areas were classified as sodic Entisols. Soils mapped as Backbay are expected to deepen in their organic matter depths closer to the shoreline, however relict drainage canals in these areas likely lower the water table, aerate the soils, and promote higher rates of C mineralization (Daniels et al. 1999; Krause et al. 2021; Lilly 1981; Xu et al. 2021). Finally, Delway series map units had 1 out of 4 classified pedons match the mapping concept (Terric Haplosaprists), with most of the discrepancies being insufficient cumulative depth of organic horizons (<40 cm thickness). For soils classified as Delway, a lack of organic matter is unexpected

(Daniels et al. 1999) because these sites that have been left undisturbed for nearly a century and the water table is nearly constant at the soil surface (peraquic conditions). Previous peat fires also likely influenced the degradation of the organic matter (Lily 1981; Poulter et al. 2006). Historically, fire was a management practice to subsidize the SOM, but natural ground fires still occurred frequently and could burn for months (Lily 1981). Drier soils are at a higher risk of burning which puts drained soils, such as the Delway soils, at a higher risk of losing carbon (Poulter et al. 2006). (For more information on changes in classification see Appendix C).

Ecosystem sites and soil series were statistically very similar, showing minimal differences in their CV values for soil properties (Table 2.1). There were generally higher CV values across the means in the soil data indicating overall higher variability in metrics taken from soil survey units (Brown, 1998). High rates of variability in field soil data studies are consistent with the dynamic nature of the sample sites. Frequent shifts in storm intensities, inconsistent precipitation rates, and modifications to surface hydrology affect the formation of soil characteristics in these environments (IPCC, 2013; Michener et al. 1997). Thus, environmental data such as pH, EC, and C:N ratios can fluctuate over time. Field investigations of wetlands formed within abandoned agricultural fields showed that past mapping (completed in 1991) was inconsistent with the condition of the environment currently, and most sites did not match the criteria for mapped soil series. For example, sites that had been classified as Brookman series forest sites had already begun to shift to ghost forest and had to be reclassified as a ghost forest ecosystem site. Other ghost forest locations had few remaining standing dead trees and had shifted to tidal marshes. Changes in vegetation can significantly influence rates of carbon sequestration (Aguilos et al. 2021; Brinson et al. 1985), which makes current

plant cover useful in predicting soil properties relative to outdated soil map units that have not been updated in decades.

Results from this study show carbon being accreted, but the annual rate of accretion was not statistically significant among any of the study ecosystems or soil types (Table 2.2). Soil data compared by ecosystem revealed that SOC pools did not vary by ecosystem or soil map unit, with an overall mean of 23.5 kg C/m². The Delway (marsh) series was predicted to have the highest rates of carbon development and storage due to its proximity to water and net primary production (McLeod et al. 2011). However, all study sites had significantly lower C:N ratios compared to unaltered marshes of the region (Figure 5), suggesting relict drainage ways may create periods of aerobic soil conditions and increased mineralization of stored SOC (Krause et al. 2021).

Comparisons between carbon pools and accretion rates across different studies showed similar results for the humid subtropical region (Adame et al. 2013; Xia et al. 2022). SOC pools were calculated to have a mean 17.70 kg C/m² to 1 m for marsh ecosystems (Adame et al. 2013), and SOC pools in coastal wetlands have been noted to range from 11.10 - 19.20 kg/m² to 1 meter (Xia et al. 2022). These values were slightly lower than the pools from this study, which ranged from approximately 16 - 26 kg/m² for 1 m SOC pools (Table 2.2). Humid subtropical climates have warmer annual temperatures and greater moisture levels, which encourages mineralization of SOC compared to cooler climates (Weintraub et al. 2003). Carbon is being stored in abandoned farm field buffers, but the rate at which it is being stored is of interest if these areas are to withstand SLR.

Sequestration rates in this study were slightly lower than other studies looking at modified and drained wetland systems in South Carolina which ranged from 0.10 - 0.25 kg C /m²/yr in management sites that were reflooded after abandonment, as compared to the 0.10 - 0.44 kg C /m²/yr rates in naturally tidal freshwater marshes (Drexler et al. 2013). Sites were disked, burned, and received nutrient applications to improve yield for rice fields in years prior and were actively managed through periodic flooding to maintain anaerobic soil conditions (Drexler et al. 2013). Sites in this study were drained for agriculture (Lilly 1981) before being abandoned, and the relict ditch lines were never filled, resulting in more aerated soils. Without consistent anaerobic conditions at the soil surface, microorganisms can decompose significantly more SOC entering the system and lowering the rate of net SOC sequestration in the abandoned fields (Krause et al. 2021; Xu et al. 2021).

The oxygenation of the abandoned fields is especially pronounced in Figure 2.5, showing just how low carbon is in this study. Based on the mean values of SOC pool and low C:N ratios, carbon accretion and storage in abandoned field sites is accumulating at a rate that is statistically similar to agricultural fields currently in production. Abandoned fields of this study should have similar soil characteristics compared to established marsh systems based on their site conditions like undisturbed soils, frequent brackish water inundation, and black needle rush vegetation. However, even though SOC is being gained to some degree, periodic soil aeration is likely driving mineralization lowering carbon accumulation and keeping soil C:N ratios low relative to unaltered marsh sites in the region (Kuhry et al. 1996).

Distinguishing Soil Factors Between Ecosystems

In wetlands that have little sedimentary input, vegetative productivity drives the soil elevation (Kirwin et al. 2013). Richness and diversity of species increases productivity and nutrient retention which, once stabilized, accretes carbon in soil profiles (Engelhardt et al. 2002). Vegetative species richness and diversity often infer wetland health, usually indicating that enough resources are available to a variety of competing species (Engelhardt et al. 2002). Normalized difference vegetative index (NDVI) has been used as an indicator of ecosystem transition by measuring the decreases of reflectance and absorption in vegetation (Martinez et al. 2024). Higher NDVI indicates a greener and denser canopy, or higher species richness while a lower NDVI can indicate diminished biomass or simply a lack of vegetation (Meneses-Tovar, 2011). The calculated NDVI from study sites reveals the relationship between the salinity gradient and vegetative health. The greener canopy of the forest had the highest NDVI (0.66), indicating more robust vegetative density and thus lower salinity and saturation levels. The ghost forest site had the second highest NDVI (0.51) likely due to the migration of marsh vegetation along the salinity gradient. Most of the Ghost Forest sites were colonized by invasive common reeds, which thrive in the salinized and inundated conditions of the ecotone. Finally, the marsh site had the lowest NDVI value (0.43) which is consistent with the elevated levels of salinity and inundation creating an environment that most vegetative species are unable to adapt to. All marsh sites had black needle rush cover, which is characterized by black or dark gray blades which could have contributed to the NDVI being lower as well. Compared to other studies, the NDVI are consistent, where values decrease moving towards ecosystems with diminished biomass (Meneses-Tovar, 2011). In another study, low marsh sites populated by *Spartina alterniflora*, were analyzed for NDVI in the Chesapeake Bay area and showed NDVI

values ranging from 0.23 - 0.26 in April and 0.41 - 0.50 in May (Nardin et al. 2021).

These values were similar to the marshes of this study, where NDVI value range of 0.30 - 0.42 in April of this study.

Spearman's correlations (Fig. 2.2) showed that distance from open water (m) had a negative relationship with 1:5 EC (dS/m) and 1:1 pH. The more distance a site had from the Pamlico Sound, the designated open water, the less salinized those soils became. Proximity to brackish estuarine water makes coastlines more susceptible to inundation and salt-water intrusion as seen through the migration of tidal marsh vegetation further inland (Aguilos et al. 2021), formation of ghost forests (Chen et al. 2023; Smart et al. 2020), as well as the changes to the chemistry and structure of soils (Riggs et al. 2003). All sites across the ecosystem gradient receive brackish water input either through preferential flow up ditches or the deposition of ocean water during storm surges (Riggs et al. 2003) which increases the exchangeable salts in soils and raises the EC (Corwin et al. 2017). Being located further inland, forest sites (mean distance from open sound: 1372 m) receive less input from brackish water and soils can flush out exchangeable salts during rainfall, lowering the levels of exchangeable salts (EC: 0.82 dS/m, Table 1). Ghost Forest and Marsh sites are frequently inundated by brackish water since they were, on average half a mile or less from the open water and expressed significantly higher levels of exchangeable salts (EC: 2.89 dS/m and 4.48 dS/m respectively). Excess soluble salts hinder most plant growth because the addition of solutes in soil water causes the osmotic potential to drop and water will not travel through the semipermeable membrane of the root (Li et al. 2022; Pagter et al. 2009). Even if a soil is inundated with water, plants not adapted to brackish or saline conditions are unable to take up water, and in their place, salt-tolerant species take root (Batzer et

al. 2014). Brackish water also contains sodium which replaces other ions, like calcium, on soil cation exchange sites which weakens the forces holding clays together and prevents the aggregation of soil peds (Amézqueta, 1998; Bronick et al. 2005; Tang et al. 2020).

Distance from open water (m) also saw weak positive correlations to SOC pools and C:N ratios, where sites further inland had higher SOC pools (kg/m^2), or storage and retention of carbon, and higher C:N ratios, or reduced nitrogen mineralization. Forest sites, being the furthest inland had the second largest SOC pools (mean SOC pool: 24.03 kg/m^2), ghost forest sites had the lowest SOC pools (mean SOC pool: 19.72 kg/m^2), and Marsh sites right on the shoreline of the sound had the largest SOC pools (mean SOC pool: 26.67 kg/m^2) (Table 2.2). Typically, areas closer to the water are saturated more often (Riggs et al. 2003), thus slowing decomposition of organic residues and reducing the aeration of soils, increasing the amount of stored organic carbon (Batzer et al. 2014). However, all study sites had altered hydrology due to relic drain lines (Richardson, 1983; Lilly, 1981) that channelize the flow of water out into the sound instead of allowing it to diffuse across the landscape (Bhattachan et al. 2018). Thus, if soils were aerated more frequently and oxygenation due to drying this would increase the decomposition of stored soil organic matter (Ise et al. 2008).

C:N ratios are proportional to mineralization and if the ratio is low then carbon can be easily mineralized by microorganisms. In Table 1, C:N ratios were all relatively low ranging from 12.11 to 14.11 across the forest, ghost forest, and marsh gradient. Forest sites were further inland which meant soils were drier, the water table being within 100 cm of the surface instead of above the surface, and conditions are favorable

for microbial respiration (Sleeter, 2021; Xu et al. 2021). Prolonged soil saturation, like in the ghost forest and marsh ecosystems, should slow mineralization, yet C:N ratios did not increase significantly at wetter sites. However, marshes maintained the highest mean depth of accretion (47 cm) and 2 m SOC pool (26.67 kg/m²) suggesting that carbon is accumulating within the soils, but periodic aerobic conditions are keeping the net rate of annual increase low relative to permanently saturated unaltered marsh systems in the region (Fig. 2.5).

Soil Properties Across Salinity Gradients

Average measured water salinity (ppt) from ditches was 1.41 (oligohaline), 10.04 (mesohaline), and 21.35 (polyhaline) for forest, ghost forest, and marsh sites, respectively (Cowardin et al. 1979). Forest sites did not see an impact on 1:1 pH from increases in salinity (Fig. 3. Left graph) since the sites were far enough inland that fresh-water input can flush salts from soil exchange sites (Hussein et al. 2001). The ghost forest and marsh sites did see a slight increase in alkaline pH values, but plateaued below pH 8, with some marsh samples decreasing as soil salinity increased. The average pH of the ocean is 8.1 (EPA, 2024), thus the mesohaline and polyhaline systems would not exceed pH 8 until the systems began increasing salinity to euhaline levels.

At the study sites, brackish water inundation or over wash flux sulfate into the terrestrial soil system (Soil Survey Staff, 2022; VanZomeran et al. 2020). Frequent inundation coupled with low topography encourages the reduction of protons in the soil solution due to the lack of oxygen and thus maintains a neutral pH (Breemen et al. 1983; Soil Survey Staff, 2022). Saturated soils retain sulfate which is reduced into sulfides not contributing to the soil acidity until it is aerated (Breemen et al. 1983; Soil Survey Staff, 2022; VanZomeran et al. 2020). If oxidized, the reduced sulfur converts to sulfuric acid which acidifies the soil (Breemen et al.

1983; Soil Survey Staff, 2022). Besides exchangeable salts, brackish water also increases the presence of sulfidic materials in the soil system, which can be detected through moist incubations and calculation of delta pH over 16 weeks (Soil Survey Staff, 2022; VanZomeren et al. 2020). If sulfides are present, pH will drop after incubation by 0.5 or more units to a pH of 4 or less, indicating that the sulfides have oxidized to sulfuric acid (Soil Survey Staff, 2022; VanZomeren et al. 2020). Since this process is largely influenced by the presence of oxygen, aerated sites in this study were largely unaffected by increases in inundation from brackish water. Thus, forest sites saw minimal changes in their pH over 16 weeks, since soils were more oxygenated and less frequently inundated with brackish water containing sulfate, the average delta pH was only -0.05 pH units (Table 2.1). However, ghost forest sites saw an average -1.35 unit change in pH, and marsh sites saw an average -1.58 unit change in pH indicating both ecosystems had appreciable sulfides within soils and classified as hyposulfidic (Table 2.1). Both ecosystems had significant positive relationships between soil delta pH (sulfide content) and salinity, especially the marsh sites at the open water edge (Figure 2.3). Short-term disturbances from drainage would not produce the same levels of acidity as prolonged anaerobic conditions would for sulfidization (Portnoy & Valiela, 1997; Portnoy & Giblen, 1997). Subsoils within coastal wetlands remain consistently anaerobic where sulfides could accumulate without being oxidized (VanZomeren et al. 2020). Therefore, variability observed in soil sulfides within ghost forest and marsh sites is likely related to depth, where surface horizons have more organic matter and periodic aeration due to the relic ditch lines (Bhattachan et al. 2018). Soil sulfidization also depends on the presence of organic matter to be mineralized by bacteria for respiration and subsequent reduction of porewater sulfate (VanZomeren et al. 2020).

In Figure 2.4, the correlation between the depth of accreted organic horizons was regressed against the salinity gradient and all sites showed moderate correlation (R^2 : 0.42). Forest sites had an average organic horizon depth of 7 cm due to more aerated soils (Table 2.1) and data points congregated at the base of the trendline (Fig. 2.4). Ghost forest sites had an average organic horizon buildup of 32 cm and marsh sites had 47 cm. Data for all sites displayed significant variability across all ecosystems, likely related to the large range in depths of organic horizons for each pedon (Fig. 2.4). Soils within abandoned farm fields are accreting organic matter in these systems, however modifications to the hydrology of the area (Bhattachan et al. 2018) and periodic fires both natural and anthropogenic (Richardson, 1983; Lilly 1981) have likely resulted in variable rates of oxidation.

Variability in SOC mineralization has resulted in overall average 0.36 ± 0.05 cm/yr rate of accretion with no significant difference ($p > 0.05$) between ecosystem sites. Older marsh sites had greater depths of accreted organic matter (Table 2.2) but lacked sufficient accretion rates to maintain high enough elevation to avoid submergence. Past studies in the APES region have shown similar net accretion rates within tidal marshes ranging from 0.24 ± 0.02 to 0.36 ± 0.05 cm/yr in intermittently flooded areas like those in this study (Craft et al. 1993). Current rates of historical sea level rise in the region from 1977-2023 were between 0.49 ± 0.06 and 0.56 ± 0.10 cm/yr (NOAA, 2023), greater than measured net accretion across all abandoned farm field sites within this study. This estimated net accretionary imbalance of -0.13 to -0.20 cm/yr has resulted in significant shoreline erosion within this region, regardless of ecosystem type (Gorzynski et al. 2024). Furthermore, the rates of sea level rise are expected to increase to 1.38 - 1.65 cm/yr by 2050 (Sweet et al. 2022) further expediting erosion and submersion of coastal wetlands within the greater Albemarle-Pamlico estuary region.

Conclusion

North Carolina is susceptible to significant erosion and inundation damage due to projected relative sea level rise. This study sought to compare different mapping concepts to determine if the conceptual mapping done by soil survey captured the soil characteristics and carbon storage capacity of the region. Comparisons of soil properties based on ecosystem and soil survey classification exhibited statistically similar results, but the ecosystem concept provided a more logical definition of forest, ghost forest, and marsh environments based on modern site characteristics. Soil carbon was found to be mineralizing faster than it was accreting in areas expected to be organic soils, likely due to the aeration from relict drainage canals lowering the water table and possible past fires in the region. Based on carbon sequestration rates and measurements of net accretion, coastal soils in this region are not accumulating SOC at a rate that can keep pace with sea level rise. With SLR expected to rise 1.38 - 1.65 cm/yr, current rates of mean net carbon accretion (0.36 cm/yr) will result in land degradation and submersion unless mineralization is slowed. In the future, active management of abandoned marginal farmland is needed to promote high rates of annual accretion from native salt-tolerant plant biomass and long-term SOC storage within permanently saturated anaerobic soils.

REFERENCES

- Adame, M.F., Kauffman, J.B, Medina, I., et al. (2013). Carbon Stocks of Tropical Coastal Wetlands within the Karstic Landscape of the Mexican Caribbean. *PLOS ONE*. <https://doi.org/10.1371/journal.pone.0056569>
- Aguilos, M., Brown, C., Minick, K., et al. (2021). Millennial-Scale Carbon Storage in Natural Pine Forests of the North Carolina Lower Coastal Plain: Effects of Artificial Drainage in a Time of Rapid Sea Level Rise. *Land*, 10(12). <https://doi.org/10.3390/land10121294>
- Aguilos M., Sun, G., Noormets, A., et al. (2021). Ecosystem Productivity and Evapotranspiration Are Tightly Coupled in Loblolly Pine (*Pinus taeda* L.) Plantations along the Coastal Plain of the Southeastern U.S. *Forests*, 12(1123). <https://doi.org/10.3390/f12081123>
- Amézketa, E. (1999). Soil Aggregate Stability: A Review. *Journal of Sustainable Agriculture*, 14(2–3); 83–151. https://doi.org/10.1300/J064v14n02_08
- Ardón, M., Montanari, S., Morse, J.L., et al. (2010). Phosphorus export from a restored wetland ecosystem in response to natural and experimental hydrologic fluctuations. *Journal of Geophysical Research*, 115(G4). <https://doi.org/10.1029/2009JG001169>
- Ardón, M., Morse, J.L., Doyle, M.W., et al. (2010). The Water Quality Consequences of Restoring Wetland Hydrology to a Large Agricultural Watershed in the Southeastern Coastal Plain. *Ecosystems*. 13; 1060-1078. <https://doi.org/10.1007/s10021-010-9374-x>
- Batzer, D.P. (Ed.), & Sharitz R.R. (Ed.). (2014). *Ecology of Freshwater and Estuarine Wetlands*. University of California Press.
- Bhattachan, A., Emanuel, R.E., Ardón, M., et al. (2018). Evaluating the effects of land-use change and future climate change on vulnerability of coastal landscapes to saltwater intrusion. *Elementa: Science of the Anthropocene*, 6(62). <https://doi.org/10.1525/elementa.316>
- Blake, G.R. and Hartge, K.H. (1986) Bulk density. In: Klute, A., Ed., *Methods of Soil Analysis, Part 1—Physical and Mineralogical Methods*, 2nd Edition, Agronomy Monograph 9, American Society of Agronomy—Soil Science Society of America, Madison, 363-382.
- Blaskó, L., Gliński, J. (Ed.), Horabik, J. (Ed.), Lipiec, J. (Ed.)(2011). *Encyclopedia of Agrophysics; Alkalinity, Physical Effects on Soils*. Encyclopedia of Earth Sciences Series. Springer, Dordrecht. https://doi.org/10.1007/978-90-481-3585-1_13
- Boelter, D.H. (1965). *Hydraulic Conductivity of Peats. Report, 100-1*. US Department of Agriculture. https://www.nrs.fs.usda.gov/pubs/jrnl/1968/nc_1968_boelter_001.pdf

- Bost, M.C., Deaton, C.D., Rodriguez, A.B., et al. (2023). Anthropogenic impacts on tidal creek sedimentation since 1900. *PLOS ONE*, 18(1), <https://doi.org/10.1371/journal.pone.0280490>
- Braswell, A.E., Heffernan, J.B., Kirwan, M.L. (2020). How Old Are Marshes on the East Coast, USA? Complex Patterns in Wetland Age Within and Among Regions. *Geophysical Research Letters*, 47(19). <https://doi.org/10.1029/2020GL089415>
- Breemen, N.V., Mulder, J., Driscoll, C.T. (1983). Acidification and Alkalinization of Soils. *Plant and Soil*, 75; 283-308. <https://doi.org/10.1007/BF02369968>
- Brinson, M.M., Bradshaw, H.D., Jones, M.N. (1985). Transitions in Forested Wetlands Along Gradients of Salinity and Hydroperiod. *Journal of the Elisha Mitchell Scientific Society*, 101(2); 76-94. <http://www.jstor.org/stable/24333326>.
- Bronick, C.J. & Lal, R. (2005) Soil structure and management: a review. *Geoderma*. 124(1-2); 3-22, <https://doi.org/10.1016/j.geoderma.2004.03.005>
- Brown, C.E. (1998). *Applied Multivariate Statistics in Geohydrology and Related Sciences*. Press.
- Buol, S.W., F.D. Hole, and R.J. McCracken. (1989). *Soil genesis and classification*. 3rd ed. Iowa State University Press, Ames.
- Charles, S.P., Kominoski, J.S., Troxler, T.G., et al. (2019) Experimental Saltwater Intrusion Drives Rapid Soil Elevation and Carbon Loss in Freshwater and Brackish Everglades Marshes. *Estuaries and Coasts*, 42; 1868-1881. <https://doi.org/10.1007/s12237-01900620-3>
- Chen, H., Rücker, A.M., Liu, Y., et al. (2023) Unique biogeochemical characteristics in coastal ghost forests – The transition from freshwater forested wetland to salt marsh under the influences of sea level rise, *Soil & Environmental Health*, 1(1); 100005, ISSN 29499194, <https://doi.org/10.1016/j.seh.2023.100005>.
- Chowdhury M.Q., Sarker, S.K., Marma, M., Rahman, M.S., Datta, A. (2024) Climate and salinity together control above ground carbon accumulation in the Sundarbans mangrove ecosystem. *Ocean & Coastal Management*, 255. <https://doi.org/10.1016/j.ocecoaman.2024.107242>
- Cohen, K.M., Finney, S.C., Gibbard, P.L. & Fan, J.X. (2023, September). *The ICS International Chronostratigraphic Chart*. Stratigraphy. <http://www.stratigraphy.org/ICSchart/ChronostratChart2023-09.pdf>
- Conner, W.H., Doyle, T.W., Krauss, K.W. (2007). *Ecology of Tidal Freshwater Forested Wetlands of the Southeastern United States*. Springer
- Corbett, D.R., Walsh, J.P., Cowart, L., et al. (2008). *Shoreline Change Within the Albemarle Pamlico Estuarine System, North Carolina*. Department of Geological

Sciences Thomas Harriot College of Arts and Sciences and Institute for Coastal Science and Policy East Carolina University

- Cortese, L., Jenson, D.J., Simard, M., et al. (2023). Using normalize difference vegetation index to infer wetlands salinity and organic contribution to vertical accretion rates. *Journal of Geophysical Research: Biogeosciences*. 128(11). <https://doi.org/10.1029/2023JG007631>
- Corwin, D.L., Yemoto, K. (2017). *Methods of Soil Analysis, Vol. 2*; “Salinity: Electrical Conductivity and Total Dissolved Solids.” Soil Science Society of America.
- Cowardin, L.M., Carter, V., Golet, F.C., et al. (1979) *Classification of wetlands and deepwater habitats of the United States*. U.S. Department of the Interior, Fish and Wildlife Service
- Creel, L. (2003, September 25). *Ripple Effects: Population and Coastal Regions*. PRB. <https://www.prb.org/resources/ripple-effects-population-and-coastal-regions/>
- Craft, C., Megonigal, P., Broome, S., et al. (2003). The Pace of Ecosystem Development of Constructed *Spartina alterniflora* Marshes. *Ecological Applications*. 13(5); 1417-1432. <http://www.jstor.org/stable/4134723>
- Craft, C.B., Seneca, E.D., & Broome, S.W. (1993) Vertical Accretion in Microtidal Regularly and Irregularly Flooded Estuarine Marshes. *Estuarine, Coastal, and Shelf Science*. 37(4); 371-386. <https://doi.org/10.1006/ecss.1993.1062>
- Czapla, K.M., Anderson, I.C., & Currin, C.A. (2020). Net Ecosystem Carbon Balance in a North Carolina, USA, Salt Marsh. *Journal of Geophysical Research: Biogeosciences*, 125(10). <https://doi.org/10.1029/2019JG005509>.
- Daniels R.B., Buol, S.W., Kleiss, H.J., & Ditzler, C.A. (1999). Soil Systems in North Carolina. *North Carolina State University - Soil Science Department*.
- Deb, S. & Mandal B.. (2021). Soils and Sediments of Coastal Ecology: A Global Carbon Sink. *Ocean and Coastal Management*. 214. <https://doi.org/10.1016/j.ocecoaman.2021.105937>.
- Desantis, L.R.G., Bhotika, S., Williams, K. And Putz, F.E. (2007). Sea-Level Rise And Drought Interactions Accelerate Forest Decline On The Gulf Coast Of Florida, Usa. *Global Change Biology*, 13; 2349-2360. <https://doi.org/10.1111/J.1365-2486.2007.01440.X>
- Dixon, T.H., Amelung, F., Ferretti, A., et al. (2006). Subsidence and Flooding in New Orleans. *Nature*, 441; 587-588. <https://doi.org/10.1038/441587a>
- Dolman, J.D. & Buol, S.W. (1968) Organic Soils on the Lower Coastal Plain of North Carolina. *Soil Science Society of America Journal*. 32(3); 297-448. <https://doi.org/10.2136/sssaj1968.03615995003200030040x>
- Dong-Soo, J.K. (2022). *Distribution and Variability of Carbon Stocks in Mid-Atlantic Tidal Marsh Soils*. [Unpublished master’s thesis]. University of Maryland.

- Dontis, E.E., Radabaugh, K.R., Chappel, A.R., et al. (2020). Carbon Storage Increases with Site Age as Created Salt Marshes Transition to Mangrove Forests in Tampa Bay, Florida (USA). *Estuaries and Coasts*, 43, 1470-1488. <https://doi.org/10.1007/s12237-020-00733-0>
- Drexler, J.Z., Krauss, K.W., Sasser, M.C., et al. (2013). A Long-Term Comparison of Carbon Sequestration Rates in Impounded and Naturally Tidal Freshwater Marshes Along the Lower Waccamaw River, South Carolina. *Wetlands*, 33; 965-974. <https://doi.org/10.1007/s13157-013-0456-3>
- Duarte, C.M., Losada I.J., & Hendriks I.E., et al. (2013). The Role of Coastal Plant Communities for Climate Change Mitigation and Adaptation. *Nature Climate Change*, 3, 961–968. <https://doi.org/10.1038/nclimate1970>.
- Edmonds, W.J., Cobb, P.R., Peacock, C.D. (1986). Characterization and Classification of Seaside- Salt Marsh Soils on Virginia’s Eastern Shore. *Soil Science Society of America Journal*, 50(3); 672-678. <https://doi.org/10.2136/sssaj1986.03615995005000030026x>
- Elsley-Quirk, T., Watson, E.B., & K. Raper, et al. (2022). Relationships between Ecosystem Properties and Sea-Level Rise Vulnerability of Tidal Wetlands of the U.S. Mid-Atlantic. *Environmental Monitoring and Assessment*, 194(4). <https://doi.org/10.1007/s10661-02209949-y>.
- Engelhardt, K.A.M. & Ritchie, M.E. (2002). The Effect of Aquatic Plant Species Richness on Wetland Ecosystem Processes. *Ecology*. 83(10); 2911-2924. [https://doi.org/10.1890/0012-9658\(2002\)083\[2911:TEOAPS\]2.0.CO;2](https://doi.org/10.1890/0012-9658(2002)083[2911:TEOAPS]2.0.CO;2)
- Finotello, A., Marani, M., & Carniello, L., et al. (2020). Control of Wind-Wave Power on Morphological Shape of Salt Marsh Margins. *Water Science and Engineering*, 13(1), 45–56. <https://doi.org/10.1016/j.wse.2020.03.006>.
- Frankard, P., Ghiette, P., Hindryckx, M., et al. (1998). Peatlands of Wallony (S-Belgium). *Suo: Mires and Peat*. 49(2); 33-47. <https://hdl.handle.net/2268/17527>
- Freshwater Inflows - Salinity* (n.d.). Texas A&M University Corpus Christi. Retrieved Sept. 20, 2024, from: <https://www.freshwaterinflow.org/salinity/>
- Gedan, K.B., Fernández-Pascual, E. (2019). Salt marsh migration into salinized agricultural fields: A novel assembly of plant communities. *Journal of Vegetation Science*, 30(5); 1007-1016. <https://doi.org/10.1111/jvs.12774>
- Gee, G.W. and Bauder, J.W. (1986). Particle-size Analysis. In *Methods of Soil Analysis*, A. Klute (Ed.). Soil Science Society of America
- Gianopulos, K., Kendig, K., Pyne, M. (2021). *Guide to Common Wetland Plants of North Carolina*. North Carolina Department of Environmental Quality, Division of Water Resources.

- Gorczyński, L. E. (2022). *Quantification of Coastal Wetland Blue Carbon Stocks along Salinity Gradients in the Albemarle-Pamlico Estuary*. [Unpublished master's thesis]. North Carolina State University.
- Gorczyński, L.E., Wilson, A.R., Odhiambo, B.K., et al. (2024). Coastal Forest Change and Shoreline Erosion across a Salinity Gradient in a Micro-Tidal Estuary System. *Forests*, 15(1069). <https://doi.org/10.3390/f15061069>
- Guimond, J.A., Michael, H.A. (2020). Effects of Marsh Migration on Flooding, Saltwater Intrusion, and Crop Yield in Coastal Agricultural Land Subject to Storm Surge Inundation. *Water Resources Research*, 57(2). <https://doi.org/10.1029/2020WR028326>
- Haywood, B.J., Hayes, M.P., & White, J.R., Cook, R.L. (2020). Potential Fate of Wetland Soil Carbon in a Deltaic Coastal Wetland Subjected to High Relative Sea Level Rise. *Science of The Total Environment*, 711. <https://doi.org/10.1016/j.scitotenv.2019.135185>.
- Herbert, E.R., Boone, P., Burgin, A.J., et al. (2015). A global perspective on wetland salinization: ecological consequences of a growing threat to freshwater wetlands. *Ecosphere*. 6(10); 1-43. <https://doi.org/10.1890/ES14-00534.1>
- Hinson, A.L., Feagin, R.A., & Eriksson, M., et al. (2017). The Spatial Distribution of Soil Organic Carbon in Tidal Wetland Soils of the Continental United States. *Global Change Biology*, 23 (12), 5468–5480. <https://doi.org/10.1111/gcb.13811>.
- Holland Consulting Planners (HCP). (2008). Hyde County, NC - CAMA Core Land Use Plan. Hyde County Board of Commissioners.
- Holmquist, J.R., Windham-Myers L., & Bliss N. (2018). Accuracy and Precision of Tidal Wetland Soil Carbon Mapping in the Conterminous United States. *Scientific Reports*, 8. <https://doi.org/10.1038/s41598-018-26948-7>
- Hussein, A.H., & Rabenhorst, M.C. (2001). Tidal Inundation of Transgressive Coastal Areas. *Soil Science Society of America Journal*, 65, 536–44. <https://doi.org/10.2136/sssaj2001.652536x>.
- Ise, T., Dunn, A.L., Wofsy, S.C., et al. (2008). High sensitivity of peat decomposition to climate change through water-table feedback. *Nature Geoscience*, 1(11). [0.1038/ngeo331](https://doi.org/10.1038/ngeo331)
- Illustration describes a barrier island from ocean to lagoon* | U.S. Geological Survey. (n.d.) <https://www.usgs.gov/media/images/illustration-describes-barrier-island-ocean-lagoon>
- IPCC (2013) Climate change 2013: the physical science basis. Contribution of Working Group I to the fifth assessment report of the intergovernmental panel on climate change. Cambridge University Press, Cambridge, New York
- Jackson, C.R. & Pringle, C.M., (2010). Ecological Benefits of Reduced Hydrologic Connectivity in Intensively Developed Landscapes. *BioScience*. 60(1); 37-46. <https://doi.org/10.1525/bio.2010.60.1.8>

- Jackson, R.B., Lajtha, K., Crow, S.E. (2017). The Ecology of Soil Carbon: Pools, Vulnerabilities, and Biotic and Abiotic Controls. *Annual Review of Ecology, Evolution, and Systematics*, 48:419-445. <https://doi.org/10.1146/annurev-ecolsys-112414-054234>
- Johnston, J., Cassalho, F., Misesse, T., & Ferreira, C.M. (2021). Projecting the effects of land subsidence and sea level rise on storm surge flooding in Coastal North Carolina. *Scientific Reports*, 11. <https://doi.org/10.1038/s41598-021-01096-7>
- Jolley, R.L., Lockaby B.G., Cavalcanti, G.G. (2009). Productivity of Ephemeral Headwater Riparian Forests Impacted by Sedimentation in the Southeastern United States Coastal Plain. *Journal of Environmental Quality*, 38(3); 965-979. <https://doi.org/10.2134/jeq2008.0206>
- Kauffman, J.B., Giovanonni, L., Kelly, J., et al. (2020). Total ecosystem carbon stocks at the marine-terrestrial interface: Blue carbon of the Pacific Northwest Coast, United States. *Global Change Biology*, 26(10); 5679-5692. <https://doi.org/10.1111/gcb.15248>
- Kirwan, M. L., Megonigal, J.P., & Noyce, G.L., et al. (2023). Geomorphic and Ecological Constraints on the Coastal Carbon Sink. *Nature Reviews Earth & Environment*, 4, 393–406. <https://doi.org/10.1038/s43017-023-00429-6>.
- Kirwin, M.L., Megonigal, J.P. (2013). Tidal wetland stability in the face of human impacts and sea-level rise. *Nature*, 504; 53-60. <https://doi-org.prox.lib.ncsu.edu/10.1038/nature12856>
- Knutson, T. (2024). *Global Warming and Hurricanes – An Overview of Current Research Results*. NOAA: Geophysical Fluid Dynamics Laboratory. <https://www.gfdl.noaa.gov/global-warming-and-hurricanes/>
- Krause, L., McCullough, K.J., Kane, E.S., et al. (2021) Impacts of historical ditching on peat volume and carbon in northern Minnesota USA peatlands. *Journal of Environmental Management*, 296; 13090. <https://doi.org/10.1016/j.jenvman.2021.113090>.
- Krauss, K.W., Noe, G.B., Duberstein, J.A., et al. (2018). The role of the upper tidal estuary in wetland blue carbon storage and flux. *Global Biogeochemical Cycles*, 32, 817–839. <http://dx.doi.org/10.1029/2018GB005897>
- Krauss, K.W., Whitbeck, J.L., Howard, R.J. (2012). On the relative roles of hydrology, salinity, temperature, and root productivity in controlling soil respiration from coastal swamps (freshwater). *Plant and Soil*, 358; 265-274. <https://doi.org/10.1007/s11104-012-1182-y>
- Kuhry, P., & Vitt, D. H. (1996). Fossil Carbon/Nitrogen Ratios as a Measure of Peat Decomposition. *Ecology*, 77(1), 271–275. <https://doi.org/10.2307/2265676>
- Li, Q., Song, Z., & Xia, S., et al. (2023). Substrate Quality Overrides Soil Salinity in Mediating Microbial Respiration in Coastal Wetlands. *Land Degradation & Development*, 34(15), 4546–4560. <https://doi.org/10.1002/ldr.4792>.

- Li, Y., Henrion, M., Moore, A., et al. (2024). Factors controlling peat soil thickness and carbon storage in temperate peatlands based on UAV high-resolution remote sensing. *Geoderma*, 449. <https://doi.org/10.1016/j.geoderma.2024.117009>
- Li, Y.L., Ge, Z.N., Xie, L.N., et al. (2022). Effects of waterlogging and elevated salinity on the allocation of photosynthetic carbon in estuarine tidal marsh: a mesocosm experiment. *Plant and Soil*, 482; 211-227. <https://doi.org/10.1007/s11104-022-05687-9>
- Lilly, J.P. (1981). *The Blackland Soils of North Carolina. Their Characteristics and Management for Agriculture*. North Carolina Agricultural Research Service. <https://vernonjames.ces.ncsu.edu/wp-content/uploads/2019/02/BLACKLANDSOILSOFNC.pdf? fwd=no>
- Lindsey, R. (2022). *Climate Change: Global Sea Level*. Understanding Climate. NOAA <https://www.climate.gov/news-features/understanding-climate/climate-change-globalsea-level>.
- Loder, A.L., Finkelstein, S.A. (2020). Carbon Accumulation in Freshwater Marsh Soils: a Synthesis for Temperate North America. *Wetlands*, 40, 1173-1187. <https://doi.org/10.1007/s13157-019-01264-6>
- Lovelock, C. E., & Reef, R., (2020). Variable Impacts of Climate Change on Blue Carbon. *One Earth*, 3(2), 195–211. <https://doi.org/10.1016/j.oneear.2020.07.010>.
- Lynch, J.M., Peacock, S.L. (1982). *Natural Areas Inventory of Hyde County, North Carolina*. Coastal Zone Information Center. <https://www.govinfo.gov/content/pkg/CZIC-qh76-5-n8-195-1982/html/CZIC-qh76-5-n8-195-1982.htm>
- Magolan, J.L., Halls, J.N. (2020). A Multi-Decadal Investigation of Tidal Creek Wetland Changes, Water Level Rise, and Ghost Forests. *Remote Sensing*, 12(7). <https://doi.org/10.3390/rs12071141>
- Martinez, M., Ardón, M., Gray, J. (2024). Detecting Trajectories of Regime Shifts and Loss of Resilience in Coastal Wetlands using Remote Sensing. *Ecosystems*. 27; 1060-1075. <https://doi-org.prox.lib.ncsu.edu/10.1007/s10021-024-00938-5>
- Maxwell, T. L., Rovai, A. S., & Adame, M. F., et al. (2023). Global Dataset of Soil Organic Carbon in Tidal Marshes. *Scientific Data*, 10(797). <https://doi.org/10.1038/s41597-02302633-x>.
- Maxwell, T. L., Spalding, M. D., & Friess, D.A., et al. (2024). *Soil Carbon in the World's Tidal Marshes*. bioRxiv. <https://doi.org/10.1101/2024.04.26.590902>.
- Mauchamp A., Méthy M. (2004) Submergence-induced damage of photosynthetic apparatus in *Phragmites australis*. *Environmental and Experimental Botany*, 51(3) :227–235. <https://doi.org/10.1016/j.envexpbot.2003.11.002>

- Mazzotti, S., Lambert, A., Van der Kooij, M., et al. (2009). Impact of anthropogenic subsidence on relative sea-level rise in the Fraser River delta. *Geology*, 37(9); 771-774. <https://doi.org/10.1130/G25640A.1>
- McLeod, E., Chmura, G.L., & Bouillon, S., et al. (2011). A Blueprint for Blue Carbon: Toward an Improved Understanding of the Role of Vegetated Coastal Habitats in Sequestering CO₂. *Frontiers in Ecology and the Environment*, 9(10), 552–60. <https://doi.org/10.1890/110004>.
- Meneses-Tovar, C.L. (2011). NDVI as indicator of degradation. *Unasylva*. 238. 62. <https://www.fao.org/4/i2560e/i2560e07.pdf>
- Miller, C. B., Bost, M.C., & McKee, B.A., et al. (2022). Carbon Accumulation Rates Are Highest at Young and Expanding Salt Marsh Edges. *Communications Earth & Environment*, 3(173). <https://doi.org/10.1038/s43247-022-00501-x>.
- Miller M.M., Shirzaei, M. (2021). Assessment of Future Flood Hazards for Southeastern Texas: Synthesizing Subsidence, Sea-Level Rise, and Storm Surge Scenarios. *Geophysical Research Letters*, 48(8). <https://doi.org/10.1029/2021GL092544>
- Minden, V., Andratschke, S., Spalke, J. (2012) Plant trait-environment relationships in salt marshes: Deviations from predictions by ecological concepts. *Perspectives in Plant Ecology, Evolution and Systematics*, 14(3); 183-192. <https://doi.org/10.1016/j.ppees.2012.01.002>
- Mitsch, W.J., Zhang, L., Waletzko, E., et al. (2014). Validation of the ecosystem services of created wetlands: Two decades of plant succession, nutrient retention, and carbon sequestration in experimental riverine marshes. *Ecological Engineering*, 72, 11-24. <https://doi.org/10.1016/j.ecoleng.2014.09.108>
- Moorhead, K.K. & Brinson, M.M. (1995). Response of Wetlands to Rising Sea Level in the Lower Coastal Plain of North Carolina. *Ecological Applications*. 5(1); 261-271. <https://doi.org/10.2307/1942068>
- Moreno-Mateos, D., Power, M.E., Comín, F.A., et al. (2012). Structural and Functional Loss in Restored Wetland Ecosystems. *PLOS Biology*. <https://doi.org/10.1371/journal.pbio.1001247>
- Morrissey, E.M., Gillespie, J.L., & Morina, J.C. (2013). Salinity affects microbial activity and soil organic matter content in tidal wetlands. *Global Change Biology*. 20(4). 1351-1362. <https://doi.org/10.1111/gcb.12431>
- Nardin, W., Taddia, Y., Quitadamo, M., et al. (2021). Seasonality and Characterization Mapping of Restored Tidal Marsh by NDVI Imageries Coupling UAVs and Multispectral Camera. *Remote Sensing*. 13(21). <https://doi.org/10.3390/rs13214207>
- NASA. (n.d.). *How Long Have Sea Levels Been Rising? How Does Recent Sea-Level Rise Compare to That over the Previous Centuries?* <https://sealevel.nasa.gov/faq/13/howlong->

[have-sea-levels-been-rising-how-does-recent-sea-level-rise-compare-to-that-overthe-previous/](#)

NC Division of Water Resources. (2024). *North Carolina Wetlands Information*. Published by the North Carolina Division of Water Resources, Water Sciences Section. Retrieved Sept., 13, 2024 from: <https://www.ncwetlands.org/learn/aboutncswetlands/types>

NOAA *North Carolina: Coastal Management*. (2024). NOAA: Coastal Management. <https://coast.noaa.gov/states/north-carolina.html>.

Noordwijk, M.V., Aynekulu, E., & Hijbeek, R., et al. 2023. Soils as Carbon Stores and Sinks: Expectations, Patterns, Processes, and Prospects of Transitions. *Annual Review of Environment and Resources*, 48 (1): 177–205. <https://doi.org/10.1146/annurev-environ112621-083121>.

North American Vertical Datum of 1988 (NAVD 88) - Vertical Datum - Datums - National Geodetic Survey. (2018). National Geodetic Survey. <https://www.ngs.noaa.gov/datums/vertical/north-american-vertical-datum-1988.shtml>

North Carolina Wildlife Resources Commission. (n.d.). *Coastal Plain Habitats*. <https://www.ncwildlife.org/wildlife-habitat/habitats/coastal-plain-habitats>

North Carolina's Sea Level is Rising. (n.d.). Accessed February 20, 2024. <https://sealevelrise.org/states/north-carolina>

North Carolina Spatial Data Download (n.d.). Accessed June 13, 2024. <https://sdd.nc.gov/>.

North Dakota State University (NDSU) Extension Service (n.d.). *Saline and Sodic Soils*. <https://www.ndsu.edu/agriculture/sites/default/files/2021-05/Saline-and-Sodic-Soils-22.pdf>

Ohenhen, L.O., Shirzaei, M., Ojha, C., et al. (2023). Hidden vulnerability of US Atlantic coast to sea-level rise due to vertical land motion. *Nature Communications*, 14(2038). <https://doi.org/10.1038/s41467-023-37853-7>

Pagter, M., Bragato, C., Malagoli, M., et al. (2009) Osmotic and ionic effects of NaCl and Na₂SO₄ salinity on *Phragmites australis*. *Aquatic Botany*, 90(1); 43-51. <https://doi.org/10.1016/j.aquabot.2008.05.005>

Pendleton, L., Donato, D.C., & Murray, B.C., et al. (2012). Estimating Global 'Blue Carbon' Emissions from Conversion and Degradation of Vegetated Coastal Ecosystems *PLoS ONE*, 7(9). <https://doi.org/10.1371/journal.pone.0043542>.

Pierfelice, K.N., Lockaby, B.G., Krauss, K.W., et al. (2015). Salinity Influences on Aboveground and Belowground Net Primary Productivity in Tidal Wetlands. *Journal of Hydrologic Engineering*, 22(1). [https://doi.org/10.1061/\(ASCE\)HE.1943-5584.0001223](https://doi.org/10.1061/(ASCE)HE.1943-5584.0001223)

- Portnoy, J.W., Giblin A.E. (1997). Biogeochemical effects of seawater restoration to diked salt marshes. *Ecological Applications*, 7(3); 1054-1063.
<https://seagrant.whoi.edu/wpcontent/uploads/2015/01/WHOI-R-97-003-Portnoy-J.W.-Biogeochemica.pdf>
- Portnoy, J.W., Giblin, A.E. (1997). Effects of historic tidal restrictions on salt marsh sediment chemistry. *Biogeochemistry*, 36; 275-303. From:
<https://seagrant.whoi.edu/wpcontent/uploads/2015/01/WHOI-R-97-002-Portnoy-J.-W.-Effects-of-Histo.pdf>
- Portnoy, J.W., Valiela, I. (1997). Short-term effects of salinity reduction and drainage on saltmarsh biogeochemical cycling and *Spartina* (cordgrass) production. *Estuaries and Coasts*, 20; 569-578. <https://doi.org/10.2307/1352615>
- Poulter, B., Christensen Jr., N.L., & Halpin, P.N. (2006) Carbon emissions from a temperate peat fire and its relevance to interannual variability of trace atmospheric greenhouse gases. *Journal of Geophysical Research, Atmospheres*. 111(6).
<https://doi.org/10.1029/2005JD006455>
- Reddy, A.D., Hawbaker, T.J., Wurster, F., et al. (2015). Quantifying soil carbon loss and uncertainty from a peatland wildfire using multi-temporal LiDAR. *Remote Sensing of Environment*, 170; 306-316. <https://doi.org/10.1016/j.rse.2015.09.017>
- Relative Sea Level Trend, 8651370 Duck, North Carolina*. (2023) NOAA.
https://tidesandcurrents.noaa.gov/sltrends/sltrends_station.shtml?id=8651370
- RESTORE. (2017). *Back Barrier Marsh: A Key Component of Caminada Headland Restoration*. Restore the Mississippi River Delta
- Richardson, C.J. (1983). Pocosins: Vanishing Wetlands or Valuable Wetlands? *Bioscience*, 33(10); 626-633. <https://doi.org/10.2307/1309491>
- Ricker, M.C., Lockaby, B.G. (2015). Soil Organic Carbon Stocks in a Large Eutrophic Floodplain Forest of the Southeastern Atlantic Coastal Plain, USA. *Wetlands*, 35; 291-301. <https://doi.org/10.1007/s13157-014-0618-y>
- Ricker, M.C., Stolt, M.H., Zavada, M.S. (2014). Comparison of Soil Organic Carbon Dynamics in Forested Riparian Wetlands and Adjacent Uplands. *Soil Science Society of America Journal*, 78(5), 1817-1827. <https://doi.org/10.2136/sssaj2014.01.0036>
- Riggs, S. R., Ames, D.V., et al. (2003). *Drowning The North Carolina Coast : Sea-Level Rise And Estuarine Dynamics*. North Carolina Sea Grant College Program.
- Rossi, A.M., Rabenhorst, M.C. (2019). Organic carbon dynamics in soils of Mid-Atlantic barrier island landscapes. *Geoderma*, 337. <https://doi.org/10.1016/j.geoderma.2018.10.028>
- Roy, K., Peltier, W.R. (2015). Glacial isostatic adjustment, relative sea level history and mantle viscosity: reconciling relative sea level model predictions for the U.S. East coast with

- geological constraints. *Geophysical Journal International*, 201(2); 1156-1181.
<https://doi.org/10.1093/gji/ggv066>
- Sanger, D. & Parker C. (2016). *Guide to the Salt Marshes and Tidal Creeks of the Southeastern United States*. South Carolina Department of Natural Resources.
<https://www.saltmarshguide.org/wp-content/uploads/2016/11/SaltMarshTidalCreekGuide.pdf>
- Schoeneberger, P.J., D.A. Wysocki, E.C. Benham, and Soil Survey Staff. (2012) *Field book for describing and sampling soils, Version 3.0*. Natural Resources Conservation Service, National Soil Survey Center, Lincoln, NE.
- Scott, M., Lindsey, R. (2022). *Understanding Blue Carbon: NOAA*. Understanding Climate. NOAA <https://www.climate.gov/news-features/understanding-climate/understandingblue-carbon>
- Shirzaei, M., Bürgmann, R. (2018). Global climate change and local land subsidence exacerbate inundation risk to the San Francisco Bay Area. *Science Advances*, 4(3).
<https://doi.org/10.1126/sciadv.aap9234>
- Simonson, Roy. (1987). Historical Aspects of Soil Survey and Soil Classification. *ASA, CSSA, and SSSA Books*. <https://doi.org/10.2136/1987.historicalaspectssoil.C2>.
- Sleeter, R.R. (2021). Modeling the Impacts of Hydrology and Management on Carbon Balance at the Great Dismal Swamp, Virginia and North Carolina, USA. In *Wetland Carbon and Environmental Management* (eds K.W. Krauss, Z. Zhu and C.L. Stagg)
<https://doi.org/10.1002/9781119639305.ch21>
- Smart, S.L., Taillie, P.J., Poulter, B., et al. (2020) Aboveground carbon loss associated with the spread of ghost forests as sea levels rise. *Environmental Research Letters*, 15(10).
<https://doi.org/10.1088/1748-9326/aba136>
- So, H.B., Alymore, L.A.G. (1993). How do sodic soils behave – the effects of sodicity on soil physical behavior. *Australian Journal of Soil Research*. 31(6); 761-777.
<https://doi.org/10.1071/SR9930761>
- Soil Survey of Pamlico County, North Carolina : United States. Natural Resources Conservation Service*. (1987). North Carolina. <https://archive.org/details/pamlicoNC1987>.
- Soil Survey Staff. (2022). Kellogg Soil Survey Laboratory Methods Manual - Soil Survey Investigations Report No.42, Version 6.0. Lincoln, NE: U.S. Government Printing Office
- Soil Survey Staff. (2022). Keys to Soil Taxonomy, 13th Edition. Washington, DC: U.S. Government Printing Office
- Soil Survey Staff (2019). Web Soil Survey; USDA-NRCS: Washington, DC: U.S.

- South Carolina Department of Natural Resources. (2020). *Marine- Tidal Creeks*.
<https://www.dnr.sc.gov/marine/habitat/tidalcreeks.html>
- Spearman's Rank Order Correlation* (n.d.). Laerd Statistics. Retrieved May, 22, 2024, from
<https://statistics.laerd.com/statistical-guides/spearmans-rank-order-correlation-statisticalguide.php>
- Spivak, A.C., Sanderman, J., & Bowen, J.L., et al. (2019). Global-Change Controls on Soil Carbon Accumulation and Loss in Coastal Vegetated Ecosystems. *Nature Geoscience*, 12:685–92. <https://doi.org/10.1038/s41561-019-0435-2>.
- Stagg, C.L., Schoolmaster Jr. D.R., Piazza, S.C., et al. (2017). A Landscape-Scale Assessment of Above- and Belowground Primary Production in Coastal Wetlands: Implications for Climate Change-Induced Community Shifts. *Estuaries and Coasts*. 40; 856-879.
<https://doi.org/10.1007/s12237-016-0177-y>
- Stolt, M., Turenne J., Payne, M. (2017). Subaqueous Soil Survey. In: Soil Survey Manual. 505523
- Sweet, W.V., Hamlington, R.E., & Kopp, C.P., et al. (2022). “Global and Regional Sea Level Rise Scenarios for the United States: Updated Mean Projections and Extreme Water Level Probabilities Along U.S. Coastlines. NOAA Technical Report NOS 01.” National Oceanic and Atmospheric Administration, National Service: 111
- Tang, S., She, D., & Wang, H. (2020) Effect of salinity on soil structure and soil hydraulic characteristics. *Canadian Journal of Soil Science*. 101(1); 61-73.
<https://doi.org/10.1139/cjss-2020-0018>
- Thorne, K., Macdonald, G., Guntenspergen, G., et al. (2018). U.S. Pacific coastal wetland resilience and vulnerability to sea-level rise. *Science Advances*. 4(2).
<https://doi.org/10.1126/sciadv.aao3270>
- Titus, Jg, & C Richman. (2001). Maps of Lands Vulnerable to Sea Level Rise: Modeled Elevations along the US Atlantic and Gulf Coasts. *Climate Research*, 18:205–28.
<https://doi.org/10.3354/cr018205>.
- Tully K., Gedan K., Epanchin-Niell R., et al. (2019). The Invisible Flood: The Chemistry, Ecology, and Social Implications of Coastal Saltwater Intrusion. *BioScience*, 69(5); 368–378, <https://doi.org/10.1093/biosci/biz027>
- Turcotte, D.L. & Schubert G. (2002). *Geodynamics* - 2nd ed. Cambridge University Press.
- Understanding the Science of Ocean and Coastal Acidification*. (2024). United States Environmental Protection Agency (EPA). Retrieved Aug., 27, 2024, from:
<https://www.epa.gov/ocean-acidification/understanding-science-ocean-and-coastalacidification>

- Ury, E., Yang, X., Wright, J.P., et al. (2021). Rapid deforestation of a coastal landscape driven by sea-level rise and extreme events. *Ecological Application*, 31(5).
<http://dx.doi.org/10.1002/eap.2339>
- VanZomerem, C.M., Berkowitz, J.F., Piercy, C.D., et al. (2020). Acid Sulfate Soils in Coastal Environments - A Review of Basic Concepts and Implications for Restoration. (ERDC/EL SR -20-4). US Army Corps of Engineers.
<https://apps.dtic.mil/sti/trecms/pdf/AD1110187.pdf>
- Vincent Manetta, Joseph. 2023. "Distribution and Variability of Blue Carbon in Tidal Marsh Soils of Southern New England." University of Rhode Island.
- Von Post, L. & Granlund, E. (1926). Peat resources in southern Sweden – Sveriges geologiska undersökning, Yearbook.
- Wang, F., Lu, X., Tang, J. (2019). Tidal wetland resilience to sea level rise increases their carbon sequestration capacity in United States. *Nature Communications*, 10 (5434).
<https://doi.org/10.1038/s41467-019-13294-z>
- Wasson, K., Ganju, N.K., & Defne, Z., et al. (2019). Understanding Tidal Marsh Trajectories: Evaluation of Multiple Indicators of Marsh Persistence. *Environmental Research Letters*, 14(12). <https://doi.org/10.1088/1748-9326/ab5a94>.
- Weintraub, M., Schimel, J. (2003) Interactions between Carbon and Nitrogen Mineralization and Soil Organic Matter Chemistry in Arctic Tundra Soils. *Ecosystems* 6, 0129–0143.
<https://doi.org/10.1007/s10021-002-0124-6>
- Xia, S., Song, Z., Zwieten, L.V., et al. (2022). Storage, patterns and influencing factors for soil organic carbon in coastal wetlands of China. *Global Change Biology*, 28(20); 6065-6085.
<https://doi.org/10.1111/gcb.16325>
- Xu, Z., Wang, S., Wang, Z. et al. (2021) Effect of drainage on microbial enzyme activities and communities dependent on depth in peatland soil. *Biogeochemistry*. 155; 323–341.
<https://doi.org/10.1007/s10533-021-00828-1>
- Zhong, B., & Xu, Y.J. (2011). Scale Effects of Geographical Soil Datasets on Carbon Estimation in Louisiana, USA: A Comparison of STATSGO and SSURGO. *Pedosphere*, 21(4): 491–501. [https://doi.org/10.1016/S1002-0160\(11\)60151-3](https://doi.org/10.1016/S1002-0160(11)60151-3).

APPENDICES

Appendix A

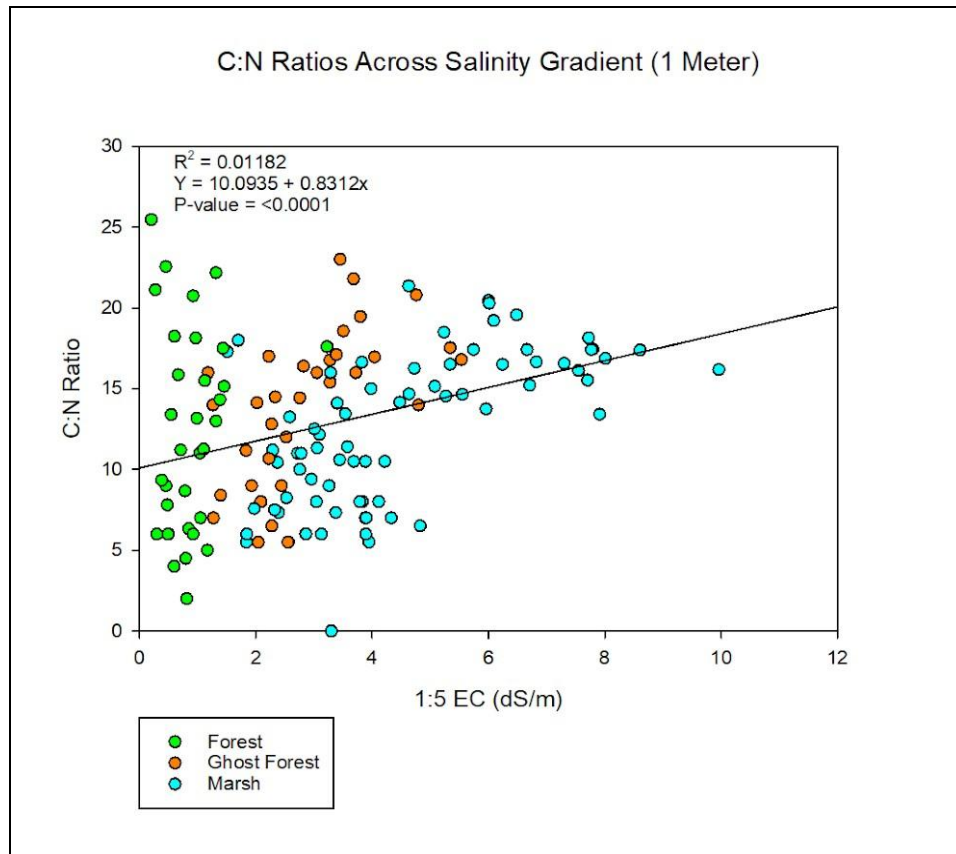


Figure A1. C:N ratios by horizon for each ecosystem across the salinity gradient. Results showed no relationship between more stable C:N ratios and increases in salinity. Graph also showed heteroskedastic shape, meaning that R^2 and P-value could not be used for interpretation.

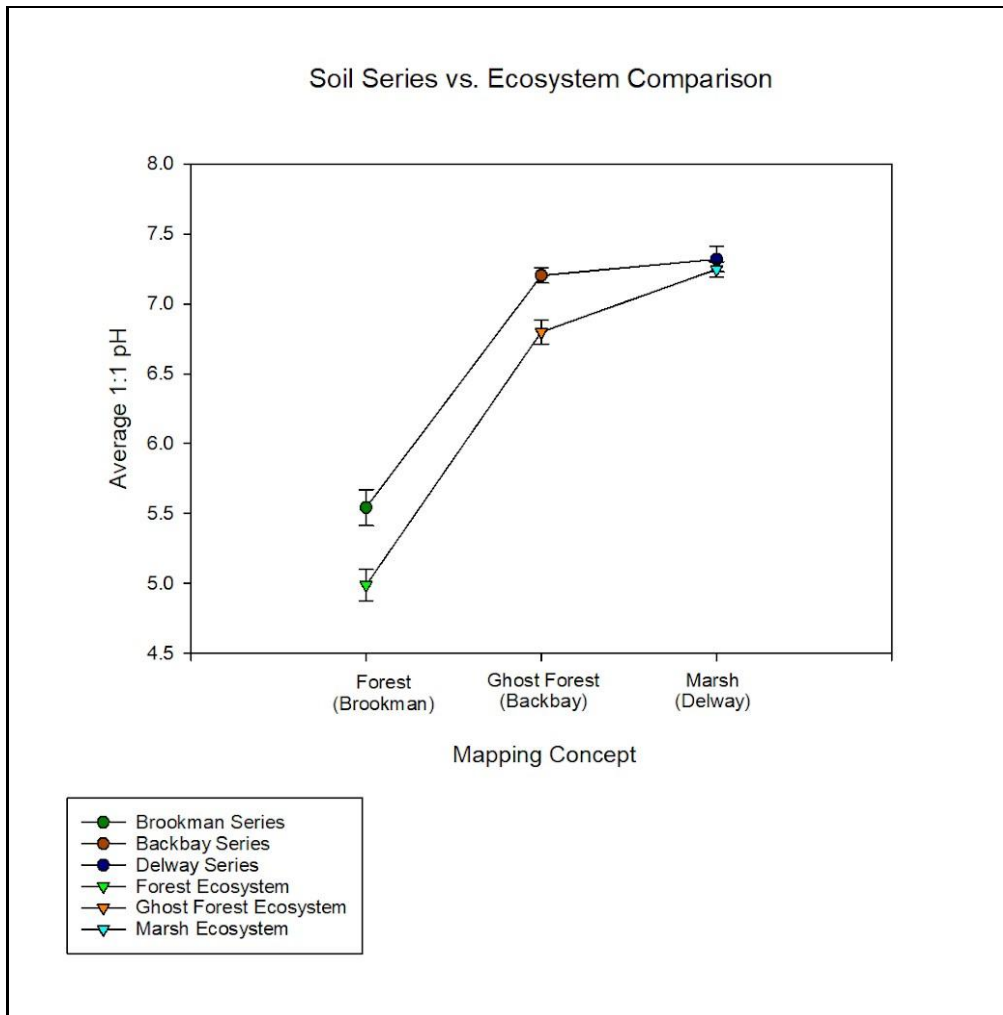


Figure A2. Representation of covariate relationship between mapped Soil Series and Ecosystem type. Similarities reveal that soil series were classified based on the soil characteristics of representative ecosystems.

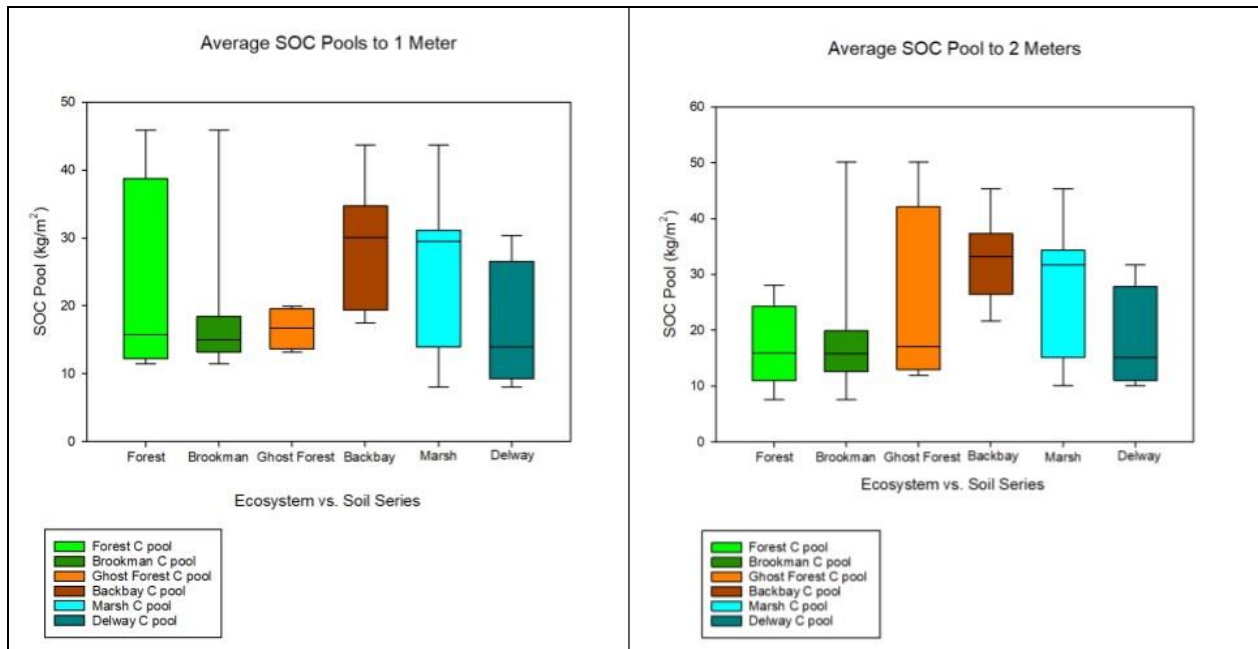


Figure A3. Box plots of SOC pools across Soil Series and Ecosystem type. Distributions of box plots reveal how much carbon data the current series classification misses when classifying on concept alone and only sample to 1 meter depths. Generally, the soil series maintained similar carbon pools in 1 and 2 meters.

Appendix B:

Blue Carbon storage data is lacking, with little information on its extent, storage, and fate in the wake of SLR. Thick vegetation and frequent inundation can make terrain difficult to travel and carry equipment through, leading to the areas being overlooked for sampling and therefore missing accurate data on blue carbon storage. Looking for methods to quantify distribution and storage potential is imperative as we look for new ways to manage carbon pools as greenhouse gas content continues to rise and global temperatures increase.

There is a general uncertainty in global soil organic carbon (SOC) stocks, especially for 'blue carbon' stocks in coastal ecosystems, and they are often overestimated. Estimates on global carbon pools typically come from terrestrial and marine environments but the coastal ecosystems that provide blue carbon sinks are underrepresented. In Holmquist et al (2018), mapping data was synthesized from the SSURGO database and researchers found that there was a 42.8% misclassification of organic soils as minerals. The synthesis also found that current SSURGO data lacked precision compared to independently generated maps and that a lack of precision has the potential to overestimate carbon stocks.

Carbon content for each horizon was multiplied by respective bulk density to determine soil organic carbon density. SOC density was then multiplied by horizon depth and 0.1 for measured carbon stock in kg/m².

Equation 1:

$$(BD \text{ (g/cm}^3\text{)} * C \text{ \%}) * (\text{depth (cm)}*0.1) = \text{kg C/m}^2$$

Estimates were made for pedons that were described but not sampled. Field descriptions were used to gather data on horizon type and texture to use in classifying unsampled horizons into multipliers. Depths were also noted for unsampled horizons for calculations on estimated SOC stock using said multipliers. Calculations were consistent with equations from the Kim

(2022) thesis and the Manetta (2023) thesis, both being companion studies to this one, with modifications to more accurately describe the variations in the NC soils.

To verify the validity of this method, data from sampled horizons were run through the same method to calculate their SOC estimates. Depths for individual horizons were multiplied by the SOC densities that correspond to that horizon's fluidity and designation. The SOC estimates were then compared to the lab analysis for carbon percentages using a simple regression.

For this study, some pedons were described in-field, but no samples were collected. To estimate the carbon stocks at these sites, the depth of each horizon was multiplied by a soil organic carbon (SOC) class multiplier. Multipliers were determined using the horizons that were sampled from the field. A horizon's fluidity and taxonomic designation were used to reclassify them into Oi/Oe, Oa, Mucky A, A, Fluid subsoil, and Sandy subsoil groups (Table 6). SOC class multipliers were then determined by multiplying the average bulk density (g/cm³) by the average C % for each multiplier group.

Equation 2:

$$(\text{mean BD (g/cm}^3\text{)} * \text{mean (C \%)}) = \text{SOC class multiplier (g/cm}^3\text{)}$$

Once the SOC class multiplier was determined, the depth for each described horizon was multiplied by its corresponding class to estimate the SOC stock for unsampled pedons.

Equation 3:

$$\text{Depth (cm)} * \text{SOC class multiplier (g/cm}^3\text{)} = \text{Estimate SOC stock (g/cm}^2\text{)}$$

The estimated SOC stock (g/cm²) would be converted to kg/m² for further analysis and calculation. To verify the validity of this method, sampled pedons analyzed in the lab had SOC estimates calculated using the same method. The estimates were regressed against their measured SOC stocks to determine how accurate the prediction was (Fig. 6). Regression analysis revealed a highly significant correlation (R²: 0.95).

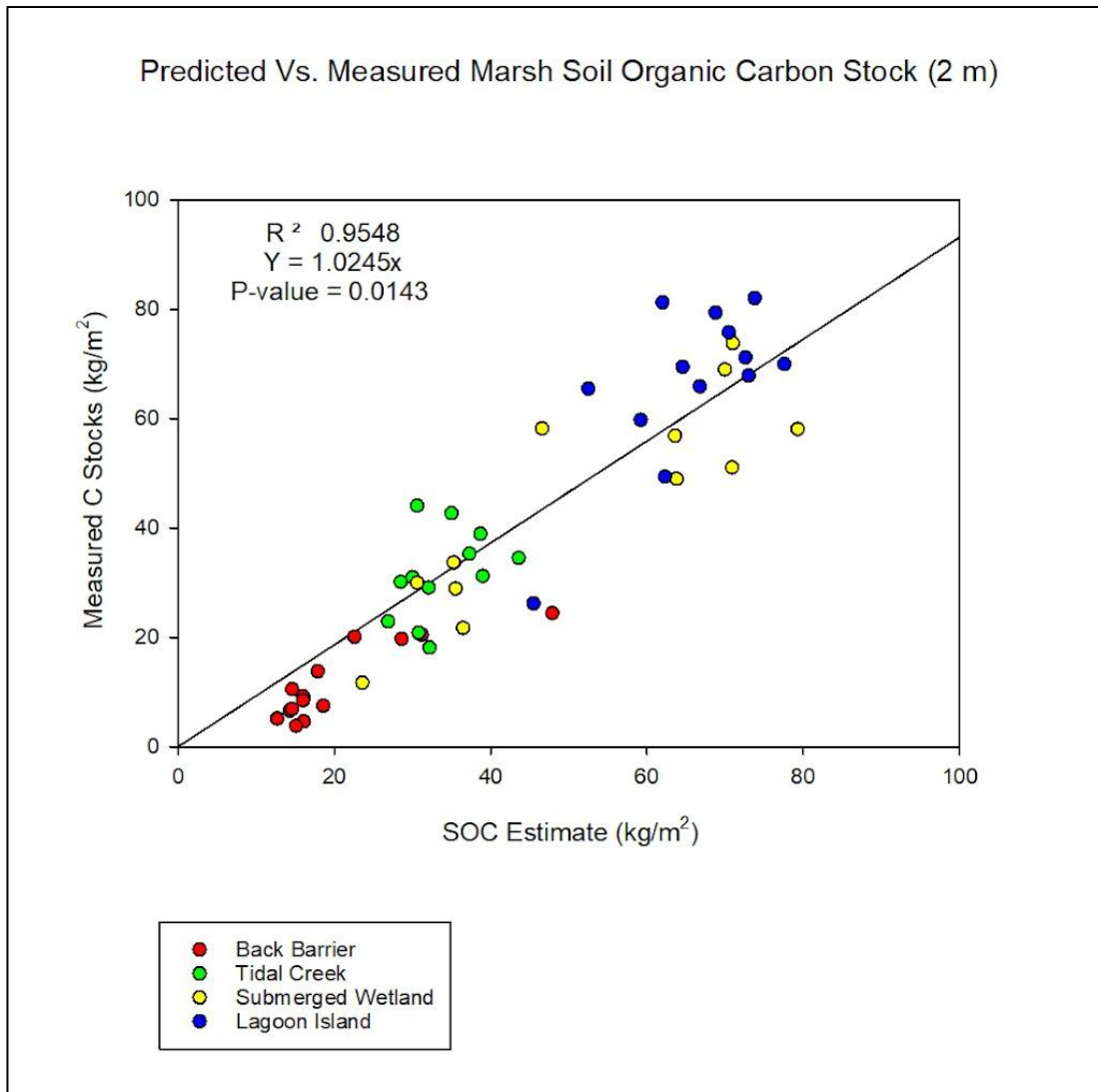


Fig. B1: Regression analysis between estimates and measurements for the same pedons.

In Figure 6, it's worth noting the two outliers from the BB and LI sites. First, the BB point has a higher SOC estimate than its companion points. In the field, this pedon was described as having only 3 horizons, and the final horizon was described at 49 - 132 cm, making it 83 cm in depth. This bottom horizon also saw a spike of organic matter and was described as a buried organic horizon, meaning that the SOC multiplier was 0.404 instead of the 0.05 for sandy subsoils that most other subsoil horizons were described with. The combination of having a large horizon depth and a larger SOC multiplier calculated the largest SOC estimate for the BB sites. The LI outlier had a similar issue. In this case, it was described as having only 2 horizons, both

of which were measured to have high carbon, but only one was designated as an organic horizon, and the other was classified as a mucky mineral A horizon. The LI PGU sites all came out as highly organic and therefore had higher SOC multipliers. However, since the pedon was described as having only 2 horizons, one of which was mineral, its overall SOC estimate was calculated to be much lower than the average estimate for all LI sites.

Based on the outliers in Figure 6, understanding horizon description in the field becomes imperative for understanding carbon density. If a pedon cannot be described in proper detail in the field, specifically horizon designations, depth, texture, and texture modifiers then carbon may be over or underestimated. Carbon pools are driven by the depth of the O and mucky A horizons and if these cannot be distinguished, or if a researcher neglects these details to opt for a faster description, then the SOC estimates would be inaccurate.

The estimates calculated cannot be treated as legitimate data and this method does not replace physical sampling in the field, however, the method has useful applications for estimations. General estimations for carbon stocks can be used in future studies to give us a better understanding of the distribution and extent of blue carbon in those hard-to-access areas.

Appendix C:

Site characteristics were investigated in field and through online applications such as ArcGIS Pro and Google Earth. The Guide to Common Wetland Plants of North Carolina was used to verify field notes on dominant plant species (Gianopulos, et al. 2021).

Table C1. Summary of Water and Sampling Data Taken at Each Transect (Chapter 2)

Transects	Salinity (ppt)	Dissolved Oxygen (mg/L)	Water pH	Sampled Pedons
1	14.62	0.97	7.04	7
2	13.74	0.56	7.20	5
3	14.90	0.72	7.93	6
			Total	18

Table C2. Site Location and vegetation by Pedon (Chapter 2)

Pedon	Ecosystem Mapped (2023)	Soil Series Mapped (1910)	Distance to Open Water (m)	Live Trees	Dead Trees	Dominant Shrubs	Dominant Emergents
1.1	Marsh	Delway	155	-	-	-	<i>J. roemerianus</i>
1.3	Marsh	Backbay	812	-	-	-	<i>J. roemerianus</i>
1.5	Ghost Forest	Brookman	992	7	6	<i>M. cerifera</i> , <i>C. thyoides</i> (saplings)	<i>P. australis</i>
1.6	Ghost Forest	Brookman	1100	9	27	<i>M. cerifera</i>	<i>J. roemerianus</i> , <i>P. australis</i> , <i>S. alterniflora</i>
2.1	Marsh	Backbay	16	1	-	-	<i>J. roemerianus</i> , <i>S. alterniflora</i>
2.2	Ghost Forest	Backbay	71	14	16	-	<i>J. roemerianus</i> , <i>S. alterniflora</i>
2.4	Forest	Brookman	432	12	8	<i>M. cerifera</i> , <i>C. thyoides</i> (saplings)	<i>P. australis</i> , <i>T. radicans</i>
3.1	Marsh	Delway	52	-	-	-	<i>J. roemerianus</i>
3.2	Marsh	Backbay	266	5	1	-	<i>S. patens</i> , <i>I. frutescens</i>
3.3	Ghost Forest	Brookman	519	-	1	-	<i>S. patens</i> , <i>J. roemerianus</i>
3.6	Forest	Brookman	1242	5	-	<i>M. cerifera</i>	<i>S. alterniflora</i> , <i>T. radicans</i>

Table C3-1: Pedon Horizon data PI 1-1

Horizons	Depth (cm)	Von Post	Texture				Bulk Density (g/cm ³)	1:1 DI pH			Elements (%)	
			Sand (%)	Silt (%)	Clay (%)	Initial pH		Final pH	1:5 EC (dS/m)	C	N	
A	0-13	-	91.6	3.5	5.0	0.68	7.05	7.06	1.92	2.19	0.16	
ACse	13-30	-	95.9	0.5	3.7	1.26	7.16	6.08	0.95	0.29	0.02	
Cseg	30-55	-	96.3	0.0	3.7	1.50	7.61	5.08	0.62	0.06	0.02	
CAseg	55-72	-	96.8	0.8	2.5	1.39	7.71	5.70	0.70	0.10	0.02	
C'seg	72-114	-	91.5	4.8	3.7	1.42	7.55	7.23	0.85	0.04	0.02	

Table C3-2: Pedon Horizon data PI 1-3

Horizons	Depth (cm)	Von Post	Texture				Bulk Density (g/cm ³)	1:1 DI pH			Elements (%)	
			Sand (%)	Silt (%)	Clay (%)	Initial pH		Final pH	1:5 EC (dS/m)	C	N	
Ase	0-12	-	84.0	3.8	12.2	0.32	7.12	5.09	3.46	9.65	0.38	
CAse	12-24	-	87.1	7.5	5.4	1.15	7.08	4.73	4.12	0.57	0.03	
Cseg1	24-40	-	94.1	3.4	2.5	1.63	7.18	4.03	2.72	0.03	0.02	
Cseg2	40-102	-	96.8	0.0	3.2	1.47	7.19	4.35	3.21	0.05	0.02	

Table C3-3: Pedon Horizon data PI 1-5

Horizons	Depth (cm)	Von Post	Texture				Bulk Density (g/cm ³)	1:1 DI pH			Elements (%)	
			Sand (%)	Silt (%)	Clay (%)	Initial pH		Final pH	1:5 EC (dS/m)	C	N	
Ase1	0-17	-	70.2	14.3	15.5	0.85	7.44	5.71	4.64	6.04	0.25	
Ase2	17-26	-	83.3	8.9	7.8	1.04	6.97	4.20	4.92	2.28	0.12	
Cseg1	26-63	-	96.7	0.0	3.3	3.05	7.45	3.64	2.70	0.03	0.02	
Cseg2	63-90	-	96.3	0.0	3.7	2.73	7.18	4.24	2.60	0.03	0.02	
Cseg3/Ase	90-107	-	94.6	0.5	4.9	2.86	7.08	4.09	2.92	0.19	0.02	

Table C3-4: Pedon Horizon data PI 2-1

Horizons	Depth (cm)	Von Post	Texture				Bulk Density (g/cm ³)	1:1 DI pH			Elements (%)	
			Sand (%)	Silt (%)	Clay (%)	Initial pH		Final pH	1:5 EC (dS/m)	C	N	
Oa/A	0-13	-	82.6	5.6	11.8	0.71	5.89	6.30	2.27	5.11	0.29	
Cseg1	13-29	-	97.5	0.0	2.5	1.50	7.17	5.51	1.28	0.13	0.02	
Cseg2	29-69	-	96.8	0.0	3.2	1.42	7.14	5.10	1.43	0.03	0.02	
Cseg3	69-101	-	96.3	0.0	3.7	1.46	7.21	5.42	2.72	0.03	0.02	

Table C3-5: Pedon Horizon data PI 2-3

Horizons	Depth (cm)	Von Post	Texture				Bulk Density (g/cm ³)	1:1 DI pH			Elements (%)	
			Sand (%)	Silt (%)	Clay (%)	Initial pH		Final pH	1:5 EC (dS/m)	C	N	
Oe	0-5	H4	-	-	-	0.43	6.73	5.44	4.61	17.66	0.94	
ACse	5-19	-	86.7	5.9	7.4	1.14	6.93	4.33	4.19	3.58	0.19	
Cseg1	19-65	-	90.7	6.8	2.5	1.46	7.27	5.15	2.89	0.03	0.02	
Cseg2	65-105	-	97.5	0.0	2.5	1.45	7.31	5.30	3.06	0.03	0.02	

Table C3-6: Pedon Horizon data PI 2-5A

Horizons	Depth (cm)	Von Post	Texture				Bulk Density (g/cm ³)	1:1 DI pH			Elements (%)	
			Sand (%)	Silt (%)	Clay (%)	Initial pH		Final pH	1:5 EC (dS/m)	C	N	
Oase	0-14	H8	-	-	-	0.20	6.77	4.40	7.12	12.29	0.74	
ACse	14-32	-	90.8	3.2	6.0	1.01	7.60	4.91	7.43	0.71	0.05	
Cseg1	32-76	-	97.5	0.0	2.5	1.37	7.49	5.16	7.38	0.03	0.02	
Cseg2	76-103	-	96.3	0.0	3.7	1.45	7.44	5.17	7.30	0.03	0.02	

Table C3-7: Pedon Horizon data PI 2-5B

Horizons	Depth (cm)	Von Post	Texture				Bulk Density (g/cm ³)	1:1 DI pH			Elements (%)	
			Sand (%)	Silt (%)	Clay (%)	Initial pH		Final pH	1:5 EC (dS/m)	C	N	
Oase	0-14	H8	-	-	-	0.22	6.78	6.80	6.79	18.04	1.03	
ACse	14-32	-	90.8	3.2	6.0	1.00	7.10	4.61	7.02	0.63	0.07	
Cseg1	32-76	-	97.5	0.0	2.5	1.42	7.24	4.94	6.93	0.03	0.02	
Cseg2	76-103	-	96.3	0.0	3.7	1.48	7.31	5.12	7.07	0.03	0.02	

Table C3-8: Pedon Horizon data PI 2-5C

Horizons	Depth (cm)	Von Post	Texture				Bulk Density (g/cm ³)	1:1 DI pH			Elements (%)	
			Sand (%)	Silt (%)	Clay (%)	Initial pH		Final pH	1:5 EC (dS/m)	C	N	
Oase	0-14	H8	-	-	-	0.22	6.49	5.44	6.24	12.75	0.51	
ACse	14-32	-	90.8	3.2	6.0	1.33	7.09	5.50	6.90	0.59	0.03	
Cseg1	32-76	-	97.5	0.0	2.5	1.44	7.05	5.03	6.90	0.03	0.02	
Cseg2	76-103	-	96.3	0.0	3.7	1.54	7.11	5.16	7.01	0.08	0.02	

Table C3-9: Pedon Horizon data PI 3-1

Horizons	Depth (cm)	Von Post	Texture				Bulk Density (g/cm ³)	1:1 DI pH			Elements (%)	
			Sand (%)	Silt (%)	Clay (%)	Initial pH		Final pH	1:5 EC (dS/m)	C	N	
Ase	0-4	-	92.7	2.8	4.4	0.77	7.63	8.03	2.48	4.21	0.41	
ACseg	4-25	-	96.3	0.0	3.7	1.40	7.87	8.66	2.18	0.09	0.02	
Cseg1	25-63	-	97.5	0.0	2.5	1.44	8.00	8.81	2.40	0.03	0.02	
Cseg2	63-103	-	96.3	0.0	3.7	1.56	7.95	9.01	2.48	0.08	0.02	

Table C3-10: Pedon Horizon data PI 3-3

Horizons	Depth (cm)	Von Post	Texture				Bulk Density (g/cm ³)	1:1 DI pH			Elements (%)	
			Sand (%)	Silt (%)	Clay (%)	Initial pH		Final pH	1:5 EC (dS/m)	C	N	
Ase	0-8	-	89.5	0.5	10.0	0.58	7.14	8.08	5.38	5.98	0.39	
CAse	8-23	-	93.3	1.7	5.0	1.46	7.60	8.47	3.64	0.20	0.02	
Cseg1	23-60	-	97.5	0.0	2.5	1.53	7.77	8.35	2.73	0.03	0.02	
Cseg2	60-101	-	98.8	0.5	0.8	1.53	7.73	7.96	2.59	0.03	0.02	

Table C3-11: Pedon Horizon data PI 3-5

Horizons	Depth (cm)	Von Post	Texture				Bulk Density (g/cm ³)	1:1 DI pH			Elements (%)	
			Sand (%)	Silt (%)	Clay (%)	Initial pH		Final pH	1:5 EC (dS/m)	C	N	
Oese	0-17	H4	-	-	-	0.23	5.73	4.98	3.18	16.50	1.02	
CAse	17-28	-	96.3	0.8	2.9	1.47	6.78	4.54	3.04	0.36	0.02	
Cseg	28-62	-	96.7	0.0	3.3	1.48	7.01	5.12	2.69	0.08	0.02	
CA'seg	62-78	-	97.6	0.7	1.6	1.46	7.07	5.00	2.61	0.03	0.02	
C'seg	78-100	-	96.3	0.0	3.7	1.37	7.37	5.28	2.45	0.05	0.02	

Table C3-12: Pedon Horizon data PI 4-1

Horizons	Depth (cm)	Von Post	Texture				Bulk Density (g/cm ³)	1:1 DI pH			Elements (%)	
			Sand (%)	Silt (%)	Clay (%)	Initial pH		Final pH	1:5 EC (dS/m)	C	N	
A	0-25	-	69.7	12.4	18.0	0.18	5.81	6.51	3.10	10.66	0.78	
Cseg	25-69	-	96.3	0.0	3.7	1.45	6.29	4.59	1.44	0.12	0.02	
2Oaseb/Cseg	69-114	-	90.2	4.9	4.9	0.76	7.14	5.12	1.78	3.09	0.18	
2Oeseb	114- 123	H5	-	-	-	0.19	7.46	5.78	1.49	14.13	0.79	

Table C3-13: Pedon Horizon data PI 4-3

Horizons	Depth (cm)	Texture				Bulk Density (g/cm ³)	1:1 DI pH			Elements (%)	
		Von Post	Sand (%)	Silt (%)	Clay (%)		Initial pH	Final pH	1:5 EC (dS/m)	C	N
Oe	0-6	H5	-	-	-	0.22	6.38	6.44	4.12	15.92	0.99
Ase	6-21	-	89.2	4.9	5.9	0.98	5.83	4.07	2.33	2.31	0.16
Cseg1	21-40	-	96.3	0.8	3.0	1.39	6.78	4.62	1.99	0.14	0.02
Cseg2	40-88	-	96.9	0.6	2.5	1.44	7.26	4.53	2.48	0.04	0.02
2Oaseb/Cseg	88- 154+	-	89.7	4.6	5.7	0.48	7.28	5.08	3.62	4.05	0.23

Table C3-14: Pedon Horizon data PI 4-5

Horizons	Depth (cm)	Texture				Bulk Density (g/cm ³)	1:1 DI pH			Elements (%)	
		Von Post	Sand (%)	Silt (%)	Clay (%)		Initial pH	Final pH	1:5 EC (dS/m)	C	N
Ase	0-24	-	75.3	11.2	13.5	0.45	7.42	5.43	4.39	5.81	0.35
Cseg	24-49	-	92.5	2.0	5.5	1.31	7.69	4.39	1.63	0.35	0.02
2Oaseb	49-132	H9	-	-	-	0.16	7.40	5.21	1.48	12.00	0.59

Table C3-15: Pedon Horizon data PIV 1-1

Horizons	Depth (cm)	Von Post	Texture				Bulk Density (g/cm ³)	1:1 DI pH			Elements (%)	
			Sand (%)	Silt (%)	Clay (%)	Initial pH		Final pH	1:5 EC (dS/m)	C	N	
Ase	0-17	-	84.5	3.6	11.9	0.67	6.65	7.00	1.87	5.31	0.33	
Cg	17-55	-	90.0	8.0	2.0	1.53	7.12	5.31	2.11	0.16	0.04	
Cseg1	55-104	-	89.5	8.5	2.0	1.36	7.82	8.77	2.13	0.04	0.04	
Cseg2	104-144	-	90.5	7.6	1.9	1.55	8.37	8.26	2.26	0.12	0.04	
2Cg	144-180	-	90.2	8.3	1.5	1.27	8.09	8.24	2.97	0.04	0.04	

Table C3-16: Pedon Horizon data PIV 2-1

Horizons	Depth (cm)	Von Post	Texture				Bulk Density (g/cm ³)	1:1 DI pH			Elements (%)	
			Sand (%)	Silt (%)	Clay (%)	Initial pH		Final pH	1:5 EC (dS/m)	C	N	
Ase	0-18	-	85.2	3.6	11.2	0.58	7.19	7.59	0.34	9.03	0.65	
Cseg1	18-31	-	98.2	0.0	1.8	1.48	7.19	8.25	0.27	0.44	0.04	
Cseg2	31-81	-	98.9	0.4	0.7	1.59	7.53	7.08	0.46	0.07	0.04	
2Aseb	81-102	-	89.6	6.2	4.1	0.73	7.01	6.40	0.52	4.95	0.28	
2Cseg1	102-171	-	99.0	0.3	0.7	1.50	7.42	8.15	0.20	0.07	0.04	
2Cseg2	171-217+	-	94.1	2.8	3.2	1.39	8.26	8.40	0.24	0.23	0.04	

Table C3-17: Pedon Horizon data BI 1-2

Horizons	Depth (cm)	Von Post	Texture				Bulk Density (g/cm ³)	1:1 DI pH			Elements (%)	
			Sand (%)	Silt (%)	Clay (%)	Initial pH		Final pH	1:5 EC (dS/m)	C	N	
Aseg	0-23	-	37.1	41.3	21.6	0.78	7.35	7.32	7.07	5.61	0.32	
Cseg1	23-65	-	32.0	43.3	24.7	0.54	7.47	6.23	6.96	3.48	0.26	
Cseg2	65-107	-	78.1	10.4	11.6	1.10	7.62	8.21	5.68	1.30	0.11	
Cseg3	107-140	-	69.3	17.4	13.3	1.01	7.47	7.59	6.41	1.53	0.12	
Cseg4	140-185	-	80.1	7.4	12.6	1.30	7.60	7.87	6.33	1.26	0.10	

Table C3-18: Pedon Horizon data BI 1-4

Horizons	Depth (cm)	Von Post	Texture				Bulk Density (g/cm ³)	1:1 DI pH			Elements (%)	
			Sand (%)	Silt (%)	Clay (%)	Initial pH		Final pH	1:5 EC (dS/m)	C	N	
Aseg	0-25	-	33.4	45.3	21.4	0.74	7.49	7.37	9.56	4.92	0.40	
Cseg1	25-66	-	54.0	31.3	14.8	0.50	7.49	4.77	6.96	2.86	0.20	
Cseg2	66-127	-	59.8	24.1	16.0	0.68	7.46	4.39	6.60	2.70	0.17	
Cseg3	127-165	-	65.1	14.8	20.1	0.89	7.46	5.36	6.26	1.90	0.13	
Cseg4	165-200+	-	86.5	3.3	10.2	1.27	7.62	8.31	5.33	0.62	0.04	

Table C3-19: Pedon Horizon data BI 1-6

Horizons	Depth (cm)	Von Post	Texture			Bulk Density (g/cm ³)	1:1 DI pH			Elements (%)	
			Sand (%)	Silt (%)	Clay (%)		Initial pH	Final pH	1:5 EC (dS/m)	C	N
Aseg	0-21	-	48.6	32.5	18.9	0.58	7.62	7.72	10.37	4.19	0.32
Cseg1	21-71	-	49.8	33.0	17.3	0.62	7.40	7.79	8.92	3.61	0.23
Cseg2	71-107	-	54.4	24.8	20.8	0.82	7.74	8.09	6.39	2.45	0.17
Cseg3	107-184	-	76.8	9.9	13.3	1.53	7.81	8.24	6.69	1.35	0.07

Table C3-20: Pedon Horizon data BI 2-1

Horizons	Depth (cm)	Von Post	Texture			Bulk Density (g/cm ³)	1:1 DI pH			Elements (%)	
			Sand (%)	Silt (%)	Clay (%)		Initial pH	Final pH	1:5 EC (dS/m)	C	N
Ase	0-21	-	45.8	35.0	19.2	0.47	7.65	7.62	10.18	4.79	0.38
Cseg1	21-74	-	60.8	21.3	17.9	1.14	7.70	7.63	6.79	2.30	0.16
Cseg2	74-133	-	61.1	22.8	16.1	0.91	7.75	8.32	7.10	2.40	0.13
Cseg3	133-150	-	50.7	25.5	23.8	0.72	7.78	8.21	7.13	2.60	0.15

Table C3-21: Pedon Horizon data BI 2-3

Horizons	Depth (cm)	Von Post	Texture				Bulk Density (g/cm ³)	1:1 DI pH			Elements (%)	
			Sand (%)	Silt (%)	Clay (%)	Initial pH		Final pH	1:5 EC (dS/m)	C	N	
Ase	0-40	-	63.8	19.7	16.4	0.66	7.76	7.73	8.52	2.40	0.19	
Cseg1	40-104	-	69.6	14.5	15.9	0.81	7.93	8.21	6.86	1.56	0.10	
Cseg2	104- 150	-	83.5	4.4	12.1	1.09	8.06	8.25	6.02	1.40	0.06	

Table C3-22: Pedon Horizon data BI 2-5

Horizons	Depth (cm)	Von Post	Texture				Bulk Density (g/cm ³)	1:1 DI pH			Elements (%)	
			Sand (%)	Silt (%)	Clay (%)	Initial pH		Final pH	1:5 EC (dS/m)	C	N	
Ase	0-10	-	60.5	25.3	14.2	0.37	7.10	6.07	7.50	3.35	0.22	
Cseg1	10-23	-	96.7	1.6	1.7	1.23	7.65	6.53	4.55	0.05	0.02	
Cseg2	23-47	-	46.9	34.5	18.6	0.56	7.24	8.05	6.69	3.41	0.22	
Cseg3	47-76	-	35.2	40.0	24.8	0.51	7.05	8.04	5.89	3.40	0.25	
Cseg4	76-140	-	86.0	3.9	10.1	1.07	7.51	8.97	6.63	0.90	0.06	

Table C3-23: Pedon Horizon data BI 3-2A

Horizons	Depth (cm)	Von Post	Texture			Bulk Density (g/cm ³)	1:1 DI pH			Elements (%)	
			Sand (%)	Silt (%)	Clay (%)		Initial pH	Final pH	1:5 EC (dS/m)	C	N
Aseg	0-36	-	63.9	21.4	14.7	1.02	7.28	7.79	6.95	1.72	0.15
Cseg1	36-101	-	88.0	5.8	6.2	1.20	7.85	8.54	5.16	0.41	0.03
Cseg2	101-142	-	77.1	12.8	10.1	1.44	7.83	8.48	4.73	0.55	0.04

Table C3-24: Pedon Horizon data BI 3-2B

Horizons	Depth (cm)	Von Post	Texture			Bulk Density (g/cm ³)	1:1 DI pH			Elements (%)	
			Sand (%)	Silt (%)	Clay (%)		Initial pH	Final pH	1:5 EC (dS/m)	C	N
Aseg	0-36	-	63.9	21.4	14.7	0.88	7.40	7.70	6.63	1.75	0.16
Cseg1	36-101	-	88.0	5.8	6.2	1.08	7.87	8.31	5.13	0.30	0.03
Cseg2	101-142	-	77.1	12.8	10.1	1.41	7.72	8.73	5.54	1.02	0.06

Table C3-25: Pedon Horizon data BI 3-2C

Horizons	Depth (cm)	Von Post	Texture			Bulk Density (g/cm ³)	1:1 DI pH			Elements (%)	
			Sand (%)	Silt (%)	Clay (%)		Initial pH	Final pH	1:5 EC (dS/m)	C	N
Aseg	0-36	-	63.9	21.4	14.7	0.85	7.18	7.79	6.49	2.84	0.27
Cseg1	36-101	-	88.0	5.8	6.2	1.38	7.82	8.16	6.15	0.60	0.04
Cseg2	101-142	-	77.1	12.8	10.1	1.36	7.77	8.57	5.27	0.68	0.05

Table C3-26: Pedon Horizon data BI 3-4

Horizons	Depth (cm)	Von Post	Texture			Bulk Density (g/cm ³)	1:1 DI pH			Elements (%)	
			Sand (%)	Silt (%)	Clay (%)		Initial pH	Final pH	1:5 EC (dS/m)	C	N
Aseg	0-42	-	79.3	8.6	12.1	0.77	7.28	4.70	6.75	1.64	0.12
Cseg1	42-98	-	75.5	20.4	4.1	0.65	7.42	4.32	6.21	1.64	0.12
Cseg2	98-125	-	83.4	4.4	12.1	1.19	7.34	5.00	6.15	0.89	0.08
Cseg3	125-150	-	92.7	1.5	5.9	1.59	7.46	3.85	5.49	0.33	0.04

Table C3-27: Pedon Horizon data BI 3-6

Horizons	Depth (cm)	Von Post	Texture			Bulk Density (g/cm ³)	1:1 DI pH			Elements (%)	
			Sand (%)	Silt (%)	Clay (%)		Initial pH	Final pH	1:5 EC (dS/m)	C	N
Ase	0-29	-	37.4	44.9	17.7	0.44	7.32	7.67	9.27	6.03	0.46
ACseg	29-52	-	28.4	55.1	16.6	0.40	7.20	7.66	8.34	5.69	0.42
Cseg1	52-104	-	34.3	41.9	23.8	0.47	7.43	8.03	6.51	4.11	0.30
Cseg2	104-152	-	88.3	0.8	11.0	1.77	7.60	8.43	6.25	0.68	0.04

Table C3-28: Pedon Horizon data BI 4-1

Horizons	Depth (cm)	Von Post	Texture				Bulk Density (g/cm ³)	1:1 DI pH			Elements (%)	
			Sand (%)	Silt (%)	Clay (%)	Initial pH		Final pH	1:5 EC (dS/m)	C	N	
Aseg	0-16	-	39.5	41.3	19.1	0.45	7.42	7.55	6.73	5.08	0.42	
Cseg1	16-83	-	66.5	19.6	13.9	0.68	7.70	8.01	5.11	2.53	0.16	
Cseg2	83-153	-	79.9	7.4	12.8	0.99	7.84	8.49	4.56	1.36	0.07	
Cseg3	153- 180	-	60.8	19.8	19.4	1.06	7.57	8.16	5.08	1.66	0.12	
Cseg4	180- 200+	-	83.5	5.2	11.4	1.32	7.65	8.27	4.62	0.69	0.05	

Table C3-29: Pedon Horizon data BI 4-3

Horizons	Depth (cm)	Von Post	Texture				Bulk Density (g/cm ³)	1:1 DI pH			Elements (%)	
			Sand (%)	Silt (%)	Clay (%)	Initial pH		Final pH	1:5 EC (dS/m)	C	N	
Aseg	0-18	-	34.1	41.6	24.3	0.40	7.20	6.40	6.64	4.93	0.42	
Cseg1	18-65	-	38.4	38.0	23.5	0.41	7.52	5.78	5.73	3.66	0.29	
Cseg2	65-135	-	76.2	11.1	12.7	0.92	7.58	4.44	6.89	1.57	0.12	

Table C3-30: Pedon Horizon data BI 4-5

Horizons	Depth (cm)	Von Post	Texture			Bulk Density (g/cm ³)	1:1 DI pH			Elements (%)	
			Sand (%)	Silt (%)	Clay (%)		Initial pH	Final pH	1:5 EC (dS/m)	C	N
Aseg	0-11	-	68.6	16.8	14.7	0.57	7.29	4.11	5.86	3.05	0.18
Cseg1	11-33	-	80.6	8.5	10.9	1.09	7.49	4.58	4.55	1.23	0.08
Cseg2	33-105	-	90.3	0.5	9.2	1.32	7.77	8.04	3.43	0.75	0.05
Cseg3	105-150	-	29.2	44.2	26.5	0.68	7.50	7.07	4.13	2.95	0.24

Table C3-31: Pedon Horizon data JB 1-2

Horizons	Depth (cm)	Von Post	Texture			Bulk Density (g/cm ³)	1:1 DI pH			Elements (%)	
			Sand (%)	Silt (%)	Clay (%)		Initial pH	Final pH	1:5 EC (dS/m)	C	N
Oese	0-34	H5	-	-	-	0.23	6.20	5.51	4.34	12.37	0.64
Oase1	34-51	H7	-	-	-	0.22	6.98	5.61	4.17	13.06	0.63
Oase2	51-73	H9	-	-	-	0.21	6.85	5.59	4.11	16.53	0.66
Oase3	73-128	H9	-	-	-	0.20	6.86	5.66	4.81	18.42	0.64
2Ase	128-169	-	60.3	24.2	15.5	1.02	6.86	4.40	3.41	2.71	0.10
2Eseg	169-182	-	63.2	23.3	13.5	2.26	7.17	3.81	2.27	0.57	0.03
2Btg	182-200+	-	61.0	20.6	18.4	1.89	7.22	4.32	2.20	0.41	0.02

Table C3-32: Pedon Horizon data JB 1-4

Horizons	Depth (cm)	Von Post	Texture			Bulk Density (g/cm ³)	1:1 DI pH			Elements (%)	
			Sand (%)	Silt (%)	Clay (%)		Initial pH	Final pH	1:5 EC (dS/m)	C	N
Oe	0-16	H4	-	-	-	0.24	6.10	4.88	4.05	25.51	1.21
Oese	16-34	H5	-	-	-	0.10	6.91	5.28	3.84	29.13	1.07
2Oase	34-62	H7	-	-	-	0.24	6.91	5.36	3.20	24.43	0.85
3Ase1	62-72	-	53.1	33.5	13.4	0.92	6.89	5.84	2.85	3.86	0.15
3Ase2	72-102	-	52.6	33.7	13.7	1.08	6.66	6.00	2.26	3.02	0.10
3ACse	102-134	-	49.5	32.5	18.0	1.42	6.64	5.57	2.43	1.81	0.08
3Cseg	134-150	-	46.6	35.6	17.8	1.77	6.67	5.32	2.22	1.43	0.07

Table C3-33: Pedon Horizon data JB 1-6

Horizons	Depth (cm)	Von Post	Texture			Bulk Density (g/cm ³)	1:1 DI pH			Elements (%)	
			Sand (%)	Silt (%)	Clay (%)		Initial pH	Final pH	1:5 EC (dS/m)	C	N
Oese	0-29	H5	-	-	-	0.05	5.86	4.89	3.34	30.90	1.46
2Oese	29-52	H5	-	-	-	0.10	6.63	5.52	2.25	26.36	1.03
3Ase	52-86	-	51.2	29.3	19.5	0.93	6.05	5.53	2.07	4.99	0.19
3Cseg	86-120	-	56.5	25.5	18.0	1.87	5.68	5.18	1.81	0.89	0.05

Table C3-34: Pedon Horizon data RB 1-2

Horizons	Depth (cm)	Von Post	Texture			Bulk Density (g/cm ³)	1:1 DI pH			Elements (%)	
			Sand (%)	Silt (%)	Clay (%)		Initial pH	Final pH	1:5 EC (dS/m)	C	N
Oese1	0-32	H5	-	-	-	0.11	7.26	6.00	4.62	16.78	0.73
Oese2	32-74	H6	-	-	-	0.25	7.45	6.28	3.96	12.31	0.48
2ACse	74-93	-	35.4	48.4	16.1	0.50	7.25	4.93	3.53	6.85	0.35
3Ase	93-125	-	44.7	36.7	18.6	0.63	7.20	5.27	4.16	7.73	0.34
3Cseg	125-200+	-	57.6	19.3	23.1	2.16	7.74	3.62	1.85	0.50	0.03

Table C3-35: Pedon Horizon data RB 1-4

Horizons	Depth (cm)	Von Post	Texture			Bulk Density (g/cm ³)	1:1 DI pH			Elements (%)	
			Sand (%)	Silt (%)	Clay (%)		Initial pH	Final pH	1:5 EC (dS/m)	C	N
Ase	0-38	-	54.1	26.6	19.3	0.39	5.49	5.24	4.63	7.70	0.36
ACse	38-52	-	44.6	39.8	15.6	0.48	7.13	5.64	4.17	5.76	0.34
2Ase	52-78	-	42.6	38.7	18.7	1.50	7.67	5.30	1.95	0.63	0.04
2Cg	78-100	-	40.9	35.9	23.2	1.26	7.27	6.37	2.32	0.26	0.03

Table C3-36: Pedon Horizon data RB 1-6

Horizons	Depth (cm)	Von Post	Texture				Bulk Density (g/cm ³)	1:1 DI pH			Elements (%)	
			Sand (%)	Silt (%)	Clay (%)	Initial pH		Final pH	1:5 EC (dS/m)	C	N	
Oese	0-27	H5	-	-	-	0.11	5.50	4.72	3.18	16.16	0.88	
2ACse	27-47	-	47.6	33.7	18.7	0.99	7.42	5.54	2.89	1.89	0.11	
2Cg1	47-69	-	37.7	33.9	28.4	1.20	7.45	6.78	1.67	0.25	0.03	
2Cg2	69-100+	-	32.5	33.1	34.3	1.13	6.97	5.53	2.48	0.17	0.03	

Table C3-37: Pedon Horizon data RB 2-2

Horizons	Depth (cm)	Von Post	Texture				Bulk Density (g/cm ³)	1:1 DI pH			Elements (%)	
			Sand (%)	Silt (%)	Clay (%)	Initial pH		Final pH	1:5 EC (dS/m)	C	N	
Oese	0-37	H6	-	-	-	0.14	5.56	4.77	2.81	19.14	1.07	
Oase	37-72	H7	-	-	-	0.16	6.80	5.66	4.10	18.53	0.76	
2Ase	72-86	-	48.9	34.5	16.6	0.28	6.89	5.77	2.82	8.20	0.32	
2Cseg1	86-104	-	57.8	28.6	13.6	1.12	7.17	6.21	1.72	0.55	0.02	
2Cseg2	104-138	-	58.7	18.5	22.8	1.87	7.28	5.00	1.91	0.30	0.02	

Table C3-38: Pedon Horizon data RB 2-4

Horizons	Depth (cm)	Von Post	Texture			Bulk Density (g/cm ³)	1:1 DI pH			Elements (%)	
			Sand (%)	Silt (%)	Clay (%)		Initial pH	Final pH	1:5 EC (dS/m)	C	N
Oe	0-18	H4	-	-	-	0.07	5.36	4.61	3.11	19.98	1.04
Oase1	18-42	H8	-	-	-	0.23	6.65	5.35	2.53	17.27	0.88
Oase2	42-54	H8	-	-	-	0.21	7.17	5.70	3.58	18.97	0.98
2Ase	54-72	-	37.7	48.7	13.7	0.73	7.17	6.21	2.72	5.86	0.25
2Ese	72-82	-	47.3	43.5	9.3	1.68	7.43	5.04	1.89	0.57	0.02
2BCtg	82-100	-	41.2	37.7	21.1	1.66	7.70	3.81	1.32	0.40	0.02

Table C3-39: Pedon Horizon data RB 2-6

Horizons	Depth (cm)	Von Post	Texture			Bulk Density (g/cm ³)	1:1 DI pH			Elements (%)	
			Sand (%)	Silt (%)	Clay (%)		Initial pH	Final pH	1:5 EC (dS/m)	C	N
Oise	0-13	H3	-	-	-	0.08	6.30	4.89	2.04	38.07	1.39
Oase1	13-28	H7	-	-	-	0.11	6.81	5.55	2.34	31.13	1.49
Oase2	28-76	H7	-	-	-	0.08	6.93	5.54	3.26	29.49	1.16
Oase3	76-101	H9	-	-	-	0.14	6.75	5.57	3.43	26.77	1.02
2Ase1	101-119	-	57.5	25.1	17.4	0.67	6.79	5.73	3.47	9.54	0.37
2Ase2	119-134	-	53.6	28.3	18.0	1.00	6.44	5.62	2.80	5.56	0.22
2Ase3	134+	-	-	-	-	0.94	6.34	5.59	2.50	4.93	0.20

Table C3-40: Pedon Horizon data SB 1-1

Horizons	Depth (cm)	Von Post	Texture			Bulk Density (g/cm ³)	1:1 DI pH			Elements (%)	
			Sand (%)	Silt (%)	Clay (%)		Initial pH	Final pH	1:5 EC (dS/m)	C	N
Oese	0-42	H5	-	-	-	0.25	6.86	5.34	4.88	14.33	0.77
Oase1	42-65	H7	-	-	-	0.12	6.78	5.57	6.16	13.06	0.54
Oase2	65-90	H7	-	-	-	0.14	6.79	5.12	6.12	12.24	0.55
Oase3	90-114	H9	-	-	-	0.26	6.73	5.01	6.27	12.53	0.53
O'ese	114-137	H5	-	-	-	0.18	6.80	4.87	5.12	22.58	0.89
2Oase	137-162	H7	-	-	-	0.18	6.66	4.30	5.40	22.39	0.81
3Ase1	162-190	-	52.7	42.2	5.1	0.22	6.65	5.56	6.46	11.27	0.48
3Ase2	190-200+	-	56.9	34.5	8.6	0.40	6.71	3.79	4.18	2.37	0.08

Table C3-41: Pedon Horizon data SB 1-4A

Horizons	Depth (cm)	Von Post	Texture			Bulk Density (g/cm ³)	1:1 DI pH			Elements (%)	
			Sand (%)	Silt (%)	Clay (%)		Initial pH	Final pH	1:5 EC (dS/m)	C	N
Oese1	0-34	H5	-	-	-	0.14	7.01	5.67	4.50	15.53	0.67
Oese2	34-72	H5	-	-	-	0.20	6.93	5.04	4.99	14.40	0.70
Oase1	72-107	H9	-	-	-	0.16	7.04	4.76	5.11	12.86	0.63
2Oase2	107-142	H8	-	-	-	0.34	6.79	4.31	6.21	24.22	0.74
3Ase	142-162	-	52.4	30.2	17.4	1.13	6.79	4.61	5.83	13.01	0.72
3ACse	162-175	-	71.2	15.3	13.5	1.59	6.89	5.70	3.62	2.05	0.06

Table C3-42: Pedon Horizon data SB 1-4B

Horizons	Depth (cm)	Von Post	Texture			Bulk Density (g/cm ³)	1:1 DI pH			Elements (%)	
			Sand (%)	Silt (%)	Clay (%)		Initial pH	Final pH	1:5 EC (dS/m)	C	N
Oese1	0-34	H5	-	-	-	0.13	6.94	5.14	4.59	19.29	0.89
Oese2	34-72	H5	-	-	-	0.25	7.09	5.37	5.90	13.38	0.39
Oase1	72-107	H9	-	-	-	0.22	7.04	5.54	6.11	12.11	0.45
2Oase2	107-142	H8	-	-	-	0.24	6.88	5.16	6.11	22.24	0.63
3Ase	142-162	-	52.4	30.2	17.4	0.51	6.83	5.35	6.15	7.15	0.27
3ACse	162-175	-	71.2	15.3	13.5	1.79	6.80	5.75	4.32	2.91	0.09

Table C3-43: Pedon Horizon data SB 1-4C

Horizons	Depth (cm)	Von Post	Texture			Bulk Density (g/cm ³)	1:1 DI pH			Elements (%)	
			Sand (%)	Silt (%)	Clay (%)		Initial pH	Final pH	1:5 EC (dS/m)	C	N
Oese1	0-34	H5	-	-	-	0.27	7.20	5.08	5.74	17.56	0.76
Oese2	34-72	H5	-	-	-	0.20	7.23	5.34	5.89	16.38	0.68
Oase1	72-107	H9	-	-	-	0.14	7.19	5.61	5.06	12.75	0.53
2Oase2	107-142	H8	-	-	-	0.26	6.88	5.12	6.06	22.71	0.67
3Ase	142-162	-	52.4	30.2	17.4	0.25	6.90	5.31	5.05	9.35	0.33
3ACse	162-175	-	71.2	15.3	13.5	1.47	6.90	5.82	3.80	4.38	0.15

Table C3-44: Pedon Horizon data SB 1-6

Horizons	Depth (cm)	Von Post	Texture			Bulk Density (g/cm ³)	1:1 DI pH			Elements (%)	
			Sand (%)	Silt (%)	Clay (%)		Initial pH	Final pH	1:5 EC (dS/m)	C	N
Oese	0-30	H4				0.14	6.78	5.72	4.20	30.02	0.94
Oase	30-58	H7				0.26	7.01	5.89	6.74	13.89	0.64
Ase	58-82	-	37.6	41.9	20.5	0.30	7.03	5.95	5.18	11.01	0.47
O'ase	82-110	H8				0.24	7.05	5.65	8.17	15.68	0.57
2Oase	110- 135	H9				0.24	6.97	5.61	4.50	13.61	0.43
3Ase	135- 169	-	71.6	19.0	9.4	1.11	6.88	5.53	3.33	3.26	0.12
3ACse	169- 200+	-	73.4	16.6	10.0	1.79	6.80	5.95	3.26	1.33	0.05

Table C3-45: Pedon Horizon data BPIS 1-2

Horizons	Depth (cm)	Von Post	Texture			Bulk Density (g/cm ³)	1:1 DI pH			Elements (%)	
			Sand (%)	Silt (%)	Clay (%)		Initial pH	Final pH	1:5 EC (dS/m)	C	N
Oese1	0-34	H5	-	-	-	0.12	7.21	6.62	2.62	27.87	1.41
Oese2	34-127	H5	-	-	-	0.13	7.04	6.41	3.34	27.29	1.14
Oase	127- 156	H7	-	-	-	0.14	7.04	6.19	3.29	19.81	0.85
Cseg	156- 184	-	38.5	40.8	20.8	0.48	6.92	5.75	3.17	4.23	0.22

Table C3-46: Pedon Horizon data BPIS 1-4

Horizons	Depth (cm)	Von Post	Texture			Bulk Density (g/cm ³)	1:1 DI pH			Elements (%)	
			Sand (%)	Silt (%)	Clay (%)		Initial pH	Final pH	1:5 EC (dS/m)	C	N
Oase	0-30	H7	-	-	-	0.10	5.58	5.79	1.18	32.38	1.85
Ase	30-100	-	32.7	42.1	25.3	0.23	7.08	4.96	2.46	8.86	0.59

Table C3-47 Pedon Horizon data BPIS 1-6

Horizons	Depth (cm)	Von Post	Texture			Bulk Density (g/cm ³)	1:1 DI pH			Elements (%)	
			Sand (%)	Silt (%)	Clay (%)		Initial pH	Final pH	1:5 EC (dS/m)	C	N
Oise	0-39	H3	-	-	-	0.54	5.55	5.31	1.72	19.78	1.08
Oase	39-92	H7	-	-	-	0.09	6.95	5.81	3.24	33.27	1.28
Oese1	92-137	H6	-	-	-	0.08	7.12	5.80	3.60	32.55	1.29
Oese2	137- 159	H5	-	-	-	0.09	6.86	6.36	3.22	20.71	0.81
2Ase	159- 180	-	54.5	28.0	17.5	0.20	7.01	5.69	2.64	4.45	0.20
2Cseg	180- 186	-	89.1	8.4	2.5	0.52	7.05	3.20	2.24	1.00	0.05

Table C3-48: Pedon Horizon data BUIS 1-1

Horizons	Depth (cm)	Von Post	Texture			Bulk Density (g/cm ³)	1:1 DI pH			Elements (%)	
			Sand (%)	Silt (%)	Clay (%)		Initial pH	Final pH	1:5 EC (dS/m)	C	N
Oa	0-17	H7	-	-	-	0.22	5.22	4.48	0.77	18.67	0.98
Oase	17-84	H7	-	-	-	0.36	6.93	5.86	1.65	12.37	0.83
Ase	84-107	-	32.8	50.0	17.2	0.22	6.99	5.81	0.19	10.87	0.72
ACse	107-200+	-	33.6	55.3	11.1	0.67	7.28	3.50	1.76	3.78	0.26

Table C3-49: Pedon Horizon data BUIS 1-3

Horizons	Depth (cm)	Von Post	Texture			Bulk Density (g/cm ³)	1:1 DI pH			Elements (%)	
			Sand (%)	Silt (%)	Clay (%)		Initial pH	Final pH	1:5 EC (dS/m)	C	N
Oase	0-20	H7	-	-	-	0.10	7.07	6.57	2.33	33.49	1.61
Oese	20-74	H5	-	-	-	0.09	7.03	6.29	2.57	23.14	1.12
2Ase	74-109	-	37.0	42.0	21.0	0.32	6.94	6.51	2.50	11.49	0.64
2ACseg	109-164	-	41.7	47.8	10.5	0.89	7.03	3.39	2.59	3.05	0.21
2Cseg	164-184	-	68.1	23.4	8.5	1.06	7.05	2.90	2.67	1.63	0.10

Table C3-50: Pedon Horizon data BUIS 1-5

Horizons	Depth (cm)	Von Post	Texture			Bulk Density (g/cm ³)	1:1 DI pH			Elements (%)	
			Sand (%)	Silt (%)	Clay (%)		Initial pH	Final pH	1:5 EC (dS/m)	C	N
Oase	0-17	H7	-	-	-	0.12	7.06	5.75	2.74	26.17	1.29
Oese	17-113	H6	-	-	-	0.09	7.23	6.30	3.14	33.78	1.39
O'ase	113- 161	H7	-	-	-	0.41	7.15	6.39	2.61	13.21	0.51
2ACseg	161- 178	-	43.5	32.4	24.1	0.52	7.03	3.98	2.94	7.79	0.34

Table C3-51 Pedon Horizon data CCIS 1-2

Horizons	Depth (cm)	Von Post	Texture			Bulk Density (g/cm ³)	1:1 DI pH			Elements (%)	
			Sand (%)	Silt (%)	Clay (%)		Initial pH	Final pH	1:5 EC (dS/m)	C	N
Oese	0-8	H5	-	-	-	0.09	6.50	5.78	1.89	29.55	1.64
Oase1	8-41	H7	-	-	-	0.16	6.82	5.51	0.82	32.52	1.38
Oase2	41-81	H7	-	-	-	0.14	6.84	5.04	1.20	32.55	1.43
2Oase3	81-104	H8	-	-	-	0.16	6.98	5.63	2.35	31.29	1.35
2Oase4	104- 118	H8	-	-	-	0.21	7.06	5.98	2.04	26.61	1.03
3Aseg	118- 147	-	73.8	12.0	14.1	0.65	6.88	5.91	2.79	10.81	0.40
3Cseg	147- 179	-	95.8	1.7	2.5	1.35	7.10	5.46	1.79	0.84	0.03

Table C3-52 Pedon Horizon data CCIS 1-4

Horizons	Depth (cm)	Von Post	Texture			Bulk Density (g/cm ³)	1:1 DI pH			Elements (%)	
			Sand (%)	Silt (%)	Clay (%)		Initial pH	Final pH	1:5 EC (dS/m)	C	N
Oese1	0-18	H4	-	-	-	0.18	6.71	5.78	1.13	26.03	1.42
Oese2	18-38	H5	-	-	-	0.13	7.32	5.18	2.14	23.08	1.25
Oase1	38-65	H7	-	-	-	0.35	7.18	6.96	2.13	11.96	0.69
Oase2	65-115	H8	-	-	-	0.30	6.99	6.27	3.14	18.12	0.94
2Aseg	115- 154	-	41.2	38.9	19.9	0.37	6.90	5.72	2.96	8.67	0.39
2Cseg	154- 173	-	87.7	7.4	4.9	1.23	7.04	3.32	1.87	0.77	0.06

Table C3-53 Pedon Horizon data KHW 1-2

Horizons	Depth (cm)	Von Post	Texture			Bulk Density (g/cm ³)	1:1 DI pH			Elements (%)	
			Sand (%)	Silt (%)	Clay (%)		Initial pH	Final pH	1:5 EC (dS/m)	C	N
Oase	0-32	H7	-	-	-	0.12	5.42	4.56	1.42	29.51	1.55
Oese	32-55	H6	-	-	-	0.15	5.55	4.42	1.39	32.20	1.70
O'ase1	55-70	H7	-	-	-	0.28	5.71	4.51	1.46	20.92	1.00
O'ase2	70-120	H8	-	-	-	0.17	5.41	4.65	1.51	30.72	1.27
2Cseg1	120- 141	-	71.4	18.6	10.0	1.11	6.46	5.48	0.79	2.01	0.10
2Cseg2	141- 150	-	78.4	14.2	7.4	1.35	6.51	4.11	0.90	2.23	0.11

Table C3-54 Pedon Horizon data SLIS 1-1

Horizons	Depth (cm)	Von Post	Texture			Bulk Density (g/cm ³)	1:1 DI pH			Elements (%)	
			Sand (%)	Silt (%)	Clay (%)		Initial pH	Final pH	1:5 EC (dS/m)	C	N
Oase1	0-38	H7	-	-	-	0.12	4.95	4.27	1.68	16.98	0.82
Oase2	38-59	H7	-	-	-	0.32	6.43	4.48	1.16	15.03	0.79
Oase3	59-92	H7	-	-	-	0.34	6.55	3.94	1.56	12.38	0.72
Oase4	91-118	H8	-	-	-	0.22	6.35	3.78	1.74	25.09	1.15
Oase5	118- 191	H8	-	-	-	0.15	6.27	5.36	1.59	21.13	0.90

Table C3-55 Pedon Horizon data SLIS 1-3A

Horizons	Depth (cm)	Von Post	Texture			Bulk Density (g/cm ³)	1:1 DI pH			Elements (%)	
			Sand (%)	Silt (%)	Clay (%)		Initial pH	Final pH	1:5 EC (dS/m)	C	N
Oese1	0-28	H5	-	-	-	0.08	6.89	6.06	1.41	31.99	1.66
Oese2	28-82	H4	-	-	-	0.14	6.90	4.56	1.79	45.60	1.79
Oese3	82-136	H6	-	-	-	0.11	6.70	5.32	2.19	30.76	1.20
Oase	136- 150	H7	-	-	-	0.12	6.79	5.43	1.96	20.53	0.84
Ase	150- 170	-	66.9	19.0	14.1	0.29	6.58	5.33	1.82	10.44	0.47
ACse	170- 182	-	95.7	1.0	3.2	1.07	6.69	2.95	1.30	0.58	0.03

Table C3-56 Pedon Horizon data SLIS 1-3B

Horizons	Depth (cm)	Von Post	Texture				Bulk Density (g/cm ³)	1:1 DI pH			Elements (%)	
			Sand (%)	Silt (%)	Clay (%)	Initial pH		Final pH	1:5 EC (dS/m)	C	N	
Oese1	0-28	H5	-	-	-	0.09	6.85	5.79	1.53	29.16	1.46	
Oese2	28-82	H4	-	-	-	0.12	6.70	5.76	1.98	41.18	1.76	
Oese3	82-136	H6	-	-	-	0.13	6.87	5.52	2.16	32.91	1.36	
Oase	136- 150	H7	-	-	-	0.25	6.44	4.58	2.13	17.49	0.69	
Ase	150- 170	-	66.9	19.0	14.1	0.38	6.80	4.56	1.73	8.93	0.30	
ACse	170- 182	-	95.7	1.0	3.2	0.84	6.72	2.92	1.73	0.32	0.03	

Table C3-57 Pedon Horizon data SLIS 1-3C

Horizons	Depth (cm)	Von Post	Texture				Bulk Density (g/cm ³)	1:1 DI pH			Elements (%)	
			Sand (%)	Silt (%)	Clay (%)	Initial pH		Final pH	1:5 EC (dS/m)	C	N	
Oese1	0-28	H5	-	-	-	0.09	6.84	5.90	1.53	28.63	1.42	
Oese2	28-82	H4	-	-	-	0.16	6.74	5.92	1.75	36.41	1.65	
Oese3	82-136	H6	-	-	-	0.10	6.58	4.64	2.13	31.35	1.25	
Oase	136- 150	H7	-	-	-	0.21	6.54	4.94	2.03	28.52	1.19	
Ase	150- 170	-	66.9	19.0	14.1	0.33	6.41	4.17	1.91	11.08	0.52	
ACse	170- 182	-	95.7	1.0	3.2	1.17	6.62	2.98	1.48	0.43	0.04	

Table C3-58 Pedon Horizon data SLIS 1-5

Horizons	Depth (cm)	Von Post	Texture				Bulk Density (g/cm ³)	1:1 DI pH			Elements (%)	
			Sand (%)	Silt (%)	Clay (%)	Initial pH		Final pH	1:5 EC (dS/m)	C	N	
Oese1	0-33	H6	-	-	-	0.16	6.90	5.36	1.37	37.12	1.46	
Oese2	33-79	H4	-	-	-	0.16	7.02	5.66	2.65	39.70	1.67	
Oese3	79-118	H6	-	-	-	0.10	7.02	6.67	2.97	32.89	1.30	
Ase1	118- 168	-	42.5	38.2	19.2	0.58	6.85	6.38	2.71	5.09	0.24	
Ase2	168- 189	-	77.7	12.9	9.4	1.11	6.70	3.50	2.55	2.33	0.13	

Table C3-59 Pedon Horizon data VTIS 1-2

Horizons	Depth (cm)	Von Post	Texture				Bulk Density (g/cm ³)	1:1 DI pH			Elements (%)	
			Sand (%)	Silt (%)	Clay (%)	Initial pH		Final pH	1:5 EC (dS/m)	C	N	
Oase1	0-26	H7	-	-	-	0.19	7.02	5.37	1.36	15.11	1.00	
Oase2	26-45	H7	-	-	-	0.16	7.05	4.46	1.64	20.18	0.95	
Oase3	45-81	H8	-	-	-	0.18	6.97	4.73	2.67	15.74	0.71	
Oase4	81-139	H8	-	-	-	0.13	6.95	4.86	2.23	20.16	0.89	
Cseg	139- 200+	-	84.5	0.8	14.6	1.22	7.16	4.28	1.84	2.80	0.13	

Table C3-60 Pedon Horizon data 1.1

Horizons	Depth (cm)	Von Post	Texture			Bulk Density (g/cm ³)	1:1 DI pH			Elements (%)	
			Sand (%)	Silt (%)	Clay (%)		Initial pH	Final pH	1:5 EC (dS/m)	C	N
Oe	0-24	H5	-	-	-	0.183	6.95	6.34	5.740	21.08	1.21
Oase	24-45	H7	-	-	-	0.107	7.15	4.59	7.305	15.24	0.92
2Ase	45-64	-	29	50.4	20.5	0.579	7.39	4.46	7.725	6.71	0.37
2Apse	64-81	-	43.6	30.4	26	1.450	7.61	4.01	6.007	2.66	0.13
2Btseg1	81-142	-	43.2	27.1	29.7	2.026	7.61	5.03	3.983	0.30	0.02
2Btseg2	142- 168	-	62.7	16.7	20.6	1.406	7.75	6.53	3.887	0.21	0.02
2BCseg	168- 207	-	71.4	9.7	18.9	1.674	7.67	7.81	3.948	0.11	0.02
2Cseg1	207- 228	-	29.9	25.5	44.5	1.534	7.86	7.93	3.057	0.34	0.03
2Cseg2	228+	-	29.3	29.9	40.8	1.383	7.54	7.35	2.717	0.55	0.05

Table C3-61 Pedon Horizon data 1.3 rep1

Horizons	Depth (cm)	Von Post	Texture				Bulk Density (g/cm ³)	1:1 DI pH			Elements (%)	
			Sand (%)	Silt (%)	Clay (%)	Initial pH		Final pH	1:5 EC (dS/m)	C	N	
Oese	0-22	H4	-	-	-	0.116	6.63	5.76	7.797	17.61	1.01	
2Apse	22-37	-	-	-	-	0.696	6.94	5.88	5.553	2.93	0.20	
2Ase	37-60	-	43.5	28.7	27.8	1.050	7.55	4.16	4.633	2.79	0.19	
2Btseg1	60-78	-	67.1	17.2	15.7	1.648	7.27	5.9	2.756	0.50	0.05	
2Btseg2	78-110	-	58.1	21.2	20.7	1.566	7.43	5.83	2.528	0.33	0.04	
2BCseg	110- 151	-	66.1	15.7	18.3	1.498	7.31	5.81	2.291	0.56	0.05	
2Cseg1	151- 203	-	73.9	11.6	14.5	1.407	6.85	6.64	1.839	0.11	0.02	
2Cseg2	203+	-	81.4	7.8	10.8	1.742	6.83	3.4	1.701	0.18	0.01	

Table C3-62 Pedon Horizon data 1.3 rep2

Horizons	Depth (cm)	Von Post	Texture				Bulk Density (g/cm ³)	1:1 DI pH			Elements (%)	
			Sand (%)	Silt (%)	Clay (%)	Initial pH		Final pH	1:5 EC (dS/m)	C	N	
Oese1	0-16	H4	-	-	-	0.099	7.14	5.32	5.340	25.09	1.52	
Oese2	16-24	H4	-	-	-	0.136	7.05	5.51	6.092	29.77	1.55	
Oese3	24-34	H5	-	-	-	0.219	6.65	5.37	5.235	22.01	1.19	
2Ase	34-61	-	55.9	22.5	21.6	1.021	7.11	5	4.724	4.39	0.27	
2Bseg1	61-72	-	62.8	16.7	20.5	1.728	7.45	5.14	3.538	1.48	0.11	
2Bseg2	72-87	-	61.6	17.9	20.6	1.675	7.29	5.24	3.092	0.73	0.06	
2Bseg3	87-124	-	55.8	21.3	22.9	1.686	7.16	5.34	2.955	0.47	0.05	
2Bseg4	124- 141	-	59.9	17.3	22.8	1.492	7.03	5.63	2.585	0.53	0.04	
2Cseg	141- 191		72.6	11.3	16.1	1.620	6.96	6.86	2.561	0.11	0.02	
2Cg	191+		82.5	6.8	10.7	1.765	6.58	6.69	2.861	0.06	0.01	

Table C3-63 Pedon Horizon data 1.3 rep3

Horizons	Depth (cm)	Von Post	Texture				Bulk Density (g/cm ³)	1:1 DI pH			Elements (%)	
			Sand (%)	Silt (%)	Clay (%)	Initial pH		Final pH	1:5 EC (dS/m)	C	N	
Oase	0-15	H7	-	-	-	0.156	7.05	4.48	6.014	22.93	1.13	
Ase1	15-34	-	42.4	31.6	26.1	0.502	7.17	5.5	6.824	9.67	0.58	
Ase2	34-51	-	37	36	27	0.624	7.06	4.73	5.957	6.60	0.48	
Ase3	51-80	-	49.3	30.3	20.4	0.727	7.27	5.96	3.403	2.68	0.19	
Bseg1	80-107	-	66.8	15.9	17.3	1.588	7.26	5.84	3.444	0.53	0.05	
Bseg2	107- 150	-	65.8	13.6	20.6	1.250	7.37	5.92	3.575	0.57	0.05	
Bseg3	150- 172	-	69.4	13.9	16.8	1.375	7.66	4.29	3.684	0.42	0.04	
Cg	172+	-	78.3	8.3	13.4	1.287	7.87	7.38	4.215	0.21	0.02	

Table C3-64 Pedon Horizon data 1.5

Horizons	Depth (cm)	Von Post	Texture				Bulk Density (g/cm ³)	1:1 DI pH			Elements (%)	
			Sand (%)	Silt (%)	Clay (%)	Initial pH		Final pH	1:5 EC (dS/m)	C	N	
Oese	0-15	H4	-	-	-	0.072	6.89	5.89	3.453	35.90	1.56	
Oase	15-22	H7	-	-	-	0.213	6.82	5.37	3.680	19.62	0.90	
Apse	22-45	-	60.8	21	18.3	1.489	6.71	5.09	2.023	0.99	0.07	
Btseg1	45-64	-	59.8	18	22.2	1.763	6.19	4.64	1.832	0.67	0.06	
Btseg2	64-87	-	42.7	25.5	31.9	1.647	6.16	5.1	1.399	0.42	0.05	
Cseg1	87-135	-	76.7	9.5	13.8	1.409	6.09	5.55	1.266	0.14	0.01	
Cseg2	135- 186	-	75.5	10.7	13.8	1.528	6.13	6.1	1.273	0.07	0.01	
Cseg3	186+	-	83.9	8.2	7.9	1.599	6.61	4.46	1.179	0.16	0.01	

Table C3-65 Pedon Horizon data 1.6

Horizons	Depth (cm)	Von Post	Texture				Bulk Density (g/cm ³)	1:1 DI pH			Elements (%)	
			Sand (%)	Silt (%)	Clay (%)	Initial pH		Final pH	1:5 EC (dS/m)	C	N	
Cseg1	0-8	-	71.8	16	12.3	0.242	6.97	5.8	3.051	4.96	0.31	
Oi	8-15	H3	-	-	-	0.225	6.71	5.8	3.798	12.07	0.62	
Apse	15-46	-	70.7	21.1	8.2	1.452	6.72	6.21	2.224	1.36	0.08	
Bseg1	46-76	-	66.6	21.9	11.5	1.525	6.37	6.25	2.275	0.64	0.05	
Bseg2	76-106	-	53.9	26.9	19.2	1.189	6.51	6.62	1.931	0.36	0.04	
C'seg2	106-161	-	68.9	14.8	16.3	1.389	5.55	5.81	2.044	0.11	0.02	
C'seg3	161+	-	79.4	9.7	11	1.376	5.5	5.75	2.090	0.08	0.01	

Table C3-66 Pedon Horizon data 2.1

Horizons	Depth (cm)	Von Post	Texture				Bulk Density (g/cm ³)	1:1 DI pH			Elements (%)	
			Sand (%)	Silt (%)	Clay (%)	Initial pH		Final pH	1:5 EC (dS/m)	C	N	
Ase1	0-10	-	16.4	62	21.7	0.416	7	4.75	1.513	7.435	0.43	
Ase2	10-50	-	34.7	45.7	19.6	0.390	6.91	4.21	8.010	7.59	0.45	
Ase3	50-86	-	35.7	49	15.3	0.712	7.56	3.77	6.666	6.27	0.36	
Ase4	86-128	-	72.3	15.7	12	1.289	7.27	3.6	4.628	2.35	0.11	
Bseg	128-154	-	79.3	6.2	14.5	1.543	8.1	6.32	3.009	0.25	0.02	
Cseg1	154-191	-	85.9	3.4	10.8	1.584	8.09	2.74	3.261	0.09	0.01	

Table C3-67 Pedon Horizon data 2.2

Horizons	Depth (cm)	Von Post	Texture				Bulk Density (g/cm ³)	1:1 DI pH			Elements (%)	
			Sand (%)	Silt (%)	Clay (%)	Initial pH		Final pH	1:5 EC (dS/m)	C	N	
Ase1	0-11	-	22.2	39.2	38.6	0.137	7.19	4.62	4.798	11.34	0.81	
Ase2	11-38	-	24.1	46.7	29.2	0.254	7.17	4.05	5.535	11.09	0.66	
Ase3	38-65	-	51.6	29.8	18.6	0.367	7.26	4.38	5.341	5.26	0.30	
Ase4	65-84	-	62.6	23.4	14	0.755	7.41	3.69	3.385	1.54	0.09	
Apse	84-103	-	57.5	27.9	14.5	1.307	7.37	3.28	3.506	1.30	0.07	
Bseg	103- 145	-	58.8	21.9	19.3	1.542	7.32	3.36	3.278	0.77	0.05	
Cseg	145+	-	70.6	13.1	16.3	1.190	7.17	3.04	3.719	0.48	0.03	

Table C3-68 Pedon Horizon data 2.4 rep1

Horizons	Depth (cm)	Von Post	Texture				Bulk Density (g/cm ³)	1:1 DI pH			Elements (%)	
			Sand (%)	Silt (%)	Clay (%)	Initial pH		Final pH	1:5 EC (dS/m)	C	N	
Oi	0-8	H1	-	-	-	0.365	5.82	5.77	1.318	13.53	0.61	
Ap	8-30	-	54.5	28.9	16.7	1.612	5.98	6	1.437	2.45	0.14	
Btg1	30-43	-	46.6	32.8	20.6	2.045	5.14	5.13	0.987	0.79	0.06	
Btg2	43-67	-	45	32	23	1.873	4.92	4.94	0.785	0.26	0.03	
Btg3	67-91	-	51.4	27.9	20.7	1.683	5.57	5.46	0.846	0.19	0.03	
Btg4	91-116	-	57.7	21.2	21.1	1.614	5.92	5.81	0.597	0.08	0.02	
BCg	116-169	-	74	10.3	15.7	1.726	5.77	5.78	0.795	0.09	0.02	
Cg	169-200+	-	88.4	4.5	7	1.716	5.08	5.22	1.049	0.07	0.01	

Table C3-69 Pedon Horizon data 2.4 rep2

Horizons	Depth (cm)	Von Post	Texture				Bulk Density (g/cm ³)	1:1 DI pH			Elements (%)	
			Sand (%)	Silt (%)	Clay (%)	Initial pH		Final pH	1:5 EC (dS/m)	C	N	
Oi	0-10	H1	-	-	-	0.051	4.56	4.52	0.205	28.27	1.11	
Ap	10-35	-	38.5	49	12.5	0.981	4.55	4.85	0.669	2.38	0.15	
Btseg1	35-85	-	36.9	30.7	32.4	1.582	4.09	4.31	0.481	0.39	0.05	
Btseg2	85-121	-	54.8	22.6	22.6	1.730	4.75	4.59	0.498	0.18	0.03	
Btseg3	121- 139	-	64.8	14.6	20.6	1.440	4.59	4.87	0.301	0.06	0.01	
Cseg1	139- 180	-	81.5	8.9	9.6	1.787	5.1	4.81	0.815	0.02	0.01	
Cseg2	180+	-	88.2	5.2	6.6	1.816	5.9	5.25	1.171	0.05	0.01	

Table C3-70 Pedon Horizon data 2.4 rep3

Horizons	Depth (cm)	Von Post	Texture				Bulk Density (g/cm ³)	1:1 DI pH			Elements (%)	
			Sand (%)	Silt (%)	Clay (%)	Initial pH		Final pH	1:5 EC (dS/m)	C	N	
Oise	0-6	H1	-	-	-	0.049	4.79	4.83	0.275	17.53	0.83	
Apse	6-31	-	58.3	32	9.8	1.569	4.84	5.3	0.924	0.83	0.04	
BA	31-44	-	52.5	33.5	14.1	1.603	4.65	5.25	0.602	3.10	0.17	
Btseg1	44-59	-	44.7	35	20.2	1.518	4.57	4.9	0.546	0.67	0.05	
Btseg2	59-91	-	40.1	37.4	22.5	1.508	4.72	4.9	0.457	0.36	0.04	
Btseg3	91-113	-	62.1	17.8	20.2	1.708	5.26	5.3	0.382	0.28	0.03	
BCseg	113- 127	-	63.9	17.5	18.6	1.812	6.04	5.13	0.922	0.12	0.02	
Cseg1	127- 151		67.8	15.6	16.6	1.604	6.01	4.86	0.493	0.06	0.01	
Cseg2	151+		84.9	6.3	8.8	1.425	5.7	5.34	1.038	0.11	0.01	

Table C3-71 Pedon Horizon data 3.1 rep1

Horizons	Depth (cm)	Von Post	Texture				Bulk Density (g/cm ³)	1:1 DI pH			Elements (%)	
			Sand (%)	Silt (%)	Clay (%)	Initial pH		Final pH	1:5 EC (dS/m)	C	N	
Ase1	0-8	-	4.7	74.9	20.4	0.462	6.51	5.98	4.475	9.77	0.69	
Ase2	8-21	-	24.1	52.9	22.9	0.162	6.5	5.6	7.549	9.195	0.57	
Ase3	21-49	-	42.3	29	28.7	0.193	6.76	4.86	7.773	11.15	0.64	
Ase4	49-61	-	58.1	25.7	16.3	1.448	7.34	4.48	6.712	1.37	0.09	
Btseg1	61-70	-	59.6	21.2	19.1	1.523	7.77	6.66	2.781	0.22	0.02	
Btseg2	70-99	-	35.2	25.6	39.2	1.420	7.68	7.23	3.129	0.18	0.03	
BCseg	99-136	-	67.8	10	22.2	1.508	7.46	7.45	3.887	0.07	0.01	
Cseg1	136- 157		80.8	5.9	13.3	2.103	7.66	7.44	4.116	0.08	0.01	
Cseg2	157- 198		78.2	8.5	13.3	1.662	7.66	7.15	3.831	0.08	0.01	
Cseg3	198- 110+		75.1	10.4	14.4	1.579	7.89	6.33	4.825	0.13	0.02	

Table C3-72 Pedon Horizon data 3.1 rep2

Horizons	Depth (cm)	Von Post	Texture				Bulk Density (g/cm ³)	1:1 DI pH			Elements (%)	
			Sand (%)	Silt (%)	Clay (%)	Initial pH		Final pH	1:5 EC (dS/m)	C	N	
Cseg	0-8	-	23.9	58.2	18	0.289	6.69	5.44	7.913	5.77	0.43	
Oase1	8-23	H8	-	-	-	0.208	6.46	3.6	8.604	12	0.69	
Ase1	23-29	-	42.8	24.7	32.4	0.201	5.75	3.43	9.962	10.68	0.66	
Ase2	29-43	-	70	20.4	9.6	1.689	7.09	3.85	5.266	1.60	0.11	
Btseg1	43-101	-	58.9	18.1	23	2.173	7.49	6.45	2.395	0.22	0.03	
Btseg2	101- 120	-	76.8	11.1	12.2	1.701	7.22	7.08	3.902	0.07	0.01	
BCseg	120- 189	-	84.8	4.8	10.3	1.665	7.06	6.9	3.892	0.06	0.01	
Cseg	189+		79.5	7.8	12.6	1.625	7.37	7.02	4.325	0.07	0.01	

Table C3-73 Pedon Horizon data 3.1 rep3

Horizons	Depth (cm)	Von Post	Texture			Bulk Density (g/cm ³)	1:1 DI pH			Elements (%)	
			Sand (%)	Silt (%)	Clay (%)		Initial pH	Final pH	1:5 EC (dS/m)	C	N
Ase1	0-21	-	45.7	31	23.3	0.269	7.26	3.4	7.708	5.28	0.34
Ase2	21-48	-	71.7	11.7	16.6	1.149	7.55	4.12	5.077	1.06	0.07
Btseg1	48-98	-	53.6	25.7	20.8	1.603	7.8	6.96	3.375	0.22	0.03
Btseg2	98-133	-	53.7	17.8	28.4	2.024	7.67	7.49	3.041	0.16	0.02
Cg	133- 188+	-	77.5	8.6	14	1.697	8.05	7.54	3.792	0.08	0.01

Table C3-74 Pedon Horizon data 3.2

Horizons	Depth (cm)	Von Post	Texture			Bulk Density (g/cm ³)	1:1 DI pH			Elements (%)	
			Sand (%)	Silt (%)	Clay (%)		Initial pH	Final pH	1:5 EC (dS/m)	C	N
Oese	0-15	H4	-	-	-	0.176	7.17	5.42	6.247	18.98	1.15
Ase1	15-34	-	56.7	25	18.3	0.501	7.05	5.6	6.486	10.96	0.56
Ase2	34-42	-	57.8	25.6	16.6	1.201	7.11	5.25	3.825	2.66	0.16
Apse	42-68	-	57.9	24.7	17.5	1.308	7.25	5.24	3.285	2.08	0.13
Btseg1	68-86	-	47.5	25.9	26.6	1.755	6.97	6.22	2.375	0.94	0.09
Btseg2	86-117	-	42.1	27.3	30.6	1.518	6.77	6.32	1.976	0.53	0.07
Cseg1	117- 159	-	72	11.7	16.3	1.601	6.79	6.52	2.324	0.15	0.02
Cseg2	159+	-	79	9.2	11.7	1.614	6.48	5.95	1.848	0.12	0.02

Table C3-75 Pedon Horizon data 3.3

Horizons	Depth (cm)	Texture				Bulk Density (g/cm ³)	1:1 DI pH			Elements (%)	
		Von Post	Sand (%)	Silt (%)	Clay (%)		Initial pH	Final pH	1:5 EC (dS/m)	C	N
Oese	0-20	H6	-	-	-	0.101	7.15	6.15	4.044	30.69	1.81
Ase	20-29	-	60.2	26.8	13.1	0.428	6.94	5.85	4.757	10.19	0.49
Apse	29-50	-	52.7	23.4	23.9	1.338	7.35	5.8	2.818	1.64	0.10
Btseg1	50-74	-	41.7	27.8	30.5	1.673	7.33	6.48	2.224	0.64	0.06
Btseg2	74-95	-	28.3	28.9	42.9	1.516	6.85	6.83	2.556	0.22	0.04
BCseg	95-116	-	74.9	9.3	15.8	1.473	7.32	6.74	2.280	0.13	0.02
Cseg1	116- 149	-	76.9	6.7	16.3	1.756	7.02	6.41	2.522	0.12	0.01
Cseg2	149+		78	10.6	11.4	1.518	7.27	6.44	2.442	0.18	0.02

Table C3-76 Pedon Horizon data 3.6

Horizons	Depth (cm)	Texture					1:1 DI pH			Elements (%)	
		Von Post	Sand (%)	Silt (%)	Clay (%)	Bulk Density (g/cm ³)	Initial pH	Final pH	1:5 EC (dS/m)	C	N
Oise1	0-4	H1	-	-	-	0.068	4.15	4.33	0.455	32.04	1.42
Oapse	4-21	-	-	-	-	0.750	4.24	4.71	0.968	16.135	0.89
Btseg1	21-53	-	36.6	35	28.4	1.556	3.99	4.22	1.454	3.18	0.21
Btseg2	53-74	-	36.5	35.2	28.3	1.418	4.8	4.76	1.385	1.72	0.12
Btseg3	74-111	-	48.4	24.8	26.8	1.704	4.5	4.69	0.712	0.56	0.05
BCg	111- 127	-	56.2	20.9	22.9	1.530	4.4	4.39	1.103	0.45	0.04
Cg1	127- 163	-	76.2	10.2	13.6	1.415	4.2	4.23	1.125	0.31	0.02
Cg2	163+	-	80.7	9	10.3	1.572	5.01	3.47	1.317	0.26	0.02

Table C4-1: Profile Description 1.1

Horizon	Depth (cm)	Description
Oe	0-24	Dark brown (10YR 3/3) broken face and rubbed, mucky peat; H5 on Von Post scale; 30% unrubbed and 20% rubbed fibers; many fine, medium, and coarse roots; neutral (6.95 pH, 1:1 water), slightly acid (6.34 pH, 1:1 water) after moist incubation; electrical conductivity (5.74 dS/m, 1:5 water); clear boundary.
Oase	24-45	Very dark brown (7.5YR 3/3) broken face and rubbed, muck; H7 on Von Post scale; 20% unrubbed and 5% rubbed fibers; many fine and medium roots, few coarse roots; slight sulfurous odor; neutral (7.15 pH, 1:1 water), very strongly acid (4.59 pH, 1:1 water) after moist incubation; electrical conductivity (7.31 dS/m, 1:5 water); clear boundary.
2Ase	45-64	Very dark grayish brown (10YR 3/2) mucky silt loam; Common fine roots; slight sulfurous odor; neutral (7.39 pH, 1:1 water), extremely acid (4.46 pH, 1:1 water) after moist incubation; electrical conductivity (7.73 dS/m, 1:5 water); clear boundary.
2Apse	64-81	Black (2.5Y 2.5/1) loam; Common fine roots; slight sulfurous odor; slightly alkaline (7.61 pH, 1:1 water), extremely acid (4.01 pH, 1:1 water) after moist incubation; strongly effervescent with 30% hydrogen peroxide; electrical conductivity (6.01 dS/m, 1:5 water); clear boundary.
2Btseg1	81-142	Gray (N5/0) clay loam; few fine roots; very dark gray (N3/0) organic stains; slightly alkaline (7.61 pH, 1:1 water), very strongly acid (5.03 pH, 1:1 water) after moist incubation; slightly effervescent with 30% hydrogen peroxide; electrical conductivity (3.98 dS/m, 1:5 water); clear boundary.
2Btseg2	142-168	Gray (N5/0) sandy clay loam; >1% charcoal fragments; common fine light olive brown (2.5Y 5/6) masses of oxidized iron; slightly alkaline (7.75 pH, 1:1 water), slightly acid (6.53 pH, 1:1 water) after moist incubation; slightly effervescent with 30% hydrogen peroxide; electrical conductivity (3.89 dS/m, 1:5 water); gradual boundary.
2BCseg	168-207	Gray (N6/0) sandy loam; common fine light olive brown (2.5Y 5/4) masses of oxidized iron; slightly alkaline (7.67 pH, 1:1 water), slightly alkaline (7.81 pH, 1:1 water) after moist incubation; slightly effervescent with 30% hydrogen peroxide; electrical conductivity (3.95 dS/m, 1:5 water); clear boundary
2Cseg1	207-228	Gray (N6/0) clay; many fine light olive brown (2.5Y 5/4) masses of oxidized iron; slightly alkaline (7.86 pH, 1:1 water), moderately alkaline

Table C4-1 (continued).

		(7.93 pH, 1:1 water) after moist incubation; slightly effervescent with 30% hydrogen peroxide; electrical conductivity (3.06 dS/m, 1:5 water); abrupt boundary.
2Cseg2	228+	Gray (N5/0) clay; slightly alkaline (7.54 pH, 1:1 water), neutral (7.35 pH, 1:1 water) after moist incubation; slightly effervescent with 30% hydrogen peroxide; electrical conductivity (2.72 dS/m, 1:5 water).

Table C4-2: Profile Description 1.3 rep1

Horizon	Depth (cm)	Description
Oese	0-22	Very dark brown (7.5YR 2.5/2) broken face and rubbed, muck; H7 von Post scale; 20% coarse wood fragments; 50% unrubbed fiber, 25% rubbed; many fine, medium, and coarse roots; moderate sulfurous odor; neutral (6.63 pH, 1:1 water), moderately acid (5.76 pH, 1:1 water) after moist incubation; electrical conductivity (7.80 dS/m, 1:5 water); abrupt boundary.
2Aapse	22-37	Very dark grayish brown (10YR 3/2) clay loam; Few fine roots; slight sulfurous odor; neutral (6.94 pH, 1:1 water), moderately acid (5.88 pH, 1:1 water) after moist incubation; electrical conductivity (5.55 dS/m, 1:5 water); clear boundary.
2Ase	37-60	Very dark gray (2.5Y 3/1) clay loam; 1% charcoal stains; few fine roots; slight sulfurous odor; slightly alkaline (7.55 pH, 1:1 water), extremely acid (4.16 pH, 1:1 water) after moist incubation; electrical conductivity (4.63 dS/m, 1:5 water); clear boundary.
2Btseg1	60-78	Gray (N5/0) sandy loam; 1% charcoal fragments; few fine light olive brown (2.5Y 5/6) masses of oxidized iron; slight sulfurous odor; neutral (7.27 pH, 1:1 water), moderately acid (5.90 pH, 1:1 water) after moist incubation; slightly effervescent with 30% hydrogen peroxide; electrical conductivity (2.76 dS/m, 1:5 water); clear boundary.
2Btseg2	78-110	Gray (N5/0) sandy clay loam; 1% charcoal fragments; few fine roots; few fine light yellowish brown (10YR 6/4) masses of oxidized iron; slightly alkaline (7.43 pH, 1:1 water), moderately acid (5.83 pH, 1:1 water) after moist incubation; slightly effervescent with 30% hydrogen peroxide; electrical conductivity (2.53 dS/m, 1:5 water); clear boundary.
2BCseg	110-151	Gray (N5/0) sandy loam; 1% charcoal fragments; few fine roots; common fine light olive brown (2.5Y 5/4) masses of oxidized iron; neutral (7.31 pH, 1:1 water), moderately acid (5.81 pH, 1:1 water) after moist incubation; slightly effervescent with 30% hydrogen peroxide; electrical conductivity (2.29 dS/m, 1:5 water); clear boundary.

Table C4-2 (continued).

2Cseg1	151-203	Gray (N5/0) sandy loam; few fine roots; many medium light olive brown (2.5Y 5/4) masses of oxidized iron; neutral (6.85 pH, 1:1 water), neutral (6.64 pH, 1:1 water) after moist incubation; slightly effervescent with 30% hydrogen peroxide; electrical conductivity (1.84 dS/m, 1:5 water); gradual boundary.
2Cseg2	203+	Gray (N5/0) loamy sand; neutral (6.83 pH, 1:1 water), ultra acid (3.4 pH, 1:1 water) after moist incubation; slightly effervescent with 30% hydrogen peroxide; electrical conductivity (1.70 dS/m, 1:5 water).

Table C4-3: Profile Description 1.3 rep2

Horizon	Depth (cm)	Description
Oese1	0-16	Very dark brown (7.5YR 2.5/2) broken face and rubbed, mucky peat; H4 von Post scale; many fine, medium, and coarse roots; moderate sulfurous odor; neutral (7.14 pH, 1:1 water), moderately acid (5.32 pH, 1:1 water) after moist incubation; electrical conductivity (5.34 dS/m, 1:5 water); gradual boundary.
Oese2	16-24	Very dark brown (10YR 2/2) broken face and rubbed, mucky peat; H4 von Post scale; many fine, medium, and coarse roots; moderate sulfurous odor; neutral (7.05 pH, 1:1 water), moderately acid (5.51 pH, 1:1 water) after moist incubation; electrical conductivity (6.09 dS/m, 1:5 water); clear boundary.
Oese3	24-34	Very dark grayish brown (10YR 3/2) broken face and rubbed, mucky peat; H5 von Post scale; many fine, medium, and coarse roots; moderate sulfurous odor; neutral (6.65 pH, 1:1 water), moderately acid (5.37 pH, 1:1 water) after moist incubation; electrical conductivity (5.24 dS/m, 1:5 water); clear boundary.
2Ase	34-61	Very dark gray (10YR 3/1) sandy clay loam; common fine and medium roots; slight sulfurous odor; neutral (7.11 pH, 1:1 water), strongly acid (5.00 pH, 1:1 water) after moist incubation; electrical conductivity (4.72 dS/m, 1:5 water); clear boundary.
2Bseg1	61-72	Dark gray (N4/0) sandy clay loam; few fine roots; slightly alkaline (7.45 pH, 1:1 water), strongly acid (5.14 pH, 1:1 water) after moist incubation; color change from 3% hydrogen peroxide; electrical conductivity (3.54 dS/m, 1:5 water); gradual boundary.
2Bseg2	72-87	Gray (N5/0) sandy clay loam; few fine roots; neutral (7.29 pH, 1:1 water), strongly acid (5.24 pH, 1:1 water) after moist incubation; slightly

Table C4-3 (continued).

		effervescent with 30% hydrogen peroxide; electrical conductivity (3.09 dS/m, 1:5 water); gradual boundary.
2Bseg3	87-124	Very dark gray (N3/0) sandy clay loam; few fine roots; neutral (7.16 pH, 1:1 water), strongly acid (5.34 pH, 1:1 water) after moist incubation; slight effervescent with 30% hydrogen peroxide; electrical conductivity (2.96 dS/m, 1:5 water); clear boundary.
2Bseg4	124-141	Gray (N4/0) sandy clay loam; few fine roots; neutral (7.03 pH, 1:1 water), moderately acid (5.63 pH, 1:1 water) after moist incubation; slightly effervescent with 30% hydrogen peroxide; electrical conductivity (2.59 dS/m, 1:5 water); clear boundary.
2Cseg	141-191	Gray (N5/0) sandy loam; few fine roots; many yellowish brown (10YR 5/6) and light olive brown (2.5Y 5/6) masses of oxidized iron; neutral (6.96 pH, 1:1 water), neutral (6.86 pH, 1:1 water) after moist incubation; slightly effervescent with 30% hydrogen peroxide; electrical conductivity (2.56 dS/m, 1:5 water); gradual boundary.
2Cg	191+	Gray (N5/0) loamy sand; many light olive brown (2.5Y 5/4) masses of oxidized iron; slightly acid (6.58 pH, 1:1 water), neutral (6.69 pH, 1:1 water) after moist incubation; electrical conductivity (2.86 dS/m, 1:5 water).

Table C4-4: Profile Description 1.3 rep3

Horizon	Depth (cm)	Description
Oase	0-15	Very dark gray (10YR 3/1) broken face and rubbed, muck; H7 von Post scale; 30% unrubbed fiber, 25% rubbed; Many fine, medium, coarse roots; slight sulfurous odor; neutral (7.05 pH, 1:1 water), extremely acid (4.48 pH, 1:1 water) after moist incubation; slightly effervescent with 30% hydrogen peroxide; electrical conductivity (6.01 dS/m, 1:5 water); clear boundary.
Ase1	15-34	Very dark grayish brown (10YR 3/2) mucky loam; 20% unrubbed fibers and 10% rubbed; many fine, medium, coarse roots; slight sulfurous odor; neutral (7.17 pH, 1:1 water), strongly acid (5.50 pH, 1:1 water) after moist incubation; slightly effervescent with 30% hydrogen peroxide; electrical conductivity (6.82 dS/m, 1:5 water); gradual boundary.
Ase2	34-51	Very dark grayish brown (10YR 3/2) mucky clay loam; common fine roots; slight sulfurous odor; neutral (7.06 pH, 1:1 water), very strongly acid (4.73 pH, 1:1 water) after moist incubation; slightly effervescent with 30% hydrogen peroxide; electrical conductivity (5.96 dS/m, 1:5 water); clear boundary.

Table C4-4 (continued).

Ase3	51-80	Black (10YR 2/1) loam; Few fine roots; slight sulfurous odor; neutral (7.27 pH, 1:1 water), moderately acid (5.96 pH, 1:1 water) after moist incubation; slightly effervescent with 30% hydrogen peroxide; electrical conductivity (3.40 dS/m, 1:5 water); clear boundary.
Bseg1	80-107	Gray (N5/0) sandy loam; neutral (7.26 pH, 1:1 water), moderately acid (5.84 pH, 1:1 water) after moist incubation; slightly effervescent with 30% hydrogen peroxide; electrical conductivity (3.44 dS/m, 1:5 water); clear boundary.
Bseg2	107-150	Gray (N5/0) sandy clay loam; many light olive brown (2.5Y 5/6) masses of oxidized iron; few very dark gray (5Y 3/1) organic stains; neutral (7.37 pH, 1:1 water), moderately acid (5.92 pH, 1:1 water) after moist incubation; slightly effervescent with 30% hydrogen peroxide; electrical conductivity (3.58 dS/m, 1:5 water); gradual boundary.
Bseg3	150-172	Gray (N5/0) sandy loam; many light olive brown (2.5Y 5/6) masses of oxidized iron; few very dark gray (5Y 3/1) organic stains; neutral (7.66 pH, 1:1 water), moderately acid (4.29 pH, 1:1 water) after moist incubation; slightly effervescent with 30% hydrogen peroxide; electrical conductivity (3.68 dS/m, 1:5 water); clear boundary.
Cg	172+	Greenish gray (10GY 5/1) sandy loam; common light olive brown (2.5Y 5/6) masses of oxidized iron; few very dark gray (5Y 3/1) organic stains; slightly alkaline (7.87 pH, 1:1 water), neutral (7.38 pH, 1:1 water) after moist incubation; electrical conductivity (4.22 dS/m, 1:5 water);

Table C4-5: Profile Description 1.5

Horizon	Depth (cm)	Description
Oese	0-15	Very dark brown (7.5YR 2.5/2) broken face and rubbed, muck; H4 von Post scale; 25% unrubbed fiber, 17% rubbed; 5% wood fragments; Many fine, medium, coarse roots; slight sulfurous odor; neutral (6.89 pH, 1:1 water), moderately acid (5.89 pH, 1:1 water) after moist incubation; electrical conductivity (3.45 dS/m, 1:5 water); clear boundary.
Oase	15-22	Very dark gray (7.5YR 3/1) broken face and rubbed, muck; H7 von Post scale; 3% unrubbed fiber, 1% rubbed; strong sulfurous odor; neutral (6.82 pH, 1:1 water), strongly acid (5.37 pH, 1:1 water) after moist incubation; electrical conductivity (3.68 dS/m, 1:5 water); abrupt boundary.
Apse	22-45	Very dark gray (N3/0) sandy loam; 3% charcoal features & phragmites rhizomes; few fine and coarse roots; slight sulfurous odor; neutral (6.71 pH, 1:1 water), very strongly acid (5.09 pH, 1:1 water) after moist

Table C4-5 (continued).

		incubation; electrical conductivity (2.02 dS/m, 1:5 water); gradual boundary.
Btseg1	45-64	Dark gray (N4/0) sandy clay loam; 1% charcoal features; common light olive brown (2.5Y 5/6) iron-stained pore linings and masses of oxidized iron slight sulfurous odor; slightly acid (6.19 pH, 1:1 water), very strongly acid (4.64 pH, 1:1 water) after moist incubation; slightly effervescent with 30% hydrogen peroxide; electrical conductivity (1.83 dS/m, 1:5 water); gradual boundary.
Btseg2	64-87	Gray (N6/0) clay loam; common light olive brown (2.5Y 5/6) iron-stained pore linings and masses of oxidized iron; slightly acid (6.16 pH, 1:1 water), strongly acid (5.10 pH, 1:1 water) after moist incubation; slightly effervescent with 30% hydrogen peroxide; electrical conductivity (1.40 dS/m, 1:5 water); clear boundary.
Cseg1	87-135	Gray (N6/0) sandy loam; common light olive brown (2.5Y 5/6) masses of oxidized iron; moderately acid (6.09 pH, 1:1 water), strongly acid (5.55 pH, 1:1 water) after moist incubation; slightly effervescent with 30% hydrogen peroxide; electrical conductivity (1.27 dS/m, 1:5 water); gradual boundary.
Cseg2	135-186	Gray (N5/0) sandy loam; common light olive brown (2.5Y 5/6) masses of oxidized iron; slightly acid (6.13 pH, 1:1 water), slightly acid (6.10 pH, 1:1 water) after moist incubation; slightly effervescent with 30% hydrogen peroxide; electrical conductivity (1.27 dS/m, 1:5 water); clear boundary.
Cseg3	186+	Dark greenish gray (10Y 4/1) loamy sand; few phragmites rhizome tubers; neutral (6.61 pH, 1:1 water), extremely acid (4.46 pH, 1:1 water) after moist incubation; slightly effervescent with 30% hydrogen peroxide; electrical conductivity (1.18 dS/m, 1:5 water).

Table C4-6: Profile Description 1.6

Horizon	Depth (cm)	Description
Cseg1	0-8	Dark grayish brown (10YR 4/2) mucky sandy loam; 30% unrubbed fiber, 10 rubbed; moderate sulfurous odor; neutral (6.97 pH, 1:1 water), moderately acid (5.80 pH, 1:1 water) after moist incubation; color change with 3% hydrogen peroxide; strongly effervescent with 30% hydrogen peroxide; electrical conductivity (3.05 dS/m, 1:5 water); clear boundary.
Oi	8-15	Very dark grayish brown (10YR 3/2) broken face and rubbed, muck; H3 von Post scale; 15% unrubbed fiber, 5% rubbed; moderate sulfurous odor; neutral (6.71 pH, 1:1 water), moderately acid (5.80 pH, 1:1 water) after moist incubation; color change with 3% hydrogen peroxide; strongly

Table C4-6 (continued).

		effervescent with 30% hydrogen peroxide; electrical conductivity (3.80 dS/m, 1:5 water); abrupt boundary.
Apse	15-46	Gray (2.5Y 5/1) sandy loam; common light olive brown (2.5Y 5/4) iron-stained pore linings and charcoal stains; moderate sulfurous odor; neutral (6.72 pH, 1:1 water), slightly acid (6.21 pH, 1:1 water) after moist incubation; strongly effervescent with 30% hydrogen peroxide; electrical conductivity (2.22 dS/m, 1:5 water); clear boundary.
Bseg1	46-76	Gray (N5/0) sandy loam; common fine roots; common light olive brown (2.5Y 5/4) iron-stained pore linings and charcoal stains; slight sulfurous odor; slightly acid (6.37 pH, 1:1 water), slightly acid (6.25 pH, 1:1 water) after moist incubation; strongly effervescent with 30% hydrogen peroxide; electrical conductivity (2.28 dS/m, 1:5 water); gradual boundary.
Bseg2	76-106	Gray (N6/0) sandy loam; common fine roots; common light olive brown (2.5Y 5/4) iron-stained pore linings; slightly acid (6.51 pH, 1:1 water), neutral (6.62 pH, 1:1 water) after moist incubation; strongly effervescent with 30% hydrogen peroxide; electrical conductivity (1.93 dS/m, 1:5 water); clear boundary.
C'seg2	106-161	Gray (N6/0) sandy loam; many strong brown (7.5YR 5/8) and yellowish brown (10YR 5/4) iron-stained pore linings; strongly acid (5.55 pH, 1:1 water), moderately acid (5.81 pH, 1:1 water) after moist incubation; violently effervescent with 30% hydrogen peroxide; electrical conductivity (2.04 dS/m, 1:5 water); clear boundary.
C'seg3	161+	Greenish gray (5GY 5/1) sandy loam; common yellowish brown (10YR 5/4) iron-stained pore linings; few fine dead roots; strongly acid (5.50 pH, 1:1 water), moderately acid (5.75 pH, 1:1 water) after moist incubation; violently effervescent with 30% hydrogen peroxide; electrical conductivity (2.09 dS/m, 1:5 water); clear boundary

Table C4-7: Profile Description 2.1

Horizon	Depth (cm)	Description
Ase1	0-10	Very dark grayish brown (2.5Y 3/2) silt loam; many fine, medium, and coarse roots; strong sulfurous odor; neutral (7.00 pH, 1:1 water), very strongly acid (4.75 pH, 1:1 water) after moist incubation; electrical conductivity (1.51 dS/m, 1:5 water); gradual boundary.
Ase2	10-50	Very dark gray (2.5Y 3/1) mucky loam; many fine roots; common medium, and coarse roots; strong sulfurous odor; neutral (6.91 pH, 1:1 water), extremely acid (4.21 pH, 1:1 water) after moist incubation; electrical conductivity (8.01 dS/m, 1:5 water); clear boundary.

Table C4-7 (continued).

Ase3	50-86	Black (2.5Y 2.5/1) mucky loam; few fine roots; 15% wood fragments; moderate sulfurous odor; slightly alkaline (7.56 pH, 1:1 water), extremely acid (3.77 pH, 1:1 water) after moist incubation; electrical conductivity (6.67 dS/m, 1:5 water); clear boundary.
Ase4	86-128	Very dark gray (5Y 3/1) sandy loam; 5% wood fragments; slight sulfurous odor; neutral (7.27 pH, 1:1 water), extremely acid (3.60 pH, 1:1 water) after moist incubation; slightly effervescent with 30% hydrogen peroxide; electrical conductivity (4.63 dS/m, 1:5 water); abrupt boundary.
Bseg	128-154	Gray (N6/0) sandy loam; few fine dead roots; few very dark gray (5Y 3/1) organic stains; moderate sulfurous odor; moderately alkaline (8.10 pH, 1:1 water), slightly acid (6.32 pH, 1:1 water) after moist incubation; slightly effervescent with 30% hydrogen peroxide; electrical conductivity (3.01 dS/m, 1:5 water); clear boundary.
Cseg1	154-191	Gray (N6/0) loamy sand; few fine dead roots; few light olive brown (2.5Y 5/4) iron-stained pore linings; moderately alkaline (8.09 pH, 1:1 water), ultra acid (2.74 pH, 1:1 water) after moist incubation; very slightly effervescent with 30% hydrogen peroxide; electrical conductivity (3.26 dS/m, 1:5 water); clear boundary.
Cg	191+	Gray (N6/0) loamy sand; few fine dead roots; moderately alkaline (8.41 pH, 1:1 water), slightly alkaline (7.54 pH, 1:1 water) after moist incubation; electrical conductivity (3.30 dS/m, 1:5 water).

Table C4-8: Profile Description 2.2

Horizon	Depth (cm)	Description
Ase1	0-11	Dark grayish brown (10YR 4/2) clay loam; many fine and coarse roots; moderate sulfurous odor; neutral (7.19 pH, 1:1 water), very strongly acid (4.62 pH, 1:1 water) after moist incubation; electrical conductivity (4.80 dS/m, 1:5 water); gradual boundary.
Ase2	11-38	Very dark grayish brown (10YR 3/2) clay loam; many fine and coarse roots; few coarse distinct iron monosulfide soft masses; moderate sulfurous odor; neutral (7.17 pH, 1:1 water), very strongly acid (4.05 pH, 1:1 water) after moist incubation; color change with 3% hydrogen peroxide; electrical conductivity (5.54 dS/m, 1:5 water); gradual boundary.
Ase3	38-65	Very dark grayish brown (10YR 3/2) loam; few fine roots; 5% wood fragments; 15% charcoal fragments; slight sulfurous odor; neutral (7.26 pH, 1:1 water), extremely acid (4.38 pH, 1:1 water) after moist incubation; electrical conductivity (5.34 dS/m, 1:5 water); gradual boundary.

Table C4-8 (continued).

Ase4	65-84	Very dark brown (10YR 2/2) sandy loam; few fine roots; 3% charcoal fragments and common charcoal stains; slight sulfurous odor; slightly alkaline (7.41 pH, 1:1 water), extremely acid (3.69 pH, 1:1 water) after moist incubation; electrical conductivity (3.39 dS/m, 1:5 water); clear boundary.
Apse	84-103	Black (10YR 2/1) sandy loam; few fine roots; slight sulfurous odor; neutral (7.37 pH, 1:1 water), ultra acid (3.28 pH, 1:1 water) after moist incubation; slightly effervescent with 30% hydrogen peroxide; electrical conductivity (3.51 dS/m, 1:5 water); clear boundary.
Bseg	103-145	Gray (N6/0) sandy loam; common light olive brown (2.5Y 5/4) iron-stained pore linings and oxidized iron masses; neutral (7.32 pH, 1:1 water), ultra acid (3.36 pH, 1:1 water) after moist incubation; color change with 3% hydrogen peroxide; slightly effervescent with 30% hydrogen peroxide; electrical conductivity (3.28 dS/m, 1:5 water); abrupt boundary.
Cseg	145+	Gray (N5/0) sandy loam; few fine roots; common light olive brown (2.5Y 5/4) iron-stained pore linings and oxidized iron masses; neutral (7.17 pH, 1:1 water), ultra acid (3.04 pH, 1:1 water) after moist incubation; very slightly effervescent with 30% hydrogen peroxide; electrical conductivity (3.72 dS/m, 1:5 water).

Table C4-9: Profile Description 2.4 rep1

Horizon	Depth (cm)	Description
Oi	0-8	Very dark gray (10YR 3/1) broken face and rubbed, peat; H1 von Post scale; no sulfurous odor; moderately acid (5.82 pH, 1:1 water), moderately acid (5.77 pH, 1:1 water) after moist incubation; electrical conductivity (1.32 dS/m, 1:5 water); clear boundary.
Ap	8-30	Very dark brown (10YR 2/2) sandy loam; weak subangular blocky structure; friable; non-fluid; no sulfurous odor; moderately acid (5.98 pH, 1:1 water), moderately acid (6.00 pH, 1:1 water) after moist incubation; electrical conductivity (1.44 dS/m, 1:5 water); abrupt boundary.
Btg1	30-43	Grayish brown (2.5Y 5/2) loam; moderate subangular blocky structure; firm; non-fluid; no sulfurous odor; many yellowish brown (10YR 5/6) iron-stained pore linings and masses of oxidized iron; strongly acid (5.14 pH, 1:1 water), strongly acid (5.13 pH, 1:1 water) after moist incubation; electrical conductivity (0.99 dS/m, 1:5 water); clear boundary.
Btg2	43-67	Gray (5Y 6/1) loam; moderate subangular blocky structure; firm; non-fluid; no sulfurous odor; very strongly acid (4.92 pH, 1:1 water), very strongly

Table C4-9 (continued).

		acid (4.94 pH, 1:1 water) after moist incubation; electrical conductivity (0.79 dS/m, 1:5 water); gradual boundary.
Btg3	67-91	Gray (5Y 5/1) sandy clay loam; moderate subangular blocky structure; firm; non-fluid; no sulfurous odor; strongly acid (5.57 pH, 1:1 water), strongly acid (5.46 pH, 1:1 water) after moist incubation; electrical conductivity (0.85 dS/m, 1:5 water); gradual boundary.
Btg4	91-116	Gray (N6/0) sandy clay loam; moderate subangular blocky structure; firm; non-fluid; no sulfurous odor; few fine roots; moderately acid (5.92 pH, 1:1 water), moderately acid (5.81 pH, 1:1 water) after moist incubation; electrical conductivity (0.60 dS/m, 1:5 water); clear boundary.
BCg	116-169	Gray (N6/0) sandy loam; weak subangular blocky structure; friable; non-fluid; no sulfurous odor; very few fine roots; few organic stains in pore linings; moderately acid (5.77 pH, 1:1 water), moderately acid (5.78 pH, 1:1 water) after moist incubation; electrical conductivity (0.79 dS/m, 1:5 water); abrupt boundary.
Cg	169-200+	Gray (N5/0) loamy sand; massive; friable; slightly fluid; no sulfurous odor; common light yellowish brown (2.5Y 6/3) masses of oxidized iron; very strongly acid (5.08 pH, 1:1 water), strongly acid (5.22 pH, 1:1 water) after moist incubation; electrical conductivity (1.05 dS/m, 1:5 water).

Table C4-10: Profile Description 2.4 rep2

Horizon	Depth (cm)	Description
Oi	0-10	Black (7.5YR 2.5/1) broken face and rubbed, peat; H1 von Post scale; many fine, medium, and coarse roots; no sulfurous odor; very strongly acid (4.56 pH, 1:1 water), very strongly acid (4.52 pH, 1:1 water) after moist incubation; slightly effervescent with 30% hydrogen peroxide; electrical conductivity (0.21 dS/m, 1:5 water); abrupt boundary.
Ap	10-35	Very dark gray (10YR 3/1) loam; weak subangular blocky structure; friable; non-fluid; many fine roots; slight sulfurous odor; very strongly acid (4.55 pH, 1:1 water), very strongly acid (4.85 pH, 1:1 water) after moist incubation; very slightly effervescent with 30% hydrogen peroxide; electrical conductivity (0.67 dS/m, 1:5 water); abrupt boundary.
Btseg1	35-85	Gray (2.5Y 6/1) clay loam; moderate subangular blocky structure; firm; non-fluid; many reddish yellow (7.5YR 6/8) iron-stained pore linings; slight sulfurous odor; extremely acid (4.09 pH, 1:1 water), extremely acid (4.31 pH, 1:1 water) after moist incubation; electrical conductivity (0.48 dS/m, 1:5 water); clear boundary.

Table C4-10 (continued).

Btseg2	85-121	Gray (5Y 5/1) sandy clay loam; moderate subangular blocky structure; firm; non-fluid; many medium and coarse roots; common reddish yellow (7.5YR 6/8) iron-stained pore linings; slight sulfurous odor; very strongly acid (4.75 pH, 1:1 water), very strongly acid (4.59 pH, 1:1 water) after moist incubation; very slightly effervescent with 30% hydrogen peroxide; electrical conductivity (0.50 dS/m, 1:5 water); clear boundary.
Btseg3	121-139	Gray (N6/0) sandy clay loam; moderate subangular blocky structure; firm; slightly fluid; few coarse roots; common light olive brown (2.5Y 5/4) and grayish brown (10YR 5/2) masses of oxidized iron and iron-stained pore linings; slight sulfurous odor; very strongly acid (4.59 pH, 1:1 water), very strongly acid (4.87 pH, 1:1 water) after moist incubation; very slightly effervescent with 30% hydrogen peroxide; electrical conductivity (0.30 dS/m, 1:5 water); gradual boundary.
Cseg1	139-180	Gray (N6/0) loamy sand; weak subangular blocky structure; friable; slightly fluid; many coarse roots; common light olive brown (2.5Y 5/6) masses of oxidized iron and iron-stained pore linings; no sulfurous odor; strongly acid (5.10 pH, 1:1 water), strongly acid (4.81 pH, 1:1 water) after moist incubation; very slightly effervescent with 30% hydrogen peroxide; electrical conductivity (0.81 dS/m, 1:5 water); gradual boundary.
Cseg2	180+	Gray (N6/0) loamy sand; massive; friable; slightly fluid; no sulfurous odor; few coarse roots; common light olive brown (2.5Y 5/6) masses of oxidized iron and iron-stained pore linings; moderately acid (5.90 pH, 1:1 water), strongly acid (5.25 pH, 1:1 water) after moist incubation; very slightly effervescent with 30% hydrogen peroxide; electrical conductivity (1.17 dS/m, 1:5 water).

Table C4-11: Profile Description 2.4 rep3

Horizon	Depth (cm)	Description
Oise	0-6	Black (7.5YR 2.5/1) broken face and rubbed, peat; H1 von Post scale; many fine, medium, and coarse roots; no sulfurous odor; very strongly acid (4.79 pH, 1:1 water), very strongly acid (4.83 pH, 1:1 water) after moist incubation; slightly effervescent with 30% hydrogen peroxide; electrical conductivity (0.27 dS/m, 1:5 water); abrupt boundary.
Apse	6-31	Very dark brown (10YR 2/2) sandy loam; weak granular structure; friable; non-fluid; many fine roots; no sulfurous odor; very strongly acid (4.84 pH, 1:1 water), strongly acid (5.30 pH, 1:1 water) after moist incubation; very slightly effervescent with 30% hydrogen peroxide; electrical conductivity (0.92 dS/m, 1:5 water); gradual boundary.

Table C4-11 (continued).

BA	31-44	Very dark brown (10YR 2/2) sandy loam; moderate granular structure; friable; non-fluid; common fine roots; no sulfurous odor; very strongly acid (4.65 pH, 1:1 water), strongly acid (5.25 pH, 1:1 water) after moist incubation; very slightly effervescent with 30% hydrogen peroxide; electrical conductivity (0.60 dS/m, 1:5 water); abrupt boundary.
Btseg1	44-59	Gray (2.5Y 5/1) loam; moderate subangular blocky structure; firm; non-fluid; many brownish yellow (10YR 6/6) iron-stained pore linings; no sulfurous odor; very strongly acid (4.57 pH, 1:1 water), very strongly acid (4.90 pH, 1:1 water) after moist incubation; very slightly effervescent with 30% hydrogen peroxide; electrical conductivity (0.55 dS/m, 1:5 water); clear boundary.
Btseg2	59-91	Gray (2.5Y 5/1) loam; strong subangular blocky structure; firm; non-fluid; many yellowish brown (10YR 5/6) iron-stained pore linings; no sulfurous odor; very strongly acid (4.72 pH, 1:1 water), very strongly acid (4.90 pH, 1:1 water) after moist incubation; very slightly effervescent with 30% hydrogen peroxide; electrical conductivity (0.46 dS/m, 1:5 water); gradual boundary.
Btseg3	91-113	Gray (N6/0) sandy clay loam; strong subangular blocky structure; firm; non-fluid; common coarse roots; many brownish yellow (10YR 6/6) iron-stained pore linings; no sulfurous odor; strongly acid (5.26 pH, 1:1 water), strongly acid (5.30 pH, 1:1 water) after moist incubation; very slightly effervescent with 30% hydrogen peroxide; electrical conductivity (0.38 dS/m, 1:5 water); gradual boundary.
BCseg	113-127	Gray (N6/0) sandy loam; weak subangular blocky structure; friable; non-fluid; many coarse roots; common yellowish brown (10YR 5/6) iron-stained pore linings; no sulfurous odor; moderately acid (6.04 pH, 1:1 water), strongly acid (5.13 pH, 1:1 water) after moist incubation; slightly effervescent with 30% hydrogen peroxide; electrical conductivity (0.92 dS/m, 1:5 water); clear boundary.
Cseg1	127-151	Gray (N6/0) sandy loam; weak subangular blocky structure; friable; slightly fluid; common coarse roots; many light yellowish brown (2.5Y 6/4) iron-stained pore linings; no sulfurous odor; moderately acid (6.01 pH, 1:1 water), very strongly acid (4.86 pH, 1:1 water) after moist incubation; slightly effervescent with 30% hydrogen peroxide; electrical conductivity (0.49 dS/m, 1:5 water); clear boundary.
Cseg2	151+	Gray (N6/0) loamy sand; massive structure; friable; slightly fluid; common coarse roots; many light olive brown (2.5Y 5/6) iron-stained pore linings; no sulfurous odor; moderately acid (5.70 pH, 1:1 water), strongly acid (5.34 pH, 1:1 water) after moist incubation; very slightly effervescent with 30% hydrogen peroxide; electrical conductivity (1.04 dS/m, 1:5 water).

Table C4-12: Profile Description 3.1 rep1

Horizon	Depth (cm)	Description
		Dark olive gray (5Y 3/2) silt loam; many fine, medium, and coarse roots; slightly acid (6.51 pH, 1:1 water), moderately acid (5.98 pH, 1:1 water) after moist incubation; color change with 3% hydrogen peroxide; slightly effervescent with 30% hydrogen peroxide; electrical conductivity (4.48 dS/m, 1:5 water); gradual boundary.
Table C4-12 (continued).		
Ase2	8-21	Very dark brown (10YR 2/2) silt loam; many fine, medium, and coarse roots; slightly acid (6.50 pH, 1:1 water), moderately acid (5.60 pH, 1:1 water) after moist incubation; color change with 3% hydrogen peroxide; slightly effervescent with 30% hydrogen peroxide; electrical conductivity (7.55 dS/m, 1:5 water); gradual boundary.
Ase3	21-49	Very dark brown (7.5YR 2.5/2) clay loam; common fine, medium, and coarse roots; few wood fragments; moderate sulfurous odor; neutral (6.76 pH, 1:1 water), very strongly acid (4.86 pH, 1:1 water) after moist incubation; color change with 3% hydrogen peroxide; slightly effervescent with 30% hydrogen peroxide; electrical conductivity (7.77 dS/m, 1:5 water); gradual boundary.
Ase4	49-61	Very dark gray (2.5Y 3/1) sandy loam; weak subangular blocky structure; friable; slightly fluid; moderate sulfurous odor; few fine roots; neutral (7.34 pH, 1:1 water), extremely acid (4.48 pH, 1:1 water) after moist incubation; slightly effervescent with 30% hydrogen peroxide; electrical conductivity (6.71 dS/m, 1:5 water); clear boundary.
Btseg1	61-70	Gray (N5/0) sandy loam; moderate subangular blocky structure; firm; slightly fluid; common olive yellow (2.5Y 6/6) iron-stained pore linings; slightly alkaline (7.77 pH, 1:1 water), neutral (6.66 pH, 1:1 water) after moist incubation; slightly effervescent with 30% hydrogen peroxide; electrical conductivity (2.78 dS/m, 1:5 water); gradual boundary.
Btseg2	70-99	Gray (N5/0) clay loam; moderate subangular blocky structure; firm; non-fluid; few fine roots; common olive yellow (2.5Y 6/6) iron-stained pore linings; slightly alkaline (7.68 pH, 1:1 water), neutral (7.23 pH, 1:1 water) after moist incubation; slightly effervescent with 30% hydrogen peroxide; electrical conductivity (3.13 dS/m, 1:5 water); clear boundary.
BCseg	99-136	Gray (N5/0) sandy clay loam; weak subangular blocky structure; friable; non-fluid; many light olive brown (2.5Y 5/6) masses of oxidized iron; slightly alkaline (7.46 pH, 1:1 water), slightly alkaline (7.45 pH, 1:1 water) after moist incubation; slightly effervescent with 30% hydrogen peroxide; electrical conductivity (3.89 dS/m, 1:5 water); gradual boundary.

Table C4-12 (continued).

Cseg1	136-157	Gray (N6/0) sandy loam; massive structure; loose; non-fluid; many light olive brown (2.5Y 5/6) masses of oxidized iron; slightly alkaline (7.66 pH, 1:1 water), slightly alkaline (7.44 pH, 1:1 water) after moist incubation; slightly effervescent with 30% hydrogen peroxide; electrical conductivity (4.12 dS/m, 1:5 water); clear boundary.
Cseg2	157-198	Gray (N6/0) sandy loam; massive structure; loose; non-fluid; few light olive brown (2.5Y 5/6) masses of oxidized iron; slightly alkaline (7.66 pH, 1:1 water), neutral (7.15 pH, 1:1 water) after moist incubation; slightly effervescent with 30% hydrogen peroxide; electrical conductivity (3.83 dS/m, 1:5 water); gradual boundary.
Cseg3	198-110+	Dark gray (N4/0) sandy loam; massive structure; loose; non-fluid; slightly alkaline (7.89 pH, 1:1 water), slightly acid (6.33 pH, 1:1 water) after moist incubation; slightly effervescent with 30% hydrogen peroxide; electrical conductivity (4.83 dS/m, 1:5 water); gradual boundary.

Table C4-13: Profile Description 3.1 rep2

Horizon	Depth (cm)	Description
Cseg	0-8	Dark grayish brown (2.5Y 4/1) mucky silt loam; common fine, medium, and coarse roots; very fluid; slight sulfurous odor; neutral (6.69 pH, 1:1 water), strongly acid (5.44 pH, 1:1 water) after moist incubation; electrical conductivity (7.91 dS/m, 1:5 water); clear boundary.
Oase1	8-23	Very dark grayish brown (10YR 3/2) broken face and rubbed, peat; H8 von Post scale; muck; very fluid; many fine, medium, and coarse roots; slight sulfurous odor; slightly acid (6.46 pH, 1:1 water), extremely acid (3.60 pH, 1:1 water) after moist incubation; electrical conductivity (8.60 dS/m, 1:5 water); gradual boundary.
Ase1	23-29	Very dark gray (10YR 3/1) clay loam; many fine, medium, and coarse roots; moderately fluid; slight sulfurous odor; moderately acid (5.75 pH, 1:1 water), ultra acid (3.43 pH, 1:1 water) after moist incubation; electrical conductivity (9.96 dS/m, 1:5 water); clear boundary.
Ase2	29-43	Dark gray (10YR 4/1) sandy loam; few fine roots; slightly fluid; common charcoal stains throughout; slight sulfurous odor; neutral (7.09 pH, 1:1 water), extremely acid (3.85 pH, 1:1 water) after moist incubation; electrical conductivity (5.27 dS/m, 1:5 water); clear boundary.
Btseg1	43-101	Olive gray (5Y 5/2) sandy clay loam; slightly fluid; common charcoal stains throughout; common light yellowish brown (2.5Y 6/4) iron-stained pore linings; slightly alkaline (7.49 pH, 1:1 water), slightly acid (6.45 pH,

Table C4-13 (continued).

		1:1 water) after moist incubation; slightly effervescent with 30% hydrogen peroxide; electrical conductivity (2.40 dS/m, 1:5 water); gradual boundary.
Btseg2	101-120	Gray (N5/0) sandy loam; slightly fluid; many light olive brown (2.5Y 5/4) iron-stained pore linings; neutral (7.22 pH, 1:1 water), neutral (7.08 pH, 1:1 water) after moist incubation; moderately effervescent with 30% hydrogen peroxide; electrical conductivity (3.90 dS/m, 1:5 water); clear boundary.
BCseg	120-189	Gray (N6/0) loamy sand; non-fluid; common charcoal stains throughout; common light yellowish brown (10YR 6/4) iron-stained pore linings; neutral (7.06 pH, 1:1 water), neutral (6.90 pH, 1:1 water) after moist incubation; moderately effervescent with 30% hydrogen peroxide; electrical conductivity (3.89 dS/m, 1:5 water); gradual boundary.
Cseg	189+	Gray (N6/0) loamy sand; non-fluid; common light yellowish brown (2.5Y 6/4) iron-stained pore linings; neutral (7.37 pH, 1:1 water), neutral (7.02 pH, 1:1 water) after moist incubation; moderately effervescent with 30% hydrogen peroxide; electrical conductivity (4.33 dS/m, 1:5 water).

Table C4-14: Profile Description 3.1 rep3

Horizon	Depth (cm)	Description
Ase1	0-21	Very dark brown (10YR 2/2) loam; few wood fragments throughout; many fine, medium, and coarse roots; moderate sulfurous odor; neutral (7.26 pH, 1:1 water), ultra acid (3.40 pH, 1:1 water) after moist incubation; electrical conductivity (7.71 dS/m, 1:5 water); abrupt boundary.
Ase2	21-48	Black (2.5Y 2.5/1) sandy loam; moderately fluid; common fine roots; slight sulfurous odor; slightly alkaline (7.55 pH, 1:1 water), extremely acid (4.12 pH, 1:1 water) after moist incubation; electrical conductivity (5.08 dS/m, 1:5 water); abrupt boundary.
Btseg1	48-98	Gray (N5/0) sandy clay loam; slightly fluid; few fine roots; common black (2.5Y 2.5/1) organic stains; many light olive brown (2.5Y 5/6) iron-stained pore linings; slightly alkaline (7.80 pH, 1:1 water), neutral (6.96 pH, 1:1 water) after moist incubation; slightly effervescent with 30% hydrogen peroxide; electrical conductivity (3.38 dS/m, 1:5 water); clear boundary.
Btseg2	98-133	Gray (N6/0) sandy clay loam; slightly fluid; many light olive brown (2.5Y 5/6) iron-stained pore linings; few black (2.5Y 2.5/1) organic stains in pore linings; slightly alkaline (7.67 pH, 1:1 water), slightly alkaline (7.49 pH, 1:1 water) after moist incubation; slightly effervescent with 30% hydrogen peroxide; electrical conductivity (3.04 dS/m, 1:5 water); clear boundary.

Table C4-14 (continued).

Cg	133-188+	Gray (N6/0) sandy loam; non-fluid; common light olive brown (2.5Y 5/6) iron-stained pore linings; common black (2.5Y 2.5/1) organic stains in pore linings; moderately alkaline (8.05 pH, 1:1 water), slightly alkaline (7.54 pH, 1:1 water) after moist incubation; electrical conductivity (3.79 dS/m, 1:5 water).
----	----------	--

Table C4-15: Profile Description 3.2

Horizon	Depth (cm)	Description
Oese	0-15	Black (2.5Y 2.5/1) broken face and rubbed, mucky peat; H4 von Post scale; 30% unrubbed fiber, 20% rubbed; many fine, medium, and coarse roots; moderate sulfurous odor; neutral (7.17 pH, 1:1 water), strongly acid (5.42 pH, 1:1 water) after moist incubation; electrical conductivity (6.25 dS/m, 1:5 water); clear boundary.
Ase1	15-34	Black (10YR 2/1) sandy loam; non-fluid; common fine, medium, and coarse roots; common charcoal stains throughout; common bark fragments throughout; moderate sulfurous odor; neutral (7.05 pH, 1:1 water), moderately acid (5.60 pH, 1:1 water) after moist incubation; electrical conductivity (6.49 dS/m, 1:5 water); clear boundary.
Ase2	34-42	Very dark gray (10YR 3/1) sandy loam; slightly fluid; common fine roots; few medium roots; slight sulfurous odor; neutral (7.11 pH, 1:1 water), strongly acid (5.25 pH, 1:1 water) after moist incubation; electrical conductivity (3.83 dS/m, 1:5 water); clear boundary.
Apse	42-68	Black (10YR 2/1) sandy loam; slightly fluid; few fine roots; slight sulfurous odor; neutral (7.25 pH, 1:1 water), strongly acid (5.24 pH, 1:1 water) after moist incubation; slightly effervescent with 30% hydrogen peroxide; electrical conductivity (3.29 dS/m, 1:5 water); gradual boundary.
Btseg1	68-86	Dark gray (5Y 4/1) sandy clay loam; slightly fluid; few fine roots; no sulfurous odor; common olive yellow (2.5Y 6/6) iron-stained pore linings; neutral (6.97 pH, 1:1 water), slightly acid (6.22 pH, 1:1 water) after moist incubation; slightly effervescent with 30% hydrogen peroxide; electrical conductivity (2.38 dS/m, 1:5 water); clear boundary.
Btseg2	86-117	Gray (N5/0) clay loam; slightly fluid; no sulfurous odor; common light olive yellow (2.5Y 5/6) iron-stained pore linings; neutral (6.77 pH, 1:1 water), slightly acid (6.32 pH, 1:1 water) after moist incubation; slightly effervescent with 30% hydrogen peroxide; electrical conductivity (1.98 dS/m, 1:5 water); clear boundary.

Table C4-15 (continued).

Cseg1	117-159	Gray (N6/0) sandy loam; non-fluid; no sulfurous odor; many strong brown (7.5YR 5/8) and brown (7.5YR 5/4) iron-stained pore linings; neutral (6.79 pH, 1:1 water), slightly acid (6.52 pH, 1:1 water) after moist incubation; slightly effervescent with 30% hydrogen peroxide; electrical conductivity (2.32 dS/m, 1:5 water); clear boundary.
Cseg2	159+	Gray (N6/0) sandy loam; non-fluid; no sulfurous odor; common light olive brown (2.5Y 5/4) iron-stained pore linings; slightly acid (6.48 pH, 1:1 water), moderately acid (5.95 pH, 1:1 water) after moist incubation; slightly effervescent with 30% hydrogen peroxide; electrical conductivity (1.85 dS/m, 1:5 water).

Table C4-16: Profile Description 3.3

Horizon	Depth (cm)	Description
Oese	0-20	Very dark grayish brown (10YR 3/2) broken face and rubbed, muck; H6 von Post scale; 40% unrubbed fiber, 20% rubbed; many fine, medium, and coarse roots; moderate sulfurous odor; neutral (7.15 pH, 1:1 water), slightly acid (6.15 pH, 1:1 water) after moist incubation; electrical conductivity (4.04 dS/m, 1:5 water).
Ase	20-29	Black (10YR 2/1) sandy loam; very fluid; many fine, medium, and coarse roots; few cypress wood fragments; moderate sulfurous odor; neutral (6.94 pH, 1:1 water), moderately acid (5.85 pH, 1:1 water) after moist incubation; electrical conductivity (4.76 dS/m, 1:5 water).
Apse	29-50	Very dark gray (10YR 3/1) sandy clay loam; slightly fluid; few fine roots; slight sulfurous odor; neutral (7.35 pH, 1:1 water), moderately acid (5.80 pH, 1:1 water) after moist incubation; very slightly effervescent to 30% hydrogen peroxide; electrical conductivity (2.82 dS/m, 1:5 water).
Btseg1	50-74	Gray (N5/0) clay loam; slightly fluid; common light olive brown (2.5Y 5/6) iron-stained pore linings and soft iron masses; few very dark gray (5Y 3/1) organic staining; slight sulfurous odor; neutral (7.33 pH, 1:1 water), slightly acid (6.48 pH, 1:1 water) after moist incubation; slightly effervescent to 30% hydrogen peroxide; electrical conductivity (2.22 dS/m, 1:5 water); gradual boundary.
Btseg2	74-95	Gray (N5/0) clay; non-fluid; many light olive brown (2.5Y 5/6) iron-stained pore linings and soft iron masses; no sulfurous odor; neutral (6.85 pH, 1:1 water), neutral (6.83 pH, 1:1 water) after moist incubation; slightly effervescent to 30% hydrogen peroxide; electrical conductivity (2.56 dS/m, 1:5 water); clear boundary.

Table C4-16 (continued).

BCseg	95-116	Gray (N6/0) sandy loam; non-fluid; many light yellowish brown (2.5Y 6/4) iron-stained pore linings and soft iron masses; no sulfurous odor; neutral (7.32 pH, 1:1 water), neutral (6.74 pH, 1:1 water) after moist incubation; slightly effervescent to 30% hydrogen peroxide; electrical conductivity (2.28 dS/m, 1:5 water); clear boundary.
Cseg1	116-149	Gray (N6/0) sandy loam; non-fluid; many light olive brown (2.5Y 5/4) iron-stained pore linings and soft iron masses; no sulfurous odor; neutral (7.02 pH, 1:1 water), slightly acid (6.41 pH, 1:1 water) after moist incubation; strongly effervescent to 30% hydrogen peroxide; electrical conductivity (2.52 dS/m, 1:5 water); abrupt boundary.
Cseg2	149+	Dark gray (N4/0) sandy loam; non-fluid; common light olive brown (2.5Y 5/6) iron-stained pore linings and soft iron masses; no sulfurous odor; neutral (7.27 pH, 1:1 water), slightly acid (6.44 pH, 1:1 water) after moist incubation; slightly effervescent to 30% hydrogen peroxide; electrical conductivity (2.44 dS/m, 1:5 water).

Table C4-17: Profile Description 3.6

Horizon	Depth (cm)	Description
Oise1	0-4	Very dark brown (7.5YR 2.5/2) broken face and rubbed, peat; H1 von Post scale; many fine, medium, and coarse roots; no sulfurous odor; extremely acid (4.15 pH, 1:1 water), extremely acid (4.33 pH, 1:1 water) after moist incubation; slightly effervescent with 30% hydrogen peroxide; electrical conductivity (0.46 dS/m, 1:5 water); clear boundary.
Oapse	4-21	Very dark brown (7.5YR 2.5/2) broken face and rubbed, peat; H1 von Post scale; many fine, medium, and coarse roots; slight sulfurous odor; extremely acid (4.24 pH, 1:1 water), very strongly acid (4.71 pH, 1:1 water) after moist incubation; slightly effervescent with 30% hydrogen peroxide; electrical conductivity (0.97 dS/m, 1:5 water); clear boundary.
Btseg1	21-53	Dark gray (10YR 4/1) clay loam; slightly fluid; common fine roots; few brown (7.5YR 4/3) iron-stained pore linings; slight sulfurous odor; extremely acid (3.99 pH, 1:1 water), extremely acid (4.22 pH, 1:1 water) after moist incubation; very slightly effervescent with 30% hydrogen peroxide; electrical conductivity (1.45 dS/m, 1:5 water); clear boundary.
Btseg2	53-74	Dark gray (10YR 4/1) clay loam; slightly fluid; few coarse roots; common brown (7.5YR 4/3) iron-stained pore linings and soft iron masses; slight sulfurous odor; very strongly acid (4.80 pH, 1:1 water), very strongly acid (4.76 pH, 1:1 water) after moist incubation; very slightly effervescent with 30% hydrogen peroxide; electrical conductivity (1.39 dS/m, 1:5 water); gradual boundary.

Table C4-17 (continued).

Btseg3	74-111	Gray (10YR 5/1) sandy clay loam; moderately fluid; few light yellowish brown (10YR 6/4) iron-stained pore linings; slight sulfurous odor; very strongly acid (4.50 pH, 1:1 water), very strongly acid (4.69 pH, 1:1 water) after moist incubation; very slightly effervescent with 30% hydrogen peroxide; electrical conductivity (0.71 dS/m, 1:5 water); gradual boundary.
BCg	111-127	Gray (N5/0) sandy clay loam; slightly fluid; few olive yellow (2.5Y 6/6) iron-stained pore linings; no sulfurous odor; extremely acid (4.40 pH, 1:1 water), extremely acid (4.39 pH, 1:1 water) after moist incubation; very slightly effervescent with 30% hydrogen peroxide; electrical conductivity (1.10 dS/m, 1:5 water); clear boundary.
Cg1	127-163	Gray (N5/0) sandy loam; moderately fluid; many brown (7.5YR 4/4) and yellowish brown (10YR 5/6) iron-stained pore linings; no sulfurous odor; extremely acid (4.20 pH, 1:1 water), extremely acid (4.23 pH, 1:1 water) after moist incubation; very slightly effervescent with 30% hydrogen peroxide; electrical conductivity (1.13 dS/m, 1:5 water); clear boundary.
Cg2	163+	Dark gray (N4/0) loamy sand; very fluid; many dark yellowish brown (10YR 4/6) iron-stained pore linings; no sulfurous odor; very strongly acid (5.01 pH, 1:1 water), ultra acid (3.47 pH, 1:1 water) after moist incubation; very slightly effervescent with 30% hydrogen peroxide; electrical conductivity (1.32 dS/m, 1:5 water); clear boundary.

Appendix D

Of the sampled tidal marsh soils, the NCSS/KSSL database has data on 7 histosol and 13 mineral tidal marsh soils in the Southeast region. Out of this pool, only 3 sampled pedons from chapter 1 have quantified carbon data 1 meter or more. This does not capture the variety of different tidal marsh soils that exist in this region. Tidal marshes were considered a non-priority area since many of the ones still existing could not be converted for agriculture or used for development (Simonson, 1987), so they were mapped using concepts over direct field validation. A catena concept, where there is an increase in organic matter further from the upland and closer to the water, was used to describe these soils. However, mapping on concepts alone misses site-specific characteristics that contribute to the formation and storage of carbon.

In the chapter 1 study, classification saw a 69% discrepancy between what was mapped prior and what was classified at a pedon-scale based on laboratory and field observations in this study. Many of the discrepancies included changes in soil chemistry, such as more or less sulfidic materials than previously expected, and differences in the depth criteria of organic materials (Histosol and histic epipedon classification).

Since the mapped classification differed from the pedon-scale classification found, it raises the question of whether the concepts used to map Southeast regional tidal marshes are accurate. For example, Backbay, a soil series mapped in the SW site, had no pedons sampled that met the series concept classification. The series is classified as a wet mineral Inceptisol with a histic epipedon, but 3 out of the 4 Backbay soil map units were identified as Histosols and the one mineral pedon was fluid mineral material versus predicted non-fluid.

Table D1:

Back Barrier (highlighted values are agreement between mapped and pedon classifications.)

Site ID	Soil Series	Mapped Classification	Epipedon Found	Classification Found
PI 1-1	Carteret	Typic Psammaquents	Ochric	Fluventic Psammaquent
PI 1-3	Carteret	Typic Psammaquents	Ochric	Haplic Sulfaquent
PI 1-5	Carteret	Typic Psammaquents	Ochric	Haplic Sulfaquent
PI 2-1	Carteret	Typic Psammaquents	Ochric	Haplic Sulfaquent
PI 2-3	Carteret	Typic Psammaquents	Ochric	Haplic Sulfaquent
PI 2-5	Carteret	Typic Psammaquents	Ochric	Haplic Sulfaquent
PI 3-1	Carteret	Typic Psammaquents	Ochric	Fluventic Psammaquent
PI 3-3	Carteret	Typic Psammaquents	Ochric	Typic Psammaquent
PI 3-5	Carteret	Typic Psammaquents	Ochric	Haplic Sulfaquent
PI 4-1	Carteret	Typic Psammaquents	Ochric	Haplic Sulfaquent
PI 4-3	Carteret	Typic Psammaquents	Ochric	Haplic Sulfaquent
PI 4-5	Carteret	Typic Psammaquents	None, Mantle	Terric Sulfisaprist
PIV 1-1	Carteret	Typic Psammaquents	Ochric	Fluventic Psammaquent
PIV 2-1	Carteret	Typic Psammaquents	Ochric	Fluventic Psammaquent

5 out of 14 = 36% agreement

Table D2

Tidal Creek (highlighted values are agreement between mapped and pedon classifications.)

Site ID	Soil Series	Mapped Classification	Epipedon Found	Classification Found
BI 1-2	Bohicket	Typic Sulfaquents	Ochric	Sodic Hydraquent
BI 1-4	Bohicket	Typic Sulfaquents	Ochric	Typic Sulfaquent
BI 1-6	Bohicket	Typic Sulfaquents	Ochric	Sodic Hydraquent
BI 2-1	Bohicket	Typic Sulfaquents	Ochric	Sodic Hydraquent
BI 2-3	Bohicket	Typic Sulfaquents	Ochric	Sodic Hydraquent
BI 2-5	Bohicket	Typic Sulfaquents	Ochric	Typic Fluvaquent
BI 3-2	Bohicket	Typic Sulfaquents	Ochric	Sodic Hydraquent
BI 3-4	Bohicket	Typic Sulfaquents	Ochric	Typic Sulfaquent
BI 3-6	Bohicket	Typic Sulfaquents	Ochric	Sodic Hydraquent
BI 4-1	Bohicket	Typic Sulfaquents	Ochric	Sodic Hydraquent
BI 4-3	Bohicket	Typic Sulfaquents	Ochric	Sulfuric Hydraquent
BI 4-5	Bohicket	Typic Sulfaquents	Ochric	Typic Sulfaquent

3 out of 12 = 25% agreement

Table D3

Submerged Wetland (highlighted values are agreement between mapped and pedon classifications.)

Site ID	Soil Series	Mapped Classification	Epipedon Found	Classification Found
JB 1-2	Longshoal	Typic Haplosaprists	None	Terric Haplosaprist
JB 1-4	Delway	Terric Haplosaprists	None	Terric Haplohemist
JB 1-6	Backbay	Histic Humaquepts	None	Terric Haplohemist
RB 1-2	Longshoal	Typic Haplosaprists	None	Terric Haplohemist
RB 1-4	Delway	Terric Haplosaprists	Ochric	Sodic Hydraquent
RB 1-6	Backbay	Histic Humaquepts	Histic	Sodic Hydraquent
RB 2-2	Longshoal	Typic Haplosaprists	None	Terric Haplohemist
RB 2-4	Delway	Terric Haplosaprists	None	Terric Sulfisaprist
RB 2-6	Backbay	Histic Humaquepts	None	Terric Haplosaprist
SB 1-1	Longshoal	Typic Haplosaprists	None	Typic Haplosaprist
SB 1-4	Delway	Terric Haplosaprists	None	Typic Haplosaprist
SB 1-6	Backbay	Histic Humaquepts	None	Terric Haplosaprist

1 out of 4 = 25% Longshoal

1 out of 4 = 25% Delway

None = 0% Backbay

Table D4

Lagoon Island (highlighted values are agreement between mapped and pedon classifications.)

Site ID	Soil Series	Mapped Classification	Epipedon Found	Classification Found
BPIS 1-2	Currituck	Terric Haplosaprists	None	Fluvaquentic Haplohemist
BPIS 1-4	Currituck	Terric Haplosaprists	Histic	Typic Hydraquent
BPIS 1-6	Currituck	Terric Haplosaprists	None	Typic Haplosaprist
BUIS 1-1	Currituck	Terric Haplosaprists	None	Terric Haplosaprist
BUIS 1-3	Currituck	Terric Haplosaprists	None	Terric Haplohemist
BUIS 1-5	Currituck	Terric Haplosaprists	None	Fluvaquentic Haplohemist
CCIS 1-2	Currituck	Terric Haplosaprists	None	Terric Haplosaprist
CCIS 1-4	Currituck	Terric Haplosaprists	None	Terric Haplosaprist
KHW 1-2	Currituck	Terric Haplosaprists	None	Terric Haplosaprist
SLIS 1-1	Currituck	Terric Haplosaprists	None	Typic Sulfisaprist
SLIS 1-3	Currituck	Terric Haplosaprists	None	Typic Haplohemist
SLIS 1-5	Currituck	Terric Haplosaprists	None	Terric Haplohemist
VTIS 1-2	Currituck	Terric Haplosaprists	None	Typic Haplosaprist

6 out of 13 = 46% agreement

Chapter 2 also expressed discrepancies between what had been mapped prior and what had been classified after sampling in this study. The sampled region is composed of non-priority soils which means that classification was done by concept instead of direct verification (Simonson, 1987). Originally, soil series were labeled as having high organic Histosols (Delway) closer to the

water and Alfisols with aquic conditions (Brookman) further inland, with organic-capped Inceptisols (Backbay) as a transition between the two regions (Soil Survey Staff, 2022). Instead, recent classification shows that carbon development is not occurring at the rate that was assumed prior. Out of the 17 pedons, 4 were mapped as Histosols and only 1 pedon had enough organic matter to classify as such. Most of the newly classified soils were found to be Entisols and Alfisols, with little organic accretion. There were 5 Histic epipedons out of the 17 pedons, with 3 having developed in the Brookman or Forest sites, which were drier than Delway or Backbay pedons.

Table D5. Classification of chapter 2 soils per the Keys to Soil Taxonomy. Highlighted values are agreements between mapped and classified pedon.

Soil Series	Mapped Classification	Epipedon Found	Classification Found	Justification
Delway	Terric Haplosaprists	None	Terric Haplosaprist	Fits Series
Delway	Terric Haplosaprists	Ochric	Sodic Hydraquent	Fluidity & Shallow Organics
Delway	Terric Haplosaprists	Ochric	Typic Endoaqualf	Shallow Organics, Dry Color
Delway	Terric Haplosaprists	Ochric	Typic Endoaqualf	No Organics, Dry Color
Backbay	Histic Humaquepts	Histic	Sodic Hydraquent	Fluidity & Shallow Organics
Backbay	Histic Humaquepts	Histic	Sodic Hydraquent	Fluidity & Shallow Organics
Backbay	Histic Humaquepts	Ochric	Sodic Hydraquent	Shallow Organics & Fluidity
Backbay	Histic Humaquepts	Ochric	Fluventic Sulfaquent	Sulfides, Carbon Distribution, & Shallow Organics
Backbay	Histic Humaquepts	Ochric	Sulfic Hydraquent	Fluidity, Sulfides, & Shallow Organics
Backbay	Histic Humaquepts	Ochric	Typic Endoaqualf	Fluidity & Shallow Organics
Brookman	Umbric Endoaqualfs	Histic	Umbric Endoaqualfs	Fits Series with Histic
Brookman	Umbric Endoaqualfs	Ochric	Sodic Hydraquent	Fluidity & Topsoil
Brookman	Umbric Endoaqualfs	Ochric	Umbric Endoaqualf	Fits Series with shallow topsoil
Brookman	Umbric Endoaqualfs	Mollic	Typic Arqiaquoll	High BS
Brookman	Umbric Endoaqualfs	Ochric	Typic Endoaqualf	Topsoil Dry Color
Brookman	Umbric Endoaqualfs	Histic	Umbric Endoaqualf	Fits Series with Histic
Brookman	Umbric Endoaqualfs	Histic	Typic Endoaqualf	Lacks Topsoil

1 out of 4 = 25% Delway

0 out of 6 = 0% Backbay

3 out of 7 = 43% Brookman

Since mapping by concept alone does not capture the variability of tidal marsh soils in the Southeast, more field validation would be needed to improve our soil mapping concepts and develop site specific block diagrams.

Appendix E

Shoreline erosion and submergence along the APES is a byproduct of the current progression of SLR outpacing the rate of coastal wetland development (Gorzynski et al. 2024; Ury et al. 2021). Elevation in this area is influenced by the geomorphology of the APES region; thus, soil organic matter accumulation is what allows coastal wetlands to remain level with average ocean height (Moorhead & Brinson, 1995; Riggs et al. 2003). In a comprehensive 2022 study, Gorzynski et al. found prominent shoreline erosion in ghost forest and marsh ecosystems. Lower bulk density organic soils, such as Terric or Typic Histosols, were identified as being easily erodible in comparison to denser mineral soils (Gorzynski et al. 2022). In a region that is predominantly comprised of organic, low bulk density soils, shoreline erosion is a prominent issue.

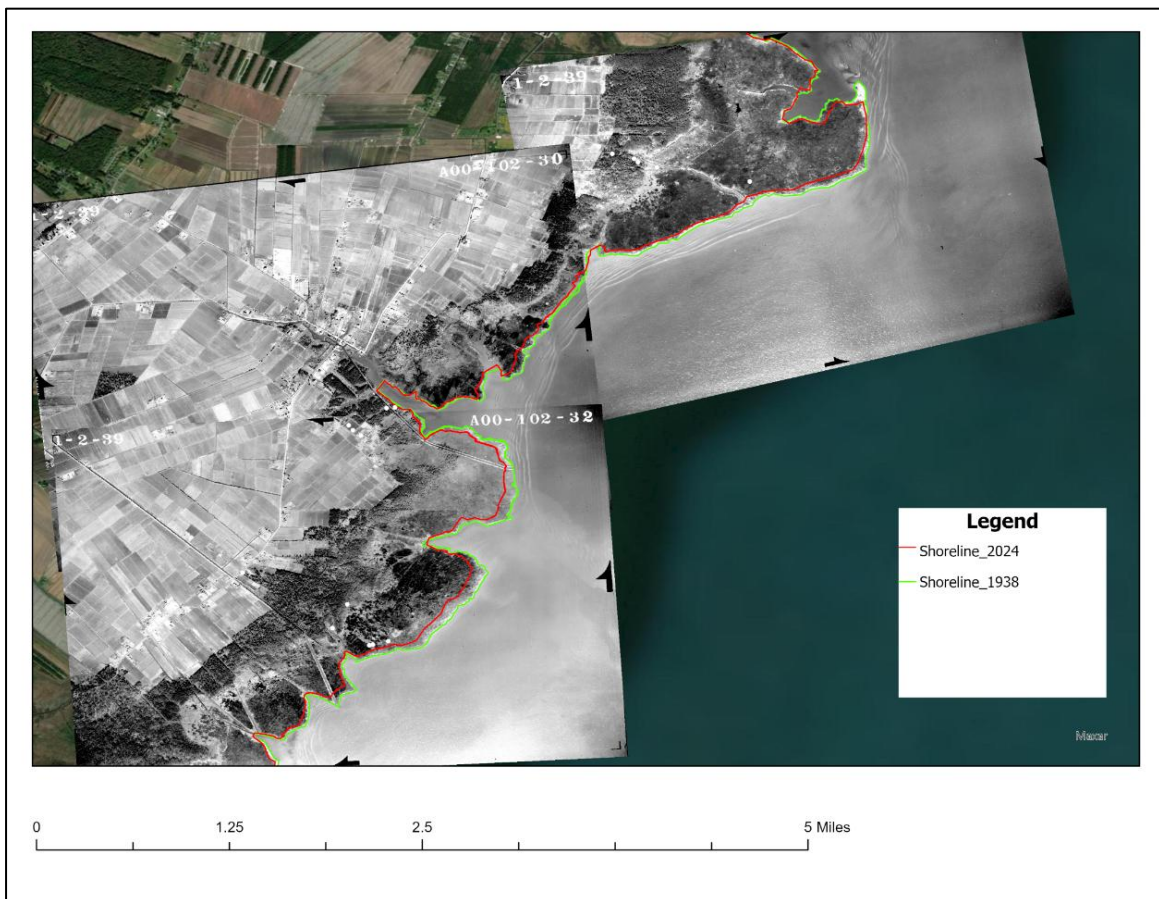


Figure E1: Shoreline georeferenced. 1938 aerial images georeferenced over 2024 shoreline.

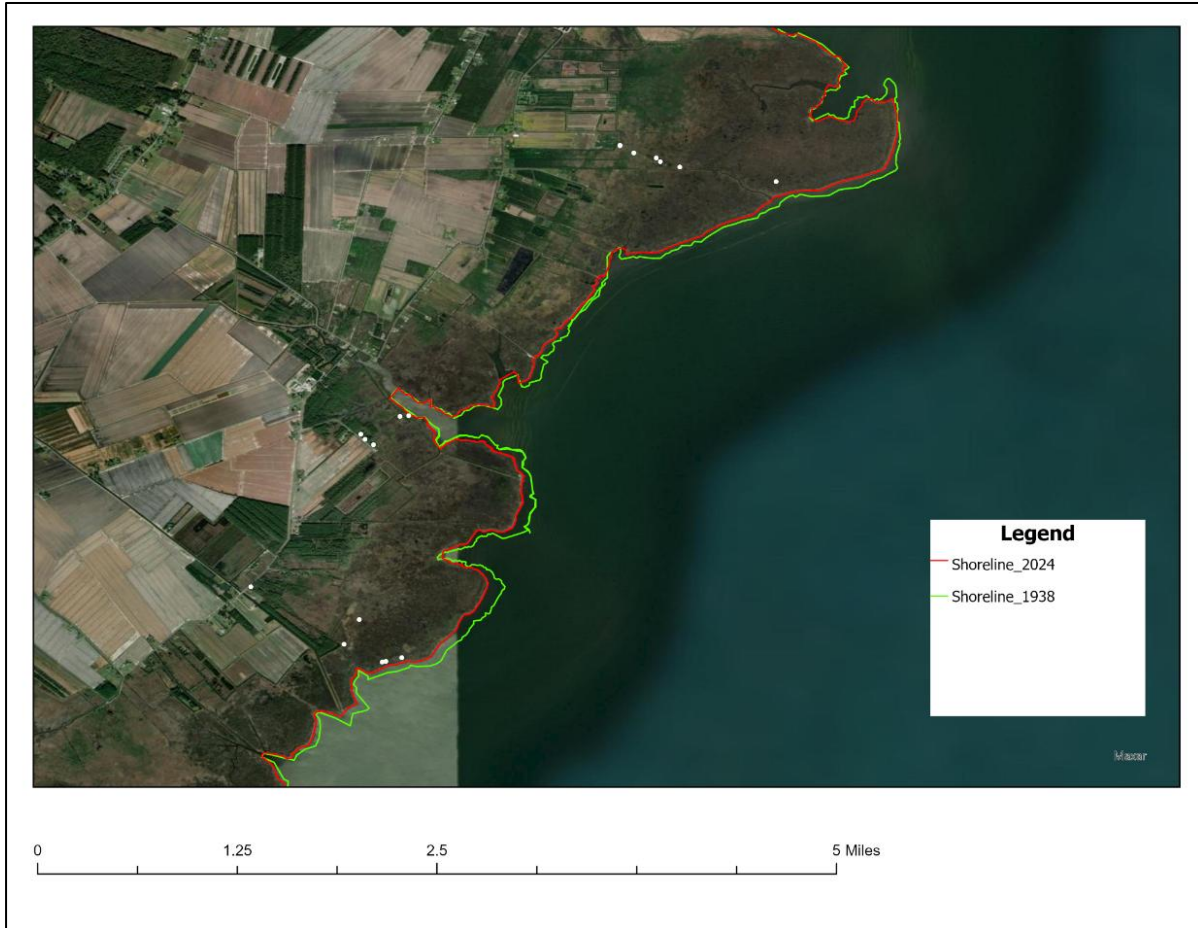


Figure E2: Shoreline Comparisons of Shoreline Erosion. 2024 shoreline next to 1938 shoreline lines to visualize how much land has been lost in study area.

To quantify the rate of change, aerial photos of a section of the Middletown, NC shoreline from 1938 were georeferenced onto 2024 shorelines. Control points were added to average the distance between shorelines, and it was determined that there has been approximately 0.54 meters/year of net erosion, which is an average of 46 meters lost total.